Wave Motion 63 (2016) 179–208

Contents lists available at ScienceDirect

Wave Motion

journal homepage: www.elsevier.com/locate/wavemoti

Polarization effects for electromagnetic wave propagation in random media

Liliana Borcea [a], Josselin Garnier [b,*]

[a] Department of Mathematics, University of Michigan, Ann Arbor, MI 48109-1043, United States

[b] Laboratoire de Probabilités et Modèles Aléatoires & Laboratoire Jacques-Louis Lions, Université Paris Diderot, 75205 Paris Cedex 13, France

HIGHLIGHTS

- Analysis of Maxwell's equations in random media.
- Quantification of the scattering mean free paths.
- Quantification of the statistical decorrelation of the waves over directions.
- Derivation of the transport equations with polarization for the energy density.
- Quantification of the depolarization.

ARTICLE INFO

Article history:
Received 23 September 2015
Received in revised form 5 January 2016
Accepted 17 February 2016
Available online 2 March 2016

Keywords:
Maxwell equations
Radiative transport
Random media
Polarization

ABSTRACT

We study Maxwell's equations in random media with small fluctuations of the electric permittivity. We consider a setup where the waves propagate toward a preferred direction, called range. We decompose the electromagnetic wave field in transverse electric and transverse magnetic plane waves, called modes, with random amplitudes that model cumulative scattering effects in the medium. Their evolution in range is described by a coupled system of stochastic differential equations driven by the random fluctuations of the electric permittivity. We analyze the solution of this system with the Markov limit theorem and obtain a detailed asymptotic characterization of the electromagnetic wave field in the long range limit. In particular, we quantify the loss of coherence of the waves due to scattering by calculating the range scales (scattering mean free paths) on which the mean amplitudes of the modes decay. We also quantify the energy exchange between the modes, and consequently the loss of polarization induced by scattering, by analyzing the Wigner transform (energy density) of the electromagnetic wave field. This analysis involves the derivation of transport equations with polarization. We study in detail these equations and connect the results with the existing literature in radiative transport and paraxial wave propagation.

1. Introduction

Understanding the interaction of electromagnetic waves with complex media through which they propagate is of great importance in applications such as radar imaging and remote sensing [1,2], optical imaging [3], laser beam propagation

* Corresponding author.
E-mail address: garnier@math.univ-paris-diderot.fr (J. Garnier).

http://dx.doi.org/10.1016/j.wavemoti.2016.02.006
0165-2125/

through the atmosphere [4], and communications [5]. As the microstructure (inhomogeneities) of such media cannot be known in detail, we model it as a random field, and thus study Maxwell's equations in random media. The goal is to describe features of the solution, the electromagnetic wave field, which do not depend on the particular realization of the random medium, just on its statistics. Of particular interest in applications are the statistical expectation of the solution, which describes the coherent part of the waves, and the second moments which describe how the waves decorrelate and depolarize, and how energy is transported in the medium.

In most applications the inhomogeneities are weak scatterers, modeled by small fluctuations of the wave speed. They have large cumulative scattering effects at long distances of propagation. Among them are the loss of coherence, manifested mathematically as an exponential decay of the statistical expectation of the wave field, and thus enhancement of the random fluctuations, and wave depolarization. The quantification of these effects depends not only on the amplitude of the fluctuations of the wave speed, but also on the relation between the basic lengths scales: the wavelength, the scale of variations of the medium (correlation length), the spatial support of the source, and the distance of propagation.

Recent mathematical studies of electromagnetic waves in random media are in [6] for layered media, in [7] for waveguides, and in [8] for beam propagation in open environments. They decompose the electromagnetic field in plane wave components, transverse to a preferred direction of propagation called range, and then analyze the evolution of their amplitudes, which are frequency and range dependent random fields. The details and results differ from one study to another, because the geometry and the scaling regimes are different. For example, the decomposition in waveguides leads to a countable set of waves, whereas in open environments, as we consider here, there is a continuum of plane waves. The regime in [8] leads to statistical wave coupling by scattering, however the waves form a narrow cone beam and they retain their initial linear polarization.

In this paper we build on the results in [7,8] to obtain a detailed characterization of polarization effects in random open environments. We consider a medium with random electric permittivity that fluctuates on a scale (correlation length) ℓ that is larger than the wavelength λ by a factor $1/\gamma$, with $\gamma \in (0, 1)$, and the waves propagate over many correlation lengths. By assuming that the support of the source is similar to the correlation length and that the fluctuations of the medium are small and smooth (i.e. their standard deviation α is small and their power spectral density decays fast enough), we identify an interesting regime where the waves propagate along a preferred direction, the range. It is between the paraxial regime studied in [8], where the waves travel in the form of a narrow cone beam, and the radiative transfer regime in [9,10], where the waves travel in all directions. In our regime the waves propagate in a cone whose opening angle is significantly larger than in the paraxial case, but smaller than 180°, so that the backscattered waves can be neglected. The validity of this regime is controlled by the parameter γ and the distance L of propagation. We take $L \gg \ell = \lambda/\gamma$ so that the scattering effects in the medium build up, but to ensure that the waves remain forward propagating, we restrict the distance to $L \sim \alpha^{-2}\ell$.

From the mathematical point of view, the advantage of having a preferred direction of propagation is that we can reduce the analysis of Maxwell's equations to the study of the range evolution of the random amplitudes of the components of the wave field. These amplitudes satisfy a system of stochastic differential equations driven by the fluctuations of the electric permittivity, and can be analyzed in detail using the Markov limit theorem [11,12]. Our main results are:

1. The quantification of the scattering mean free paths, the range scales on which the components of the electromagnetic wave field lose coherence.
2. The quantification of the statistical decorrelation of the waves over directions.
3. The derivation of the transport equations for the energy density, which allows us to quantify the depolarization of the waves and the diffusion of wave energy in direction.
4. The connection of the results to the radiative transport theory with polarization given in [13,9,14], and to the moment equations associated to the random paraxial wave equation given in [15–17] (scalar case) and [8] (electromagnetic case).

The paper is organized as follows: We state up front, in Section 2, the mathematical problem and the main results. The derivation of these results uses the formulation and scaling described in Section 3. The derivation of the wave decomposition is in Section 4. To give an intuitive interpretation of the decomposition we consider first homogeneous media. Then we give the decomposition in random media and derive the system of stochastic differential equations satisfied by the random wave amplitudes. The Markov limit of the solution of this system is obtained in Section 5. We use it in Section 6 to quantify the loss of coherence of the waves. The analysis of the second moments of the amplitudes and the derivation of the transport equations is in Section 7. They are connected to the radiative transport theory in [13,9,10] in Appendix B. We illustrate the results with numerical simulations in statistically isotropic media in Section 8. We give a detailed analysis in the high-frequency limit $\gamma \to 0$ in Section 9 and connect these results to the white-noise paraxial wave equation studied in [8] in Appendix C. We end with a summary in Section 10.

2. Statement of results

We begin in Section 2.1 with Maxwell's equations satisfied by time-harmonic electric and magnetic fields in random media. The scattering regime is defined in Section 2.2, by identifying the important scales and describing their relations. The wave decomposition in transverse electric and magnetic modes is stated in Section 2.3. The characterizations of the first and second moments of the random amplitudes of these modes are our main results, stated in Section 2.4. They are proved in Sections 6 and 7.

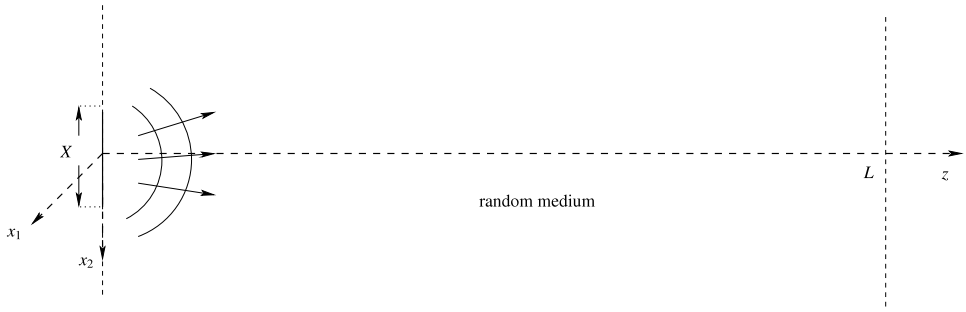

Fig. 1. Geometric setup. The source of diameter X is localized at the origin of range z, and emits waves in the direction z, in the random medium extending from $z = 0$ to $z = L$.

2.1. Maxwell's equations in random media

The time-harmonic electric and magnetic fields $\vec{\boldsymbol{E}}(\vec{\boldsymbol{x}})$ and $\vec{\boldsymbol{H}}(\vec{\boldsymbol{x}})$ satisfy Maxwell's equations

$$\vec{\nabla} \times \vec{\boldsymbol{E}}(\vec{\boldsymbol{x}}) = i\omega\mu_o \vec{\boldsymbol{H}}(\vec{\boldsymbol{x}}), \tag{1}$$

$$\vec{\nabla} \times \vec{\boldsymbol{H}}(\vec{\boldsymbol{x}}) = \vec{\boldsymbol{\mathcal{J}}}(\vec{\boldsymbol{x}}) - i\omega\varepsilon(\vec{\boldsymbol{x}})\vec{\boldsymbol{E}}(\vec{\boldsymbol{x}}), \tag{2}$$

$$\vec{\nabla} \cdot \left[\varepsilon(\vec{\boldsymbol{x}})\vec{\boldsymbol{E}}(\vec{\boldsymbol{x}})\right] = \rho(\vec{\boldsymbol{x}}), \tag{3}$$

$$\vec{\nabla} \cdot \left[\mu_o \vec{\boldsymbol{H}}(\vec{\boldsymbol{x}})\right] = 0, \tag{4}$$

for $\vec{\boldsymbol{x}} \in \mathbb{R}^3$ and frequency $\omega \in \mathbb{R}$. The setup is illustrated in Fig. 1. The excitation is with the current source density $\vec{\boldsymbol{\mathcal{J}}}$ localized at $z = 0$, that emits waves in the direction z, called range. The system of coordinates is $\vec{\boldsymbol{x}} = (\boldsymbol{x}, z)$, with vector $\boldsymbol{x} = (x_1, x_2)$ in the cross-range plane. The waves propagate in a linear medium with random electric permittivity $\varepsilon(\vec{\boldsymbol{x}})$ and constant magnetic permeability μ_o. The medium is isotropic and non-absorbing, meaning that $\varepsilon(\vec{\boldsymbol{x}})$ is scalar valued and positive. Extensions to variable magnetic permeability and to dissipative media with complex valued permittivity tensors are possible, but for simplicity we do not consider them here.

We focus attention on Eqs. (1) and (2), because the other two equations are implied by them. Eq. (4) follows by taking the divergence in (1) and the charge density $\rho(\vec{\boldsymbol{x}})$ in Eq. (3) is related to the current source $\vec{\boldsymbol{\mathcal{J}}}(\vec{\boldsymbol{x}})$ by the continuity of charge equation

$$i\omega\rho(\vec{\boldsymbol{x}}) = \vec{\nabla} \cdot \vec{\boldsymbol{\mathcal{J}}}(\vec{\boldsymbol{x}}),$$

obtained by taking the divergence of Eq. (2).

The random electric permittivity models small scale inhomogeneities in the medium. It fluctuates around the constant value ε_o, as described by

$$\varepsilon_{\mathrm{r}}(\vec{\boldsymbol{x}}) = 1 + 1_{(0,L)}(z)\, \alpha\nu\left(\frac{\vec{\boldsymbol{x}}}{\ell}\right), \tag{5}$$

where $\varepsilon_{\mathrm{r}}(\vec{\boldsymbol{x}}) = \varepsilon(\vec{\boldsymbol{x}})/\varepsilon_o$ is the relative electric permittivity, and ν is a dimensionless stationary random process of dimensionless argument in $\mathbb{R}^3$. The process has zero mean

$$\mathbb{E}\left[\nu(\vec{\boldsymbol{r}})\right] = 0, \tag{6}$$

and autocorrelation

$$\mathbb{E}\left[\nu(\vec{\boldsymbol{r}})\nu(\vec{\boldsymbol{r}}')\right] = \mathcal{R}(\vec{\boldsymbol{r}} - \vec{\boldsymbol{r}}'), \quad \forall\, \vec{\boldsymbol{r}}, \vec{\boldsymbol{r}}' \in \mathbb{R}^3. \tag{7}$$

We assume that ν is bounded and differentiable, with bounded derivative almost surely, and that $\mathcal{R}(\vec{\boldsymbol{r}})$ is integrable, with Fourier transform (power spectral density)

$$\widetilde{\mathcal{R}}(\vec{\boldsymbol{q}}) = \int_{\mathbb{R}^3} d\vec{\boldsymbol{r}}\, \mathcal{R}(\vec{\boldsymbol{r}}) e^{-i\vec{\boldsymbol{q}}\cdot\vec{\boldsymbol{r}}}. \tag{8}$$

This is a non-negative function by Bochner's theorem, and we suppose that it is either compactly supported in a ball in $\mathbb{R}^3$ of radius $O(1)$, or it is negligible outside this ball. The autocorrelation is normalized so that

$$\int_{\mathbb{R}^3} d\vec{\boldsymbol{r}}\, \mathcal{R}(\vec{\boldsymbol{r}}) = O(1), \qquad \mathcal{R}(\boldsymbol{0}) = O(1). \tag{9}$$

The length scale ℓ in (5) is the correlation length and the positive and small dimensionless parameter α quantifies the typical amplitude (standard deviation) of the fluctuations.

The indicator function $1_{(0,L)}(z)$ in (5) limits the support of the fluctuations to the range interval $z \in (0, L)$. This allows us to state easily the boundary conditions satisfied by $\vec{\boldsymbol{E}}$ and $\vec{\boldsymbol{H}}$. The truncation at $z = L$ may be understood physically in the time domain, where L is determined by the duration of the observation time. For a finite time the waves emitted by the source cannot be affected by the medium beyond some range, called here L, which is why we can truncate the random fluctuations there without affecting the solution. The truncation at $z = 0$ is consistent with the fact that in our scaling the backscattered waves are negligible. Thus, the waves that propagate from the source in the negative range direction have no effect on the waves at $z > 0$, which is why we can truncate the fluctuations at $z = 0$.

2.2. The scattering regime

There are four important length scales that define the scattering regime: the wavelength λ, the correlation length ℓ, the distance of propagation $\bar{L}$, and the support X of the source in cross-range. The wavelength is defined at the reference wave speed $c_o = 1/\sqrt{\varepsilon_o \mu_o}$ by $\lambda = 2\pi c_o/\omega$, and $\bar{L}$ is of the same order as L. The support X of the source in cross-range determines the initial opening angle of the cone (beam) of emitted waves. To define it we let the current source be of the form

$$\vec{\mathscr{J}}(\vec{\boldsymbol{x}}) = \zeta_o^{-1} \vec{\boldsymbol{J}}\left(\frac{\boldsymbol{x}}{X}\right) \delta(z), \tag{10}$$

where $\vec{\boldsymbol{J}}(\boldsymbol{r}) = \big(\boldsymbol{J}(\boldsymbol{r}), J_z(\boldsymbol{r})\big)$ is a vector-valued function of the dimensionless vector $\boldsymbol{r} \in \mathbb{R}^2$. The magnitude of $\vec{\boldsymbol{J}}$ is assumed negligible for $|\boldsymbol{r}| > 1$, so X is the diameter of the spatial support of the source. The scaling by the constant impedance $\zeta_o = \sqrt{\mu_o/\varepsilon_o}$ is chosen for convenience.

Our scattering regime is defined by the scale ordering

$$\lambda < \ell \sim X \ll \bar{L}, \tag{11}$$

and the small standard deviation α of the random fluctuations of the electric permittivity, satisfying

$$\alpha^2 \sim \ell/\bar{L}. \tag{12}$$

Here the symbol $\sim$ denotes the same order. By taking a large distance of propagation $\bar{L}$, as in (11), we ensure that the cumulative scattering effects in the random medium have a significant effect on the electromagnetic wave field. This effect is summarized in Section 2.4 by the exponential decay in z of the statistical expectation of the wave field, which is a manifestation of its randomization, the exchange of energy between the wave modes, and the diffusion of energy over directions of propagation. Because of this diffusion we restrict the propagation distance $\bar{L}$ as in (12), so that the forward going waves emitted by the source remain forward going for all $z \in (0, \bar{L})$.

2.3. Transverse electric and magnetic modes

The interaction of the waves with the random medium depends on the direction of propagation, which is why we decompose the electric and magnetic fields in plane waves with wave vector $\vec{\boldsymbol{\kappa}}$. The decomposition stated here is derived in Section 4.4, and in our scattering regime it consists of two types of forward going waves which we call modes: transverse electric and magnetic.

The decomposition of the electric field is

$$\vec{\boldsymbol{E}}(\vec{\boldsymbol{x}}) = \int_{|\boldsymbol{\kappa}|<1} \frac{d(k\boldsymbol{\kappa})}{(2\pi)^2} \beta^{-\frac{1}{2}}(\boldsymbol{\kappa}) \big[a(\boldsymbol{\kappa}, z)\, \vec{\boldsymbol{u}}(\boldsymbol{\kappa}) + a^{\perp}(\boldsymbol{\kappa}, z)\, \vec{\boldsymbol{u}}^{\perp}(\boldsymbol{\kappa})\big] e^{ik\vec{\boldsymbol{\kappa}}\cdot\vec{\boldsymbol{x}}}, \tag{13}$$

and for the magnetic field we have

$$\vec{\boldsymbol{H}}(\vec{\boldsymbol{x}}) = \zeta_o^{-1} \int_{|\boldsymbol{\kappa}|<1} \frac{d(k\boldsymbol{\kappa})}{(2\pi)^2} \beta^{-\frac{1}{2}}(\boldsymbol{\kappa}) \big[a(\boldsymbol{\kappa}, z)\, \vec{\boldsymbol{u}}^{\perp}(\boldsymbol{\kappa}) - a^{\perp}(\boldsymbol{\kappa}, z)\, \vec{\boldsymbol{u}}(\boldsymbol{\kappa})\big] e^{ik\vec{\boldsymbol{\kappa}}\cdot\vec{\boldsymbol{x}}}, \tag{14}$$

where $k = 2\pi/\lambda$ is the wavenumber and we use the notation $d(k\boldsymbol{\kappa}) = k^2 d\boldsymbol{\kappa}$. The three-dimensional wave vector is

$$\vec{\boldsymbol{\kappa}} = \big(\boldsymbol{\kappa}, \beta(\boldsymbol{\kappa})\big), \quad \boldsymbol{\kappa} = (\kappa_1, \kappa_2) \in \mathbb{R}^2. \tag{15}$$

It satisfies $|\vec{\boldsymbol{\kappa}}| = 1$, and the third component is

$$\beta(\boldsymbol{\kappa}) = \sqrt{1 - |\boldsymbol{\kappa}|^2}. \tag{16}$$

This is real valued for $|\boldsymbol{\kappa}| < 1$, meaning that the waves are propagating and not evanescent. In general there are forward and backward propagating waves, as explained in Section 4.4, but in our scattering regime the waves move forward, which is why we have $\beta(\boldsymbol{\kappa})$ with positive sign in (15).

The vectors

$$\vec{\boldsymbol{u}}(\boldsymbol{\kappa}) = \Big(\beta(\boldsymbol{\kappa})\frac{\boldsymbol{\kappa}}{|\boldsymbol{\kappa}|}, -|\boldsymbol{\kappa}|\Big), \qquad \vec{\boldsymbol{u}}^{\perp}(\boldsymbol{\kappa}) = \Big(\frac{\boldsymbol{\kappa}^{\perp}}{|\boldsymbol{\kappa}|}, 0\Big), \tag{17}$$

where $\boldsymbol{\kappa}^{\perp} = (-\kappa_2, \kappa_1)$, distinguish the two modes associated with wave vector $\vec{\boldsymbol{\kappa}}$. Note that the triplet $\{\vec{\boldsymbol{u}}(\boldsymbol{\kappa}), \vec{\boldsymbol{u}}^{\perp}(\boldsymbol{\kappa}), \vec{\boldsymbol{\kappa}}\}$ is an orthonormal basis of $\mathbb{R}^3$. Thus, Eqs. (13) and (14) are decompositions in transverse waves, which are orthogonal to the direction of propagation along $\vec{\boldsymbol{\kappa}}$. The amplitudes $a(\boldsymbol{\kappa}, z)$ are for the transverse magnetic modes, because they do not contribute to the longitudinal component of the magnetic field. They multiply the vector $\vec{\boldsymbol{u}}^{\perp}(\boldsymbol{\kappa})$ in Eq. (95). Similarly, $a^{\perp}(\boldsymbol{\kappa}, z)$ are the amplitudes of transverse electric modes, because they do not contribute to the longitudinal electric field.

For any wave vector $\vec{\boldsymbol{\kappa}}$, the electric and magnetic plane waves

$$\vec{\mathcal{E}}(\boldsymbol{\kappa}, z) = \beta^{-\frac{1}{2}}(\boldsymbol{\kappa})\big[a(\boldsymbol{\kappa}, z)\vec{\boldsymbol{u}}(\boldsymbol{\kappa}) + a^{\perp}(\boldsymbol{\kappa}, z)\vec{\boldsymbol{u}}^{\perp}(\boldsymbol{\kappa})\big],$$
$$\vec{\mathcal{H}}(\boldsymbol{\kappa}, z) = \zeta_o^{-1}\beta^{-\frac{1}{2}}(\boldsymbol{\kappa})\big[a(\boldsymbol{\kappa}, z)\vec{\boldsymbol{u}}^{\perp}(\boldsymbol{\kappa}) - a^{\perp}(\boldsymbol{\kappa}, z)\vec{\boldsymbol{u}}(\boldsymbol{\kappa})\big],$$

are orthogonal to $\vec{\boldsymbol{\kappa}}$ and to each other. The amplitudes $a(\boldsymbol{\kappa}, z)$ and $a^{\perp}(\boldsymbol{\kappa}, z)$ are random, and encode the scattering effects in the medium. In the system of coordinates with axes along $\vec{\boldsymbol{u}}(\boldsymbol{\kappa})$, $\vec{\boldsymbol{u}}^{\perp}(\boldsymbol{\kappa})$, and $\vec{\boldsymbol{\kappa}}$, which is right-handed because

$$\vec{\boldsymbol{u}}(\boldsymbol{\kappa}) \times \vec{\boldsymbol{u}}^{\perp}(\boldsymbol{\kappa}) = \vec{\boldsymbol{\kappa}}, \qquad \vec{\boldsymbol{\kappa}} \times \vec{\boldsymbol{u}}(\boldsymbol{\kappa}) = \vec{\boldsymbol{u}}^{\perp}(\boldsymbol{\kappa}), \qquad \vec{\boldsymbol{u}}^{\perp}(\boldsymbol{\kappa}) \times \vec{\boldsymbol{\kappa}} = \vec{\boldsymbol{u}}(\boldsymbol{\kappa}),$$

we can quantify the evolution of the state of polarization of the waves using the coherence matrix

$$\mathcal{P}(\boldsymbol{\kappa}, z) = \mathbb{E}\left[\begin{pmatrix} a(\boldsymbol{\kappa}, z) \\ a^{\perp}(\boldsymbol{\kappa}, z)\end{pmatrix}\begin{pmatrix} a(\boldsymbol{\kappa}, z) \\ a^{\perp}(\boldsymbol{\kappa}, z)\end{pmatrix}^{\dagger}\right] = \frac{1}{2}\begin{pmatrix} \mathfrak{S}_1(\boldsymbol{\kappa}, z) + \mathfrak{S}_2(\boldsymbol{\kappa}, z) & \mathfrak{S}_3(\boldsymbol{\kappa}, z) + i\mathfrak{S}_4(\boldsymbol{\kappa}, z) \\ \mathfrak{S}_3(\boldsymbol{\kappa}, z) - i\mathfrak{S}_4(\boldsymbol{\kappa}, z) & \mathfrak{S}_1(\boldsymbol{\kappa}, z) - \mathfrak{S}_2(\boldsymbol{\kappa}, z)\end{pmatrix}, \tag{18}$$

where $\dagger$ denotes complex conjugate and transpose, and

$$\mathfrak{S}_1(\boldsymbol{\kappa}, z) = \mathbb{E}\big[|a(\boldsymbol{\kappa}, z)|^2 + |a^{\perp}(\boldsymbol{\kappa}, z)|^2\big], \qquad \mathfrak{S}_2(\boldsymbol{\kappa}, z) = \mathbb{E}\big[|a(\boldsymbol{\kappa}, z)|^2 - |a^{\perp}(\boldsymbol{\kappa}, z)|^2\big],$$
$$\mathfrak{S}_3(\boldsymbol{\kappa}, z) = 2\mathrm{Re}\big(\mathbb{E}\big[a(\boldsymbol{\kappa}, z)\overline{a^{\perp}(\boldsymbol{\kappa}, z)}\big]\big), \qquad \mathfrak{S}_4(\boldsymbol{\kappa}, z) = 2\mathrm{Im}\big(\mathbb{E}\big[a(\boldsymbol{\kappa}, z)\overline{a^{\perp}(\boldsymbol{\kappa}, z)}\big]\big),$$

are the components of the Stokes vector $\boldsymbol{\mathfrak{S}}(\boldsymbol{\kappa}, z) = \big(\mathfrak{S}_1(\boldsymbol{\kappa}, z), \mathfrak{S}_2(\boldsymbol{\kappa}, z), \mathfrak{S}_3(\boldsymbol{\kappa}, z), \mathfrak{S}_4(\boldsymbol{\kappa}, z)\big)$. We use henceforth the bar to denote complex conjugate. The degree of polarization is defined by

$$\mathrm{Pol}(\boldsymbol{\kappa}, z) = \frac{\big(\mathfrak{S}_2(\boldsymbol{\kappa}, z)^2 + \mathfrak{S}_3(\boldsymbol{\kappa}, z)^2 + \mathfrak{S}_4(\boldsymbol{\kappa}, z)^2\big)^{1/2}}{\mathfrak{S}_1(\boldsymbol{\kappa}, z)}. \tag{19}$$

It is a number in the interval [0, 1], due to the Cauchy–Schwarz inequality

$$\big|\mathbb{E}\big[a(\boldsymbol{\kappa}, z)\overline{a^{\perp}(\boldsymbol{\kappa}, z)}\big]\big|^2 \le \mathbb{E}\big[|a(\boldsymbol{\kappa}, z)|^2\big]\mathbb{E}\big[|a^{\perp}(\boldsymbol{\kappa}, z)|^2\big].$$

The wave is fully polarized when $\mathrm{Pol}(\boldsymbol{\kappa}, z) = 1$ and unpolarized when $\mathrm{Pol}(\boldsymbol{\kappa}, z) = 0$. The mode amplitudes of fully polarized waves have a deterministic linear dependence so that

$$\mathbb{E}[|a(\boldsymbol{\kappa}, z)|^2]\mathbb{E}[|a^{\perp}(\boldsymbol{\kappa}, z)|^2] = \Big|\mathbb{E}[a(\boldsymbol{\kappa}, z)\overline{a^{\perp}(\boldsymbol{\kappa}, z)}]\Big|^2.$$

The mode amplitudes of unpolarized waves are uncorrelated and have the same mean power.

2.4. Main results

If the medium were homogeneous, the modes would be independent, with constant amplitudes $a_o(\boldsymbol{\kappa})$ and $a_o^{\perp}(\boldsymbol{\kappa})$ defined by the current source (10),

$$a_o(\boldsymbol{\kappa}) = \frac{\beta^{-1/2}(\boldsymbol{\kappa})\,|\boldsymbol{\kappa}|}{2}\int_{\mathbb{R}^2} d\boldsymbol{x}\, J_z\Big(\frac{\boldsymbol{x}}{X}\Big)e^{-i\boldsymbol{k}\boldsymbol{\kappa}\cdot\boldsymbol{x}} - \frac{\beta^{1/2}(\boldsymbol{\kappa})}{2}\frac{\boldsymbol{\kappa}}{|\boldsymbol{\kappa}|}\cdot\int_{\mathbb{R}^2} d\boldsymbol{x}\,\boldsymbol{J}\Big(\frac{\boldsymbol{x}}{X}\Big)e^{-i\boldsymbol{k}\boldsymbol{\kappa}\cdot\boldsymbol{x}}, \tag{20}$$

$$a_o^{\perp}(\boldsymbol{\kappa}) = -\frac{\beta^{-1/2}(\boldsymbol{\kappa})}{2}\frac{\boldsymbol{\kappa}^{\perp}}{|\boldsymbol{\kappa}|}\cdot\int_{\mathbb{R}^2} d\boldsymbol{x}\,\boldsymbol{J}\Big(\frac{\boldsymbol{x}}{X}\Big)e^{-i\boldsymbol{k}\boldsymbol{\kappa}\cdot\boldsymbol{x}}. \tag{21}$$

In the random medium, in the scattering regime defined by (11)–(12), the mode amplitudes $\{a(\boldsymbol{\kappa}, z), a^{\perp}(\boldsymbol{\kappa}, z)\}$ for $|\boldsymbol{\kappa}| < 1$ and $z \lesssim \bar{L}$ form a Markov process whose statistical moments can be characterized explicitly. We are interested in the first two moments which describe the loss of coherence of the waves and the transport of energy by the modes.

2.4.1. The mean mode amplitudes

Let us denote the vector of the expectations of the mode amplitudes at wave vector $\vec{\boldsymbol{\kappa}}$ by

$$\mathcal{A}(\boldsymbol{\kappa}, z) = \begin{pmatrix} \mathbb{E}[a(\boldsymbol{\kappa}, z)] \\ \mathbb{E}[a^{\perp}(\boldsymbol{\kappa}, z)] \end{pmatrix}. \tag{22}$$

Its initial value in the source plane $z = 0$ is

$$\mathcal{A}(\boldsymbol{\kappa}, 0) = \mathcal{A}_o(\boldsymbol{\kappa}) = \begin{pmatrix} a_o(\boldsymbol{\kappa}) \\ a_o^{\perp}(\boldsymbol{\kappa}) \end{pmatrix}, \tag{23}$$

and for $z > 0$ we have

$$\mathcal{A}(\boldsymbol{\kappa}, z) = \exp\Big[\mathbf{Q}(\boldsymbol{\kappa})z\Big]\mathcal{A}_o(\boldsymbol{\kappa}). \tag{24}$$

Thus, the scattering effects in the random medium do not average out, and the range evolution of the mean mode amplitudes is determined by the matrix $\mathbf{Q}(\boldsymbol{\kappa})$ in the exponential. This complex symmetric matrix is given by

$$\begin{aligned}\mathbf{Q}(\boldsymbol{\kappa}) = &-\frac{k^2\alpha^2}{4}\int_{|\boldsymbol{\kappa}'|<1}\frac{d(k\boldsymbol{\kappa}')}{(2\pi)^2}\,\boldsymbol{\Gamma}(\boldsymbol{\kappa}, \boldsymbol{\kappa}')\boldsymbol{\Gamma}(\boldsymbol{\kappa}', \boldsymbol{\kappa})\int_{\mathbb{R}^2} d\boldsymbol{x}\int_0^{\infty} dz\,\mathcal{R}\left(\frac{\vec{\boldsymbol{x}}}{\ell}\right)e^{-ik(\vec{\boldsymbol{\kappa}}-\vec{\boldsymbol{\kappa}}')\cdot\vec{\boldsymbol{x}}} \\ &-\frac{ik\alpha^2}{2}\mathcal{R}(\mathbf{0})\frac{|\boldsymbol{\kappa}|^2}{\beta(\boldsymbol{\kappa})}\begin{pmatrix}1 & 0\\ 0 & 0\end{pmatrix},\end{aligned} \tag{25}$$

for $\vec{\boldsymbol{\kappa}}, \vec{\boldsymbol{\kappa}}'$ defined as in (15), $\vec{\boldsymbol{x}} = (\boldsymbol{x}, z)$, and

$$\boldsymbol{\Gamma}(\boldsymbol{\kappa}, \boldsymbol{\kappa}') = \begin{pmatrix} \dfrac{|\boldsymbol{\kappa}||\boldsymbol{\kappa}'|}{\sqrt{\beta(\boldsymbol{\kappa})\beta(\boldsymbol{\kappa}')}} + \dfrac{\boldsymbol{\kappa}}{|\boldsymbol{\kappa}|}\cdot\dfrac{\boldsymbol{\kappa}'}{|\boldsymbol{\kappa}'|}\sqrt{\beta(\boldsymbol{\kappa})\beta(\boldsymbol{\kappa}')} & \dfrac{\boldsymbol{\kappa}}{|\boldsymbol{\kappa}|}\cdot\dfrac{\boldsymbol{\kappa}'^{\perp}}{|\boldsymbol{\kappa}'|}\sqrt{\dfrac{\beta(\boldsymbol{\kappa})}{\beta(\boldsymbol{\kappa}')}} \\ \dfrac{\boldsymbol{\kappa}^{\perp}}{|\boldsymbol{\kappa}|}\cdot\dfrac{\boldsymbol{\kappa}'}{|\boldsymbol{\kappa}'|}\sqrt{\dfrac{\beta(\boldsymbol{\kappa}')}{\beta(\boldsymbol{\kappa})}} & \dfrac{\boldsymbol{\kappa}}{|\boldsymbol{\kappa}|}\cdot\dfrac{\boldsymbol{\kappa}'}{|\boldsymbol{\kappa}'|}\dfrac{1}{\sqrt{\beta(\boldsymbol{\kappa}')\beta(\boldsymbol{\kappa})}} \end{pmatrix}. \tag{26}$$

Note that $\boldsymbol{\Gamma}(\boldsymbol{\kappa}', \boldsymbol{\kappa}) = \boldsymbol{\Gamma}(\boldsymbol{\kappa}, \boldsymbol{\kappa}')^T$ and since the autocorrelation $\mathcal{R}$ is an even function, and the power spectral density $\widetilde{\mathcal{R}}$ is non-negative, the real part of $\mathbf{Q}(\boldsymbol{\kappa})$ is a symmetric, negative definite matrix

$$\mathrm{Re}\big[\mathbf{Q}(\boldsymbol{\kappa})\big] = -\frac{k^2\ell^3\alpha^2}{8}\int_{|\boldsymbol{\kappa}'|<1}\frac{d(k\boldsymbol{\kappa}')}{(2\pi)^2}\,\boldsymbol{\Gamma}(\boldsymbol{\kappa}, \boldsymbol{\kappa}')\boldsymbol{\Gamma}^T(\boldsymbol{\kappa}, \boldsymbol{\kappa}')\,\widetilde{\mathcal{R}}\big(k\ell(\vec{\boldsymbol{\kappa}} - \vec{\boldsymbol{\kappa}}')\big). \tag{27}$$

In the case of transverse isotropic statistics of the media, where $\mathcal{R}(\vec{\boldsymbol{r}})$ with $\vec{\boldsymbol{r}} = (\boldsymbol{r}, r_z)$ depends only on $|\boldsymbol{r}|$ and r_z, we obtain by integrating in (25) over $\boldsymbol{\kappa}'$ in polar coordinates that $\mathbf{Q}(\boldsymbol{\kappa})$ is diagonal and moreover, it only depends on $|\boldsymbol{\kappa}|$. Therefore, the mean wave amplitudes decouple and they decay exponentially in z on the range scales (scattering mean free paths)

$$\mathcal{S}(\boldsymbol{\kappa}) = -1/\mathrm{Re}\big[\mathrm{Q}_{11}(\boldsymbol{\kappa})\big], \qquad \mathcal{S}^{\perp}(\boldsymbol{\kappa}) = -1/\mathrm{Re}\big[\mathrm{Q}_{22}(\boldsymbol{\kappa})\big], \tag{28}$$

which depend only on $|\boldsymbol{\kappa}|$. We refer to Section 8 for illustrations with numerical simulations in statistically isotropic media, and to Section 9 for the analysis of the high-frequency limit and connection to the white-noise paraxial regime described in Appendix C. We also show in Appendix B that, if $\mathcal{R}$ is isotropic i.e., $\mathcal{R}(\vec{\boldsymbol{r}})$ only depends on $|\vec{\boldsymbol{r}}|$, then $\mathrm{Re}(\mathbf{Q}(\boldsymbol{\kappa}))$ is proportional to the identity matrix, so the scattering mean free paths (28) are equal.

In general media the mean mode amplitudes are coupled, but they still decay exponentially in z. Indeed, matrix

$$\mathbf{S}(\boldsymbol{\kappa}) = -\mathbf{Q}(\boldsymbol{\kappa}) - \mathbf{Q}(\boldsymbol{\kappa})^{\dagger} = \frac{k^2\ell^3\alpha^2}{4}\int_{|\boldsymbol{\kappa}'|<1}\frac{d(k\boldsymbol{\kappa}')}{(2\pi)^2}\,\boldsymbol{\Gamma}(\boldsymbol{\kappa}, \boldsymbol{\kappa}')\boldsymbol{\Gamma}^T(\boldsymbol{\kappa}, \boldsymbol{\kappa}')\,\widetilde{\mathcal{R}}\big(k\ell(\vec{\boldsymbol{\kappa}} - \vec{\boldsymbol{\kappa}}')\big) \tag{29}$$

is real symmetric and positive definite. Therefore, the mean amplitudes satisfy

$$\partial_z\|\mathcal{A}(\boldsymbol{\kappa}, z)\|^2 = \mathcal{A}(\boldsymbol{\kappa}, z)^{\dagger}\Big[\mathbf{Q}(\boldsymbol{\kappa})^{\dagger} + \mathbf{Q}(\boldsymbol{\kappa})\Big]\mathcal{A}(\boldsymbol{\kappa}, z) = -\mathcal{A}(\boldsymbol{\kappa}, z)^{\dagger}\mathbf{S}(\boldsymbol{\kappa})\mathcal{A}(\boldsymbol{\kappa}, z), \tag{30}$$

and if we let $\Lambda_1(\boldsymbol{\kappa}) \geq \Lambda_2(\boldsymbol{\kappa}) > 0$ be the eigenvalues of $\mathbf{S}(\boldsymbol{\kappa})$ and use Gronwall's lemma, we get

$$e^{-z\Lambda_1(\boldsymbol{\kappa})/2}\,\|\mathcal{A}_o(\boldsymbol{\kappa})\| \leq \|\mathcal{A}(\boldsymbol{\kappa}, z)\| \leq e^{-z\Lambda_2(\boldsymbol{\kappa})/2}\,\|\mathcal{A}_o(\boldsymbol{\kappa})\|. \tag{31}$$

The scales $2/\Lambda_1(\boldsymbol{\kappa})$ and $2/\Lambda_2(\boldsymbol{\kappa})$, on which the mean wave amplitudes decay exponentially in range, are the scattering mean free paths.

The exponential decay of the mean mode amplitudes, and therefore of the mean (coherent) fields $\mathbb{E}\big[\vec{\boldsymbol{E}}(\vec{\boldsymbol{x}})\big]$ and $\mathbb{E}\big[\vec{\boldsymbol{H}}(\vec{\boldsymbol{x}})\big]$, is a manifestation of the randomization of the waves due to scattering. Energy is conserved, as shown in Section 5.3,

$$\int_{|\boldsymbol{\kappa}|<1}\frac{d(k\boldsymbol{\kappa})}{(2\pi)^2}\Big[|a(\boldsymbol{\kappa}, z)|^2 + |a^{\perp}(\boldsymbol{\kappa}, z)|^2\Big] = \text{constant}, \tag{32}$$

so the second moments cannot all decay. Therefore, the mode amplitudes have large random fluctuations.

Remark 1. The exponential decay of the coherent field is a general phenomenon in random media, and can be characterized under many scattering regimes, including when the forward scattering approximation is not valid. We refer to [18] for an overview.

2.4.2. The transport equations

The energy density (Wigner transform) of the modes at wave vector $\vec{\boldsymbol{\kappa}}$ is defined by

$$\mathcal{W}(\boldsymbol{\kappa},\vec{\boldsymbol{x}}) = \int \frac{d(k\boldsymbol{q})}{(2\pi)^2}\, \exp\big[ik\boldsymbol{q}\cdot\big(\boldsymbol{x}+\nabla\beta(\boldsymbol{q})z\big)\big] \times \mathbb{E}\left[\begin{pmatrix} a\Big(\boldsymbol{\kappa}+\dfrac{\boldsymbol{q}}{2},z\Big)\\ a^{\perp}\Big(\boldsymbol{\kappa}+\dfrac{\boldsymbol{q}}{2},z\Big)\end{pmatrix}\begin{pmatrix} a\Big(\boldsymbol{\kappa}-\dfrac{\boldsymbol{q}}{2},z\Big)\\ a^{\perp}\Big(\boldsymbol{\kappa}-\dfrac{\boldsymbol{q}}{2},z\Big)\end{pmatrix}^{\dagger}\right], \quad \vec{\boldsymbol{x}} = (\boldsymbol{x},z), \tag{33}$$

where the integral is over all $\boldsymbol{q}$ such that $|\boldsymbol{\kappa}\pm\boldsymbol{q}/2| < 1$. It satisfies the transport equation

$$\partial_z\mathcal{W}(\boldsymbol{\kappa},\vec{\boldsymbol{x}}) - \nabla\beta(\boldsymbol{\kappa})\cdot\nabla_{\boldsymbol{x}}\mathcal{W}(\boldsymbol{\kappa},\vec{\boldsymbol{x}}) = \mathbf{Q}(\boldsymbol{\kappa})\mathcal{W}(\boldsymbol{\kappa},\vec{\boldsymbol{x}}) + \mathcal{W}(\boldsymbol{\kappa},\vec{\boldsymbol{x}})\mathbf{Q}(\boldsymbol{\kappa})^{\dagger} + \frac{k^2\ell^3\alpha^2}{4}\int_{|\boldsymbol{\kappa}'|<1}\frac{d(k\boldsymbol{\kappa}')}{(2\pi)^2}\,\boldsymbol{\Gamma}(\boldsymbol{\kappa},\boldsymbol{\kappa}')\mathcal{W}(\boldsymbol{\kappa}',\vec{\boldsymbol{x}})\boldsymbol{\Gamma}(\boldsymbol{\kappa}',\boldsymbol{\kappa})\,\widetilde{\mathcal{R}}\left(k\ell(\vec{\boldsymbol{\kappa}}-\vec{\boldsymbol{\kappa}}')\right), \tag{34}$$

for $z > 0$. The derivation of this equation, given in Section 7, is one of the main results of this paper. We show some numerical illustrations in Section 8 in statistically isotropic media and relate it to the radiative transport theory in [13,9,10] in Appendix B. We consider the high frequency limit $\lambda/\ell \to 0$ in Section 9, where we can connect the results to those in the white-noise paraxial regime [8] as described in Appendix C.

The integral over $\boldsymbol{x}$ of the Wigner transform is the Hermitian, positive definite coherence matrix

$$\mathcal{P}(\boldsymbol{\kappa},z) = \mathbb{E}\left[\begin{pmatrix} a(\boldsymbol{\kappa},z)\\ a^{\perp}(\boldsymbol{\kappa},z)\end{pmatrix}\begin{pmatrix} a(\boldsymbol{\kappa},z)\\ a^{\perp}(\boldsymbol{\kappa},z)\end{pmatrix}^{\dagger}\right] = \int_{\mathbb{R}^2} d\boldsymbol{x}\,\mathcal{W}(\boldsymbol{\kappa},\vec{\boldsymbol{x}}). \tag{35}$$

Its diagonal entries are the mean mode powers, and the relation with the Stokes vector is as in (18). The coherence matrix evolves from its initial value $\mathcal{P}(\boldsymbol{\kappa},0) = \mathcal{A}(\boldsymbol{\kappa},0)\mathcal{A}(\boldsymbol{\kappa},0)^{\dagger}$ at the source according to equation

$$\partial_z\mathcal{P}(\boldsymbol{\kappa},z) = \mathbf{Q}(\boldsymbol{\kappa})\mathcal{P}(\boldsymbol{\kappa},z) + \mathcal{P}(\boldsymbol{\kappa},z)\mathbf{Q}(\boldsymbol{\kappa})^{\dagger} + \frac{k^2\ell^3\alpha^2}{4}\int_{|\boldsymbol{\kappa}'|<1}\frac{d(k\boldsymbol{\kappa}')}{(2\pi)^2}\,\boldsymbol{\Gamma}(\boldsymbol{\kappa},\boldsymbol{\kappa}')\mathcal{P}(\boldsymbol{\kappa}',z)\boldsymbol{\Gamma}(\boldsymbol{\kappa}',\boldsymbol{\kappa})\,\widetilde{\mathcal{R}}\left(k\ell(\vec{\boldsymbol{\kappa}}-\vec{\boldsymbol{\kappa}}')\right). \tag{36}$$

It follows by direct calculation, using the commutation properties of the trace and (29), that

$$\partial_z\int_{|\boldsymbol{\kappa}|<1}\frac{d(k\boldsymbol{\kappa})}{(2\pi)^2}\,\mathrm{Tr}\Big[\mathcal{P}(\boldsymbol{\kappa},z)\Big] = \int_{|\boldsymbol{\kappa}|<1}\frac{d(k\boldsymbol{\kappa})}{(2\pi)^2}\,\mathrm{Tr}\Big[\Big(\mathbf{Q}(\boldsymbol{\kappa})+\mathbf{Q}(\boldsymbol{\kappa})^{\dagger}+\mathbf{S}(\boldsymbol{\kappa})\Big)\mathcal{P}(\boldsymbol{\kappa},z)\Big] = 0, \tag{37}$$

which is consistent with the conservation identity (32). Moreover, (36) can be written in integral form as

$$\mathcal{P}(\boldsymbol{\kappa},z) = e^{\mathbf{Q}(\boldsymbol{\kappa})z}\mathcal{P}(\boldsymbol{\kappa},0)e^{\mathbf{Q}(\boldsymbol{\kappa})^{\dagger}z} + \frac{k^2\ell^3\alpha^2}{4}\int_0^z dz'\int_{|\boldsymbol{\kappa}'|<1}\frac{d(k\boldsymbol{\kappa}')}{(2\pi)^2}\,\widetilde{\mathcal{R}}\left(k\ell(\vec{\boldsymbol{\kappa}}-\vec{\boldsymbol{\kappa}}')\right) \times\Big[e^{\mathbf{Q}(\boldsymbol{\kappa})\,(z-z')}\boldsymbol{\Gamma}(\boldsymbol{\kappa},\boldsymbol{\kappa}')\Big]\mathcal{P}(\boldsymbol{\kappa}',z')\Big[e^{\mathbf{Q}(\boldsymbol{\kappa})\,(z-z')}\boldsymbol{\Gamma}(\boldsymbol{\kappa},\boldsymbol{\kappa})\Big]^{\dagger},$$

where we used the symmetry relation $\boldsymbol{\Gamma}(\boldsymbol{\kappa}',\boldsymbol{\kappa}) = \boldsymbol{\Gamma}(\boldsymbol{\kappa},\boldsymbol{\kappa}')^T$. Since $\mathcal{P}(\boldsymbol{\kappa},0)$ is Hermitian positive definite by definition, and the power spectral density $\widetilde{\mathcal{R}}$ is non-negative, we conclude that Eq. (36) has a Hermitian positive definite solution for all z, which is consistent with (35).

3. Mathematical formulation of the problem

In this section we give the mathematical formulation for the analysis of the electromagnetic wave field in the random medium with electric permittivity (5). We begin in Section 3.1 with the derivation of the 4×4 system of partial differential equations satisfied by the transverse components of the electric and magnetic fields. Our goal is to analyze the solution of this system in the scattering regime (11)–(12), made precise in Section 3.2. This scaling defines the asymptotic regime in which we can characterize the statistics of the mode amplitudes using a Markov limit.

3.1. The equations for the transverse waves

Let us eliminate from Maxwell's equations (1) and (2) the longitudinal components E_z and H_z of $\vec{\boldsymbol{E}} = (\boldsymbol{E}, E_z)$ and $\vec{\boldsymbol{H}} = (\boldsymbol{H}, H_z)$, and derive a closed system of partial differential equations for the transverse electric and magnetic fields $\boldsymbol{E}$ and $\boldsymbol{H}$. We obtain that

$$H_z(\vec{\boldsymbol{x}}) = -\frac{i}{\omega\mu_o}\nabla^\perp \cdot \boldsymbol{E}(\vec{\boldsymbol{x}}), \tag{38}$$

$$E_z(\vec{\boldsymbol{x}}) = \frac{i}{\omega\varepsilon(\vec{\boldsymbol{x}})}\left[\nabla^\perp \cdot \boldsymbol{H}(\vec{\boldsymbol{x}}) - \vec{\boldsymbol{e}}_z \cdot \boldsymbol{\mathcal{J}}(\vec{\boldsymbol{x}})\right], \tag{39}$$

where $\vec{\boldsymbol{e}}_z$ is the unit vector along the range axis, $\nabla = (\partial_{x_1}, \partial_{x_2})$ is the gradient in the transverse coordinates and $\nabla^\perp = (-\partial_{x_2}, \partial_{x_1})$ is its rotation by 90°, counterclockwise. The transverse components satisfy

$$\partial_z \boldsymbol{E}(\vec{\boldsymbol{x}}) = -i\omega\mu_o \boldsymbol{H}^\perp(\vec{\boldsymbol{x}}) - \frac{i}{\omega}\nabla\left[\frac{\nabla \cdot \boldsymbol{H}^\perp(\vec{\boldsymbol{x}})}{\varepsilon(\vec{\boldsymbol{x}})}\right] - \frac{i\zeta_o^{-1}}{\omega}\nabla_{\boldsymbol{x}}\left[\frac{J_z(\boldsymbol{x}/X)}{\varepsilon(\vec{\boldsymbol{x}})}\right]\delta(z), \tag{40}$$

$$\partial_z \boldsymbol{H}^\perp(\vec{\boldsymbol{x}}) = -i\omega\varepsilon(\vec{\boldsymbol{x}})\boldsymbol{E}(\vec{\boldsymbol{x}}) - \frac{i}{\omega\mu_o}\nabla^\perp\left[\nabla^\perp \cdot \boldsymbol{E}(\vec{\boldsymbol{x}})\right] + \zeta_o^{-1}\boldsymbol{J}(\boldsymbol{x}/X)\delta(z), \tag{41}$$

with $\boldsymbol{H}^\perp = (-H_2, H_1)$, the rotation of $\boldsymbol{H} = (H_1, H_2)$ by 90°, counterclockwise. We study the 4×4 system (40)–(41), written in more convenient form in terms of the scaled, rotated magnetic field

$$\boldsymbol{U}(\vec{\boldsymbol{x}}) = -\zeta_o \boldsymbol{H}^\perp(\vec{\boldsymbol{x}}). \tag{42}$$

The scaling by the impedance ζ_o ensures that $\boldsymbol{E}$ and $\boldsymbol{U}$ have the same physical units. Eqs. (40)–(41) become

$$\partial_z \boldsymbol{E}(\vec{\boldsymbol{x}}) = ik\boldsymbol{U}(\vec{\boldsymbol{x}}) + \frac{i}{k}\nabla\left[\frac{\nabla \cdot \boldsymbol{U}(\vec{\boldsymbol{x}})}{\varepsilon_{\mathrm{r}}(\vec{\boldsymbol{x}})}\right] - \frac{i}{k}\nabla_{\boldsymbol{x}}\left[\frac{J_z(\boldsymbol{x}/X)}{\varepsilon_{\mathrm{r}}(\vec{\boldsymbol{x}})}\right]\delta(z), \tag{43}$$

$$\partial_z \boldsymbol{U}(\vec{\boldsymbol{x}}) = ik\varepsilon_{\mathrm{r}}(\vec{\boldsymbol{x}})\boldsymbol{E}(\vec{\boldsymbol{x}}) + \frac{i}{k}\nabla^\perp\left[\nabla^\perp \cdot \boldsymbol{E}(\vec{\boldsymbol{x}})\right] - \boldsymbol{J}(\boldsymbol{x}/X)\delta(z). \tag{44}$$

3.2. Asymptotic regime

We model the separation of scales in (11)–(12) with two dimensionless parameters ϵ and γ, ordered as

$$0 < \epsilon \ll \gamma < 1, \tag{45}$$

and defined by

$$\epsilon = \frac{\lambda}{\bar{L}}, \qquad \gamma = \frac{\lambda}{\ell}. \tag{46}$$

Our primary asymptotic analysis is for $\epsilon \to 0$. The parameter γ remains finite, except in Section 9 where we study the high-frequency limit $\gamma \to 0$ in which the transport equations simplify and become equivalent to those in the white-noise paraxial regime.

We let $\bar{L}$ be the reference length scale, and introduce the scaled length variables

$$\boldsymbol{x}' = \boldsymbol{x}/(\epsilon\bar{L}), \qquad z' = z/\bar{L}, \qquad L' = L/\bar{L}, \qquad X' = X/\bar{L} = \epsilon/\gamma_J. \tag{47}$$

The scaled wavenumber is $k' = k\bar{L}\epsilon = 2\pi$ and the normalized standard deviation of the fluctuations is

$$\alpha' = \alpha/\epsilon^{1/2} = O(1). \tag{48}$$

As we will see below, the dimensionless parameter

$$\gamma_J = \gamma\ell/X = O(\gamma), \tag{49}$$

controls the opening angle of the cone (beam) emitted by the source.

Substituting (47) into (43)–(44) and dropping all the primes, since all the variables are scaled henceforth, we obtain

$$\begin{aligned}\partial_z \boldsymbol{E}^\epsilon(\boldsymbol{x}, z) = {} & \frac{ik}{\epsilon}\left[\mathbf{I} + \frac{1}{k^2}\nabla(\nabla\cdot)\right]\boldsymbol{U}^\epsilon(\boldsymbol{x}, z) - \frac{i\alpha}{k\epsilon^{1/2}}\nabla\left[\nu\left(\gamma\boldsymbol{x}, \gamma\frac{z}{\epsilon}\right)\nabla \cdot \boldsymbol{U}^\epsilon(\boldsymbol{x}, z)\right] \\ & + \frac{i\alpha^2}{k}\nabla\left[\nu^2\left(\gamma\boldsymbol{x}, \gamma\frac{z}{\epsilon}\right)\nabla \cdot \boldsymbol{U}^\epsilon(\boldsymbol{x}, z)\right] - \frac{i}{k}\nabla_{\boldsymbol{x}} J_z(\gamma_J\boldsymbol{x})\delta(z),\end{aligned} \tag{50}$$

and

$$\partial_z \boldsymbol{U}^\epsilon(\boldsymbol{x},z) = \frac{ik}{\epsilon}\left[\mathbf{I} + \frac{1}{k^2}\nabla^\perp\left(\nabla^\perp\cdot\right)\right]\boldsymbol{E}^\epsilon(\boldsymbol{x},z) + \frac{ik\alpha}{\epsilon^{1/2}}\nu\left(\gamma\boldsymbol{x},\gamma\frac{z}{\epsilon}\right)\boldsymbol{E}^\epsilon(\boldsymbol{x},z) - \boldsymbol{J}\left(\gamma_J\boldsymbol{x}\right)\delta(z), \tag{51}$$

for $0 \le z \le L$ and $\mathbf{I}$ the 2×2 identity matrix. For ranges $z < 0$ and $z > L$ the equations are simpler, as all the terms involving the process ν vanish. The fields $\boldsymbol{E}^\epsilon$ and $\boldsymbol{U}^\epsilon$ are approximations of $\boldsymbol{E}$ and $\boldsymbol{U}$ for $\epsilon \ll 1$, and Eqs. (50)–(51) follow by neglecting terms of order $\epsilon^{1/2}$ and higher in (43)–(44).

4. Wave decomposition

Because the interaction of the waves with the random medium depends on the direction of propagation, we decompose $\boldsymbol{E}^\epsilon$ and $\boldsymbol{U}^\epsilon$ over plane waves, using the Fourier transform with respect to the transverse coordinates $\boldsymbol{x}$. We denote this transform with a hat, to distinguish it from the Fourier transform with respect to the three dimensional vector $\vec{\boldsymbol{x}} = (\boldsymbol{x}, z)$. We have

$$\widehat{\boldsymbol{E}}^\epsilon(k\boldsymbol{\kappa},z) = \int_{\mathbb{R}^2} d\boldsymbol{x}\,\boldsymbol{E}^\epsilon(\boldsymbol{x},z)e^{-ik\boldsymbol{\kappa}\cdot\boldsymbol{x}}, \tag{52}$$

and similar for $\widehat{\boldsymbol{U}}^\epsilon(k\boldsymbol{\kappa},z)$, where $\boldsymbol{\kappa}$ is the scaled wave vector. The inverse transform is

$$\boldsymbol{E}^\epsilon(\boldsymbol{x},z) = \int_{\mathbb{R}^2}\frac{d(k\boldsymbol{\kappa})}{(2\pi)^2}\,\widehat{\boldsymbol{E}}^\epsilon(k\boldsymbol{\kappa},z)e^{ik\boldsymbol{\kappa}\cdot\boldsymbol{x}}. \tag{53}$$

We begin in Section 4.1 with the decomposition in homogeneous media and then consider random media in Section 4.2. We state the energy conservation in Section 4.3 and interpret the wave decomposition in terms of transverse electric and magnetic plane waves in Section 4.4.

4.1. Homogeneous media

The transformed fields in homogeneous media are $\widehat{\boldsymbol{E}}_o^\epsilon(k\boldsymbol{\kappa},z)$ and $\widehat{\boldsymbol{U}}_o^\epsilon(k\boldsymbol{\kappa},z)$. They satisfy the system of ordinary differential equations

$$\partial_z\begin{pmatrix}\widehat{\boldsymbol{E}}_o^\epsilon(k\boldsymbol{\kappa},z)\\ \widehat{\boldsymbol{U}}_o^\epsilon(k\boldsymbol{\kappa},z)\end{pmatrix} = \frac{ik}{\epsilon}\mathbf{M}(\boldsymbol{\kappa})\begin{pmatrix}\widehat{\boldsymbol{E}}_o^\epsilon(k\boldsymbol{\kappa},z)\\ \widehat{\boldsymbol{U}}_o^\epsilon(k\boldsymbol{\kappa},z)\end{pmatrix} + \frac{\delta(z)}{\gamma_J^2}\begin{pmatrix}\boldsymbol{\kappa}\widehat{J}_z\left(\frac{k\boldsymbol{\kappa}}{\gamma_J}\right)\\ -\widehat{\boldsymbol{J}}\left(\frac{k\boldsymbol{\kappa}}{\gamma_J}\right)\end{pmatrix}, \tag{54}$$

with 4×4 matrix

$$\mathbf{M}(\boldsymbol{\kappa}) = \begin{pmatrix}\mathbf{0} & \mathbf{I}-\boldsymbol{\kappa}\otimes\boldsymbol{\kappa}\\ \mathbf{I}-\boldsymbol{\kappa}^\perp\otimes\boldsymbol{\kappa}^\perp & \mathbf{0}\end{pmatrix}, \tag{55}$$

and symbol $\otimes$ denoting vector outer product. The Fourier transform of the current source $\vec{\boldsymbol{J}} = (\boldsymbol{J}, J_z)$ is

$$\widehat{\boldsymbol{J}}(k\boldsymbol{\kappa}) = \int_{\mathbb{R}^2} d\boldsymbol{x}\boldsymbol{J}(\boldsymbol{x})e^{-ik\boldsymbol{\kappa}\cdot\boldsymbol{x}}, \qquad \widehat{J}_z(k\boldsymbol{\kappa}) = \int_{\mathbb{R}^2} d\boldsymbol{x}J_z(\boldsymbol{x})e^{-ik\boldsymbol{\kappa}\cdot\boldsymbol{x}}. \tag{56}$$

Naturally, the fields are outgoing and bounded away from the source. Moreover, the Fourier transform $(\widehat{\boldsymbol{J}}(k\boldsymbol{\kappa}), \widehat{J}_z(k\boldsymbol{\kappa}))$ of the current source is supported at $|\boldsymbol{\kappa}| < 1/k$. Therefore, the excitation in Eq. (54) is supported at transverse wave vectors satisfying

$$|\boldsymbol{\kappa}| \le \frac{\gamma_J}{k} < 1. \tag{57}$$

The plane wave decomposition is based on the diagonalization of the matrix $\mathbf{M}(\boldsymbol{\kappa})$. This has two double eigenvalues $\pm\beta(\boldsymbol{\kappa})$ and the eigenvectors are

$$\boldsymbol{\psi}_\pm(\boldsymbol{\kappa}) = \begin{pmatrix}\pm\beta^{1/2}(\boldsymbol{\kappa})\frac{\boldsymbol{\kappa}}{|\boldsymbol{\kappa}|}\\ \beta^{-1/2}(\boldsymbol{\kappa})\frac{\boldsymbol{\kappa}}{|\boldsymbol{\kappa}|}\end{pmatrix} \quad\text{and}\quad \boldsymbol{\psi}_\pm^\perp(\boldsymbol{\kappa}) = \begin{pmatrix}\beta^{-1/2}(\boldsymbol{\kappa})\frac{\boldsymbol{\kappa}^\perp}{|\boldsymbol{\kappa}|}\\ \pm\beta^{1/2}(\boldsymbol{\kappa})\frac{\boldsymbol{\kappa}^\perp}{|\boldsymbol{\kappa}|}\end{pmatrix}. \tag{58}$$

They are linearly independent when $|\boldsymbol{\kappa}| \neq 1$, so they form a basis of $\mathbb{R}^4$ in which we can expand the solution of (54),

$$\begin{pmatrix} \widehat{\boldsymbol{E}}_o^\epsilon(k\boldsymbol{\kappa}, z) \\ \widehat{\boldsymbol{U}}_o^\epsilon(k\boldsymbol{\kappa}, z) \end{pmatrix} = \upsilon_o(\boldsymbol{\kappa}, z)\psi_+(\boldsymbol{\kappa}) + \upsilon_o^\perp(\boldsymbol{\kappa}, z)\psi_+^\perp(\boldsymbol{\kappa}) + \chi_o(\boldsymbol{\kappa}, z)\psi_-(\boldsymbol{\kappa}) + \chi_o^\perp(\boldsymbol{\kappa}, z)\psi_-^\perp(\boldsymbol{\kappa}). \tag{59}$$

Because the frequency is fixed, we do not include the wavenumber k in the argument of the coefficients in the expansion. Eq. (59) is the Helmholtz decomposition of the electric field and the rotated magnetic field, because the components along $\boldsymbol{\kappa}$ correspond to curl free vector fields in the $\boldsymbol{x}$ domain, and the components along $\boldsymbol{\kappa}^\perp$ to divergence free fields.

The expressions of the coefficients in (59) are obtained by substituting into (54) and using the linear independence of the eigenvectors. We obtain that

$$\upsilon_o(\boldsymbol{\kappa}, z) = a_o(\boldsymbol{\kappa})e^{\frac{ik}{\epsilon}\beta(\boldsymbol{\kappa})z}, \qquad \chi_o(\boldsymbol{\kappa}, z) = b_o(\boldsymbol{\kappa})e^{-\frac{ik}{\epsilon}\beta(\boldsymbol{\kappa})z},$$

and similar for $\upsilon_o^\perp$ and $\chi_o^\perp$. Consequently, the electric field is given by

$$\begin{aligned} \widehat{\boldsymbol{E}}_o^\epsilon(k\boldsymbol{\kappa}, z) \;=\; & 1_{(0,\infty)}(z)\left[a_o(\boldsymbol{\kappa})\beta^{1/2}(\boldsymbol{\kappa})\frac{\boldsymbol{\kappa}}{|\boldsymbol{\kappa}|} + a_o^\perp(\boldsymbol{\kappa})\beta^{-1/2}(\boldsymbol{\kappa})\frac{\boldsymbol{\kappa}^\perp}{|\boldsymbol{\kappa}|}\right]e^{\frac{ik}{\epsilon}\beta(\boldsymbol{\kappa})z} \\ & + 1_{(-\infty,0)}(z)\left[-b_o(\boldsymbol{\kappa})\beta^{1/2}(\boldsymbol{\kappa})\frac{\boldsymbol{\kappa}}{|\boldsymbol{\kappa}|} + b_o^\perp(\boldsymbol{\kappa})\beta^{-1/2}(\boldsymbol{\kappa})\frac{\boldsymbol{\kappa}^\perp}{|\boldsymbol{\kappa}|}\right]e^{-\frac{ik}{\epsilon}\beta(\boldsymbol{\kappa})z}, \end{aligned} \tag{60}$$

and the rotated magnetic field is

$$\begin{aligned} \widehat{\boldsymbol{U}}_o^\epsilon(k\boldsymbol{\kappa}, z) \;=\; & 1_{(0,\infty)}(z)\left[a_o(\boldsymbol{\kappa})\beta^{-1/2}(\boldsymbol{\kappa})\frac{\boldsymbol{\kappa}}{|\boldsymbol{\kappa}|} + a_o^\perp(\boldsymbol{\kappa})\beta^{1/2}(\boldsymbol{\kappa})\frac{\boldsymbol{\kappa}^\perp}{|\boldsymbol{\kappa}|}\right]e^{\frac{ik}{\epsilon}\beta(\boldsymbol{\kappa})z} \\ & + 1_{(-\infty,0)}(z)\left[b_o(\boldsymbol{\kappa})\beta^{-1/2}(\boldsymbol{\kappa})\frac{\boldsymbol{\kappa}}{|\boldsymbol{\kappa}|} - b_o^\perp(\boldsymbol{\kappa})\beta^{1/2}(\boldsymbol{\kappa})\frac{\boldsymbol{\kappa}^\perp}{|\boldsymbol{\kappa}|}\right]e^{-\frac{ik}{\epsilon}\beta(\boldsymbol{\kappa})z}. \end{aligned} \tag{61}$$

Recalling the Fourier transform (52), we see that this is a plane wave decomposition with wave vectors $\big(\boldsymbol{\kappa}, \pm\beta(\boldsymbol{\kappa})\big)$ multiplying $(\boldsymbol{x}, z/\epsilon)$ in the phases of the exponentials. The plus sign corresponds to forward going waves, along the positive range axis, and the negative sign to backward going waves.

In (60) we used the radiation conditions, so that the waves are outgoing and bounded, and the amplitudes are determined by the jump conditions at the source

$$\widehat{\boldsymbol{E}}_o^\epsilon(k\boldsymbol{\kappa}, 0+) - \widehat{\boldsymbol{E}}_o^\epsilon(k\boldsymbol{\kappa}, 0-) = \frac{\boldsymbol{\kappa}}{\gamma_J^2}\widehat{J}_z\left(\frac{k\boldsymbol{\kappa}}{\gamma_J}\right), \qquad \widehat{\boldsymbol{U}}_o^\epsilon(k\boldsymbol{\kappa}, 0+) - \widehat{\boldsymbol{U}}_o^\epsilon(k\boldsymbol{\kappa}, 0-) = -\frac{1}{\gamma_J^2}\widehat{\boldsymbol{J}}\left(\frac{k\boldsymbol{\kappa}}{\gamma_J}\right).$$

We obtain that

$$a_o(\boldsymbol{\kappa}) = \frac{1}{2\gamma_J^2}\left[\beta^{-1/2}(\boldsymbol{\kappa})|\boldsymbol{\kappa}|\widehat{J}_z\left(\frac{k\boldsymbol{\kappa}}{\gamma_J}\right) - \beta^{1/2}(\boldsymbol{\kappa})\frac{\boldsymbol{\kappa}}{|\boldsymbol{\kappa}|}\cdot\widehat{\boldsymbol{J}}\left(\frac{k\boldsymbol{\kappa}}{\gamma_J}\right)\right], \qquad a_o^\perp(\boldsymbol{\kappa}) = -\frac{1}{2\gamma_J^2}\beta^{-1/2}(\boldsymbol{\kappa})\frac{\boldsymbol{\kappa}^\perp}{|\boldsymbol{\kappa}|}\cdot\widehat{\boldsymbol{J}}\left(\frac{k\boldsymbol{\kappa}}{\gamma_J}\right), \tag{62}$$

$$b_o(\boldsymbol{\kappa}) = \frac{1}{2\gamma_J^2}\left[\beta^{-1/2}(\boldsymbol{\kappa})|\boldsymbol{\kappa}|\widehat{J}_z\left(\frac{k\boldsymbol{\kappa}}{\gamma_J}\right) + \beta^{1/2}(\boldsymbol{\kappa})\frac{\boldsymbol{\kappa}}{|\boldsymbol{\kappa}|}\cdot\widehat{\boldsymbol{J}}\left(\frac{k\boldsymbol{\kappa}}{\gamma_J}\right)\right], \qquad b_o^\perp(\boldsymbol{\kappa}) = a_o^\perp(\boldsymbol{\kappa}). \tag{63}$$

Note that Eq. (62) written in dimensional units are the same as (20)–(21). Moreover, as noted above, the excitation in Eq. (54) is supported at transverse wave vectors satisfying (57). Thus, there are no evanescent waves in the decompositions (60)–(61).

4.2. Random media

The Fourier transforms of the wave fields in the random medium satisfy the system of equations

$$\partial_z\begin{pmatrix} \widehat{\boldsymbol{E}}^\epsilon(k\boldsymbol{\kappa}, z) \\ \widehat{\boldsymbol{U}}^\epsilon(k\boldsymbol{\kappa}, z) \end{pmatrix} = \frac{ik}{\epsilon}\mathbf{M}(\boldsymbol{\kappa})\begin{pmatrix} \widehat{\boldsymbol{E}}^\epsilon(k\boldsymbol{\kappa}, z) \\ \widehat{\boldsymbol{U}}^\epsilon(k\boldsymbol{\kappa}, z) \end{pmatrix} + 1_{(0,L)}(z)\left[\mathcal{M}^\epsilon\begin{pmatrix} \widehat{\boldsymbol{E}}^\epsilon \\ \widehat{\boldsymbol{U}}^\epsilon \end{pmatrix}\right](k\boldsymbol{\kappa}, z), \tag{64}$$

derived from (50)–(51), with radiation conditions at $z < 0$ and $z > L$, and source conditions at $z = 0$. The leading order term in the right hand side involves the same matrix $\mathbf{M}(\boldsymbol{\kappa})$ as in the homogeneous medium. The perturbation due to the random medium is given by the integral operator $\mathcal{M}^\epsilon$ defined by

$$\begin{aligned} \left[\mathcal{M}^\epsilon\begin{pmatrix} \widehat{\boldsymbol{E}}^\epsilon \\ \widehat{\boldsymbol{U}}^\epsilon \end{pmatrix}\right](k\boldsymbol{\kappa}, z) = & \frac{ik\alpha}{\epsilon^{1/2}\gamma^2}\int\frac{d(k\boldsymbol{\kappa}')}{(2\pi)^2}\widehat{\nu}\left(\frac{k(\boldsymbol{\kappa}-\boldsymbol{\kappa}')}{\gamma}, \gamma\frac{z}{\epsilon}\right)\begin{pmatrix} \mathbf{0} & \boldsymbol{\kappa}\otimes\boldsymbol{\kappa}' \\ \mathbf{I} & \mathbf{0} \end{pmatrix}\begin{pmatrix} \widehat{\boldsymbol{E}}^\epsilon(k\boldsymbol{\kappa}', z) \\ \widehat{\boldsymbol{U}}^\epsilon(k\boldsymbol{\kappa}', z) \end{pmatrix} \\ & - \frac{ik\alpha^2}{\gamma^2}\int\frac{d(k\boldsymbol{\kappa}')}{(2\pi)^2}\widehat{\nu^2}\left(\frac{k(\boldsymbol{\kappa}-\boldsymbol{\kappa}')}{\gamma}, \gamma\frac{z}{\epsilon}\right)\begin{pmatrix} \mathbf{0} & \boldsymbol{\kappa}\otimes\boldsymbol{\kappa}' \\ \mathbf{0} & \mathbf{0} \end{pmatrix}\begin{pmatrix} \widehat{\boldsymbol{E}}^\epsilon(k\boldsymbol{\kappa}', z) \\ \widehat{\boldsymbol{U}}^\epsilon(k\boldsymbol{\kappa}', z) \end{pmatrix}, \end{aligned} \tag{65}$$

where $\widehat{\nu}$ and $\widehat{\nu^2}$ are the Fourier transforms of ν and ν^2 with respect to the first argument.

We use a similar decomposition of the waves as in the homogeneous medium, based on the same eigenvector basis $\{\boldsymbol{\psi}_\pm(\boldsymbol{\kappa}), \boldsymbol{\psi}_\pm^\perp(\boldsymbol{\kappa})\}$ that diagonalizes the matrix $\mathbf{M}(\boldsymbol{\kappa})$ in the leading term of (64). We obtain that

$$\begin{pmatrix} \widehat{\boldsymbol{E}}^\epsilon(k\boldsymbol{\kappa}, z) \\ \widehat{\boldsymbol{U}}^\epsilon(k\boldsymbol{\kappa}, z) \end{pmatrix} = \left[a^\epsilon(\boldsymbol{\kappa}, z)\boldsymbol{\psi}_+(\boldsymbol{\kappa}) + a^{\epsilon,\perp}(\boldsymbol{\kappa}, z)\boldsymbol{\psi}_+^\perp(\boldsymbol{\kappa})\right] e^{\frac{ik}{\epsilon}\beta(\boldsymbol{\kappa})z} + \left[b^\epsilon(\boldsymbol{\kappa}, z)\boldsymbol{\psi}_-(\boldsymbol{\kappa}) + b^{\epsilon,\perp}(\boldsymbol{\kappa}, z)\boldsymbol{\psi}_-^\perp(\boldsymbol{\kappa})\right] e^{-\frac{ik}{\epsilon}\beta(\boldsymbol{\kappa})z}, \tag{66}$$

where the amplitudes $a^\epsilon(\boldsymbol{\kappa}, z)$, $a^{\epsilon,\perp}(\boldsymbol{\kappa}, z)$, $b^\epsilon(\boldsymbol{\kappa}, z)$, and $b^{\epsilon,\perp}(\boldsymbol{\kappa}, z)$ are no longer constants determined by the current source density, but random fields. We keep all the components of the waves, forward and backward going, because of scattering in the random medium.

The radiation conditions are

$$a^\epsilon(\boldsymbol{\kappa}, z) = a^{\epsilon,\perp}(\boldsymbol{\kappa}, z) = 0, \quad \text{if } z < 0, \quad \text{and} \quad b^\epsilon(\boldsymbol{\kappa}, z) = b^{\epsilon,\perp}(\boldsymbol{\kappa}, z) = 0, \quad \text{if } z \geq L, \tag{67}$$

because the medium is homogeneous outside the range interval $(0, L)$. This also implies that

$$a^\epsilon(\boldsymbol{\kappa}, z) = a^\epsilon(\boldsymbol{\kappa}, L), \quad \text{and} \quad a^{\epsilon,\perp}(\boldsymbol{\kappa}, z) = a^{\epsilon,\perp}(\boldsymbol{\kappa}, L), \quad \text{if } z > L, \tag{68}$$

and

$$b^\epsilon(\boldsymbol{\kappa}, z) = b^\epsilon(\boldsymbol{\kappa}, 0-) \quad \text{and} \quad b^{\epsilon,\perp}(\boldsymbol{\kappa}, z) = b^{\epsilon,\perp}(\boldsymbol{\kappa}, 0-), \quad \text{if } z < 0. \tag{69}$$

The excitation comes from the jump conditions at the source

$$\widehat{\boldsymbol{E}}^\epsilon(k\boldsymbol{\kappa}, 0+) - \widehat{\boldsymbol{E}}^\epsilon(k\boldsymbol{\kappa}, 0-) = \frac{\boldsymbol{\kappa}}{\gamma_J^2}\widehat{J}_z\left(\frac{k\boldsymbol{\kappa}}{\gamma_J}\right), \qquad \widehat{\boldsymbol{U}}^\epsilon(k\boldsymbol{\kappa}, 0+) - \widehat{\boldsymbol{U}}^\epsilon(k\boldsymbol{\kappa}, 0-) = -\frac{1}{\gamma_J^2}\widehat{\boldsymbol{J}}\left(\frac{k\boldsymbol{\kappa}}{\gamma_J}\right),$$

which give the following initial conditions at $z = 0$,

$$a^\epsilon(\boldsymbol{\kappa}, 0+) = a_o(\boldsymbol{\kappa}), \qquad a^{\epsilon,\perp}(\boldsymbol{\kappa}, 0+) = a_o^\perp(\boldsymbol{\kappa}), \tag{70}$$

and

$$b^\epsilon(\boldsymbol{\kappa}, 0-) = b_o(\boldsymbol{\kappa}) + b^\epsilon(\boldsymbol{\kappa}, 0+), \qquad b^{\epsilon,\perp}(\boldsymbol{\kappa}, 0-) = b_o^\perp(\boldsymbol{\kappa}) + b^{\epsilon,\perp}(\boldsymbol{\kappa}, 0+). \tag{71}$$

Eqs. (70) say that the forward going waves leaving the source are the same as in the homogeneous medium. This is physical, because the waves must travel a long distance before they are affected by the small fluctuations of the electric permittivity. Eqs. (71) say that the waves at $z < 0$ are given by the superposition of those emitted by the source, modeled by $b_o(\boldsymbol{\kappa})$ and $b_o^\perp(\boldsymbol{\kappa})$, and the waves backscattered by the random medium, modeled by $b^\epsilon(\boldsymbol{\kappa}, 0+)$ and $b^{\epsilon,\perp}(\boldsymbol{\kappa}, 0+)$.

To determine the amplitudes in the random medium, we substitute Eqs. (66) into (64), and use the linear independence of the eigenvectors $\boldsymbol{\psi}_\pm(\boldsymbol{\kappa})$ and $\boldsymbol{\psi}_\pm^\perp(\boldsymbol{\kappa})$. If we let

$$\mathbf{Y}^\epsilon(\boldsymbol{\kappa}, z) = \begin{pmatrix} a^\epsilon(\boldsymbol{\kappa}, z) \\ a^{\epsilon,\perp}(\boldsymbol{\kappa}, z) \\ b^\epsilon(\boldsymbol{\kappa}, z) \\ b^{\epsilon,\perp}(\boldsymbol{\kappa}, z) \end{pmatrix}, \tag{72}$$

we obtain that

$$\frac{\partial \mathbf{Y}^\epsilon}{\partial z}(\boldsymbol{\kappa}, z) = \frac{ik\alpha}{2\gamma^2\epsilon^{1/2}} \int \frac{d(k\boldsymbol{\kappa}')}{(2\pi)^2}\, \widehat{\nu}\left(\frac{k(\boldsymbol{\kappa} - \boldsymbol{\kappa}')}{\gamma}, \gamma\frac{z}{\epsilon}\right) \mathbf{F}\left(\boldsymbol{\kappa}, \boldsymbol{\kappa}', \frac{z}{\epsilon}\right) \mathbf{Y}^\epsilon(\boldsymbol{\kappa}', z) + \frac{ik\alpha^2}{2\gamma^2} \int \frac{d(k\boldsymbol{\kappa}')}{(2\pi)^2}\, \widehat{\nu^2}\left(\frac{k(\boldsymbol{\kappa} - \boldsymbol{\kappa}')}{\gamma}, \gamma\frac{z}{\epsilon}\right) \mathbf{G}\left(\boldsymbol{\kappa}, \boldsymbol{\kappa}', \frac{z}{\epsilon}\right) \mathbf{Y}^\epsilon(\boldsymbol{\kappa}', z), \tag{73}$$

in $z \in (0, L)$, with boundary conditions (67) and (70). We are interested in the propagating waves, corresponding to $|\boldsymbol{\kappa}| < 1$ in (73), and we explain in Section 5 that in our regime the evanescent waves may be neglected. This means that we can restrict the integral in (73) to vectors $\boldsymbol{\kappa}'$ satisfying $|\boldsymbol{\kappa}'| < 1$.

The mode amplitudes are coupled in Eqs. (73) by the 4×4 complex matrices $\mathbf{F}(\boldsymbol{\kappa}, \boldsymbol{\kappa}', \zeta)$ and $\mathbf{G}(\boldsymbol{\kappa}, \boldsymbol{\kappa}', \zeta)$, with block structure

$$\mathbf{F}(\boldsymbol{\kappa}, \boldsymbol{\kappa}', \zeta) = \begin{pmatrix} \mathbf{F}^{aa}(\boldsymbol{\kappa}, \boldsymbol{\kappa}', \zeta) & \mathbf{F}^{ab}(\boldsymbol{\kappa}, \boldsymbol{\kappa}', \zeta) \\ \mathbf{F}^{ba}(\boldsymbol{\kappa}, \boldsymbol{\kappa}', \zeta) & \mathbf{F}^{bb}(\boldsymbol{\kappa}, \boldsymbol{\kappa}', \zeta) \end{pmatrix}, \tag{74}$$

and

$$\mathbf{G}(\boldsymbol{\kappa}, \boldsymbol{\kappa}', \zeta) = \begin{pmatrix} \mathbf{G}^{aa}(\boldsymbol{\kappa}, \boldsymbol{\kappa}', \zeta) & \mathbf{G}^{ab}(\boldsymbol{\kappa}, \boldsymbol{\kappa}', \zeta) \\ \mathbf{G}^{ba}(\boldsymbol{\kappa}, \boldsymbol{\kappa}', \zeta) & \mathbf{G}^{bb}(\boldsymbol{\kappa}, \boldsymbol{\kappa}', \zeta) \end{pmatrix}, \tag{75}$$

where the superscripts of the 2×2 blocks indicate which types of waves they couple. The dependence on ζ of the blocks in $\mathbf{F}$ can be factored as

$$\mathbf{F}^{aa}(\boldsymbol{\kappa}, \boldsymbol{\kappa}', \zeta) = \mathbf{\Gamma}^{aa}(\boldsymbol{\kappa}, \boldsymbol{\kappa}') e^{ik\left[\beta(\boldsymbol{\kappa}') - \beta(\boldsymbol{\kappa})\right]\zeta}, \tag{76}$$

$$\mathbf{F}^{bb}(\boldsymbol{\kappa}, \boldsymbol{\kappa}', \zeta) = \mathbf{\Gamma}^{bb}(\boldsymbol{\kappa}, \boldsymbol{\kappa}') e^{ik\left[-\beta(\boldsymbol{\kappa}') + \beta(\boldsymbol{\kappa})\right]\zeta}, \tag{77}$$

$$\mathbf{F}^{ab}(\boldsymbol{\kappa}, \boldsymbol{\kappa}', \zeta) = \mathbf{\Gamma}^{ab}(\boldsymbol{\kappa}, \boldsymbol{\kappa}') e^{-ik\left[\beta(\boldsymbol{\kappa}') + \beta(\boldsymbol{\kappa})\right]\zeta}, \tag{78}$$

$$\mathbf{F}^{ba}(\boldsymbol{\kappa}, \boldsymbol{\kappa}', \zeta) = \mathbf{\Gamma}^{ba}(\boldsymbol{\kappa}, \boldsymbol{\kappa}') e^{ik\left[\beta(\boldsymbol{\kappa}') + \beta(\boldsymbol{\kappa})\right]\zeta}, \tag{79}$$

with 2×2 real-valued matrices

$$\mathbf{\Gamma}^{aa}(\boldsymbol{\kappa}, \boldsymbol{\kappa}') = \begin{pmatrix} \dfrac{|\boldsymbol{\kappa}||\boldsymbol{\kappa}'|}{\sqrt{\beta(\boldsymbol{\kappa})\beta(\boldsymbol{\kappa}')}} + \dfrac{\boldsymbol{\kappa}}{|\boldsymbol{\kappa}|} \cdot \dfrac{\boldsymbol{\kappa}'}{|\boldsymbol{\kappa}'|}\sqrt{\beta(\boldsymbol{\kappa})\beta(\boldsymbol{\kappa}')} & \dfrac{\boldsymbol{\kappa}}{|\boldsymbol{\kappa}|} \cdot \dfrac{\boldsymbol{\kappa}'^{\perp}}{|\boldsymbol{\kappa}'|}\sqrt{\dfrac{\beta(\boldsymbol{\kappa})}{\beta(\boldsymbol{\kappa}')}} \\ \dfrac{\boldsymbol{\kappa}^{\perp}}{|\boldsymbol{\kappa}|} \cdot \dfrac{\boldsymbol{\kappa}'}{|\boldsymbol{\kappa}'|}\sqrt{\dfrac{\beta(\boldsymbol{\kappa}')}{\beta(\boldsymbol{\kappa})}} & \dfrac{\boldsymbol{\kappa}}{|\boldsymbol{\kappa}|} \cdot \dfrac{\boldsymbol{\kappa}'}{|\boldsymbol{\kappa}'|}\dfrac{1}{\sqrt{\beta(\boldsymbol{\kappa}')\beta(\boldsymbol{\kappa})}} \end{pmatrix}, \tag{80}$$

and

$$\mathbf{\Gamma}^{bb}(\boldsymbol{\kappa}, \boldsymbol{\kappa}') = \begin{pmatrix} -\dfrac{|\boldsymbol{\kappa}||\boldsymbol{\kappa}'|}{\sqrt{\beta(\boldsymbol{\kappa})\beta(\boldsymbol{\kappa}')}} - \dfrac{\boldsymbol{\kappa}}{|\boldsymbol{\kappa}|} \cdot \dfrac{\boldsymbol{\kappa}'}{|\boldsymbol{\kappa}'|}\sqrt{\beta(\boldsymbol{\kappa})\beta(\boldsymbol{\kappa}')} & \dfrac{\boldsymbol{\kappa}}{|\boldsymbol{\kappa}|} \cdot \dfrac{\boldsymbol{\kappa}'^{\perp}}{|\boldsymbol{\kappa}'|}\sqrt{\dfrac{\beta(\boldsymbol{\kappa})}{\beta(\boldsymbol{\kappa}')}} \\ \dfrac{\boldsymbol{\kappa}^{\perp}}{|\boldsymbol{\kappa}|} \cdot \dfrac{\boldsymbol{\kappa}'}{|\boldsymbol{\kappa}'|}\sqrt{\dfrac{\beta(\boldsymbol{\kappa}')}{\beta(\boldsymbol{\kappa})}} & -\dfrac{\boldsymbol{\kappa}}{|\boldsymbol{\kappa}|} \cdot \dfrac{\boldsymbol{\kappa}'}{|\boldsymbol{\kappa}'|}\dfrac{1}{\sqrt{\beta(\boldsymbol{\kappa}')\beta(\boldsymbol{\kappa})}} \end{pmatrix}, \tag{81}$$

on the diagonal. Note that $\mathbf{\Gamma}^{aa}$ is the same as the matrix $\mathbf{\Gamma}$ in (26). The off-diagonal matrices are

$$\mathbf{\Gamma}^{ab}(\boldsymbol{\kappa}, \boldsymbol{\kappa}') = \begin{pmatrix} \dfrac{|\boldsymbol{\kappa}||\boldsymbol{\kappa}'|}{\sqrt{\beta(\boldsymbol{\kappa})\beta(\boldsymbol{\kappa}')}} - \dfrac{\boldsymbol{\kappa}}{|\boldsymbol{\kappa}|} \cdot \dfrac{\boldsymbol{\kappa}'}{|\boldsymbol{\kappa}'|}\sqrt{\beta(\boldsymbol{\kappa})\beta(\boldsymbol{\kappa}')} & \dfrac{\boldsymbol{\kappa}}{|\boldsymbol{\kappa}|} \cdot \dfrac{\boldsymbol{\kappa}'^{\perp}}{|\boldsymbol{\kappa}'|}\sqrt{\dfrac{\beta(\boldsymbol{\kappa})}{\beta(\boldsymbol{\kappa}')}} \\ -\dfrac{\boldsymbol{\kappa}^{\perp}}{|\boldsymbol{\kappa}|} \cdot \dfrac{\boldsymbol{\kappa}'}{|\boldsymbol{\kappa}'|}\sqrt{\dfrac{\beta(\boldsymbol{\kappa}')}{\beta(\boldsymbol{\kappa})}} & \dfrac{\boldsymbol{\kappa}}{|\boldsymbol{\kappa}|} \cdot \dfrac{\boldsymbol{\kappa}'}{|\boldsymbol{\kappa}'|}\dfrac{1}{\sqrt{\beta(\boldsymbol{\kappa}')\beta(\boldsymbol{\kappa})}} \end{pmatrix}, \tag{82}$$

and

$$\mathbf{\Gamma}^{ba}(\boldsymbol{\kappa}, \boldsymbol{\kappa}') = \begin{pmatrix} -\dfrac{|\boldsymbol{\kappa}||\boldsymbol{\kappa}'|}{\sqrt{\beta(\boldsymbol{\kappa})\beta(\boldsymbol{\kappa}')}} + \dfrac{\boldsymbol{\kappa}}{|\boldsymbol{\kappa}|} \cdot \dfrac{\boldsymbol{\kappa}'}{|\boldsymbol{\kappa}'|}\sqrt{\beta(\boldsymbol{\kappa})\beta(\boldsymbol{\kappa}')} & \dfrac{\boldsymbol{\kappa}}{|\boldsymbol{\kappa}|} \cdot \dfrac{\boldsymbol{\kappa}'^{\perp}}{|\boldsymbol{\kappa}'|}\sqrt{\dfrac{\beta(\boldsymbol{\kappa})}{\beta(\boldsymbol{\kappa}')}} \\ -\dfrac{\boldsymbol{\kappa}^{\perp}}{|\boldsymbol{\kappa}|} \cdot \dfrac{\boldsymbol{\kappa}'}{|\boldsymbol{\kappa}'|}\sqrt{\dfrac{\beta(\boldsymbol{\kappa}')}{\beta(\boldsymbol{\kappa})}} & -\dfrac{\boldsymbol{\kappa}}{|\boldsymbol{\kappa}|} \cdot \dfrac{\boldsymbol{\kappa}'}{|\boldsymbol{\kappa}'|}\dfrac{1}{\sqrt{\beta(\boldsymbol{\kappa}')\beta(\boldsymbol{\kappa})}} \end{pmatrix}. \tag{83}$$

The diagonal blocks in $\mathbf{G}$ are

$$\mathbf{G}^{aa}(\boldsymbol{\kappa}, \boldsymbol{\kappa}', \zeta) = \begin{pmatrix} -\dfrac{|\boldsymbol{\kappa}||\boldsymbol{\kappa}'|}{\sqrt{\beta(\boldsymbol{\kappa})\beta(\boldsymbol{\kappa}')}} & 0 \\ 0 & 0 \end{pmatrix} e^{ik\left[\beta(\boldsymbol{\kappa}') - \beta(\boldsymbol{\kappa})\right]\zeta}, \tag{84}$$

$$\mathbf{G}^{bb}(\boldsymbol{\kappa}, \boldsymbol{\kappa}', \zeta) = -\overline{\mathbf{G}^{aa}(\boldsymbol{\kappa}, \boldsymbol{\kappa}', \zeta)}, \tag{85}$$

and the off-diagonal blocks are similar

$$\mathbf{G}^{ab}(\boldsymbol{\kappa}, \boldsymbol{\kappa}', \zeta) = \begin{pmatrix} -\dfrac{|\boldsymbol{\kappa}||\boldsymbol{\kappa}'|}{\sqrt{\beta(\boldsymbol{\kappa})\beta(\boldsymbol{\kappa}')}} & 0 \\ 0 & 0 \end{pmatrix} e^{-ik\left[\beta(\boldsymbol{\kappa}') + \beta(\boldsymbol{\kappa})\right]\zeta}, \tag{86}$$

$$\mathbf{G}^{ba}(\boldsymbol{\kappa}, \boldsymbol{\kappa}', \zeta) = -\overline{\mathbf{G}^{ab}(\boldsymbol{\kappa}, \boldsymbol{\kappa}', \zeta)}. \tag{87}$$

4.3. Energy conservation

The diagonal blocks of coupling matrices $\mathbf{F}$ and $\mathbf{G}$ satisfy the symmetry relations

$$\mathbf{F}^{aa}(\boldsymbol{\kappa}, \boldsymbol{\kappa}', \zeta) = \mathbf{F}^{aa}(\boldsymbol{\kappa}', \boldsymbol{\kappa}, \zeta)^{\dagger}, \qquad \mathbf{G}^{aa}(\boldsymbol{\kappa}, \boldsymbol{\kappa}', \zeta) = \mathbf{G}^{aa}(\boldsymbol{\kappa}', \boldsymbol{\kappa}, \zeta)^{\dagger}, \tag{88}$$

$$\mathbf{F}^{bb}(\boldsymbol{\kappa}, \boldsymbol{\kappa}', \zeta) = \mathbf{F}^{bb}(\boldsymbol{\kappa}', \boldsymbol{\kappa}, \zeta)^{\dagger}, \qquad \mathbf{G}^{bb}(\boldsymbol{\kappa}, \boldsymbol{\kappa}', \zeta) = \mathbf{G}^{bb}(\boldsymbol{\kappa}', \boldsymbol{\kappa}, \zeta)^{\dagger}. \tag{89}$$

Using these in (73) we obtain the conservation identity

$$\int_{|\boldsymbol{\kappa}|<1} \frac{d(k\boldsymbol{\kappa})}{(2\pi)^2}\Big[|a^\epsilon(\boldsymbol{\kappa},z)|^2 + |a^{\epsilon,\perp}(\boldsymbol{\kappa},z)|^2 - |b^\epsilon(\boldsymbol{\kappa},z)|^2 - |b^{\epsilon,\perp}(\boldsymbol{\kappa},z)|^2\Big] = \text{constant}, \tag{90}$$

independent of z.

Now let us recall that $\frac{1}{2}\mathrm{Re}\big[\vec{\boldsymbol{E}}^\epsilon \times \vec{\boldsymbol{H}}^\epsilon\big]$ is the time average of the Poynting vector of the time harmonic electromagnetic wave [19]. Its z-component is

$$-\frac{1}{2}\mathrm{Re}\Big[\boldsymbol{E}^\epsilon(\boldsymbol{x},z)\cdot\boldsymbol{H}^{\epsilon,\perp}(\boldsymbol{x},z)\Big] = \frac{\zeta_o^{-1}}{2}\mathrm{Re}\Big[\boldsymbol{E}^\epsilon(\boldsymbol{x},z)\cdot\boldsymbol{U}^\epsilon(\boldsymbol{x},z)\Big],$$

where we used (42). The integral of this is the energy flux which must be conserved

$$\int_{\mathbb{R}^2} d\boldsymbol{x}\,\mathrm{Re}\Big[\boldsymbol{E}^\epsilon(\boldsymbol{x},z)\cdot\boldsymbol{U}^\epsilon(\boldsymbol{x},z)\Big] = \text{constant}. \tag{91}$$

Our identity (90) is the statement of this energy conservation, written in terms of the wave amplitudes. It follows from (91) by substituting Eqs. (66) and using Plancherel's theorem.

4.4. Transverse electric and transverse magnetic waves

To interpret the wave decomposition (66) as an expansion of the electromagnetic wave field in transverse electric and magnetic waves, we recall the definitions (38)–(39) of the longitudinal electric and magnetic fields. After the scaling, and in the Fourier domain, these become

$$\widehat{H}_z^\epsilon(k\boldsymbol{\kappa},z) = \zeta_o^{-1}\boldsymbol{\kappa}^\perp\cdot\widehat{\boldsymbol{E}}^\epsilon(k\boldsymbol{\kappa},z), \tag{92}$$

$$\widehat{E}_z^\epsilon(k\boldsymbol{\kappa},z) = -\zeta_o\boldsymbol{\kappa}^\perp\cdot\widehat{\boldsymbol{H}}^\epsilon(k\boldsymbol{\kappa},z) = -\boldsymbol{\kappa}\cdot\widehat{\boldsymbol{U}}^\epsilon(k\boldsymbol{\kappa},z). \tag{93}$$

Then, using (66), the definition (58) of the eigenfunctions, and the inverse Fourier transform (53), we obtain that the electric field $\vec{\boldsymbol{E}}^\epsilon = (\boldsymbol{E}^\epsilon, E_z^\epsilon)$ is given by

$$\begin{aligned}\vec{\boldsymbol{E}}^\epsilon\Big(\frac{\boldsymbol{x}}{\epsilon},z\Big) = \int_{|\boldsymbol{\kappa}|<1}\frac{d(k\boldsymbol{\kappa})}{(2\pi)^2}\beta^{-\frac{1}{2}}(\boldsymbol{\kappa})\Big\{&\big[a^\epsilon(\boldsymbol{\kappa},z)\,\vec{\boldsymbol{u}}(\boldsymbol{\kappa}) + a^{\epsilon,\perp}(\boldsymbol{\kappa},z)\,\vec{\boldsymbol{u}}^\perp(\boldsymbol{\kappa})\big]e^{i\frac{k}{\epsilon}\vec{\boldsymbol{\kappa}}\cdot\vec{\boldsymbol{x}}}\\ &+\big[-b^\epsilon(\boldsymbol{\kappa},z)\,\vec{\boldsymbol{u}}^-(\boldsymbol{\kappa}) + b^{\epsilon,\perp}(\boldsymbol{\kappa},z)\,\vec{\boldsymbol{u}}^\perp(\boldsymbol{\kappa})\big]e^{i\frac{k}{\epsilon}\vec{\boldsymbol{\kappa}}^-\cdot\vec{\boldsymbol{x}}}\Big\},\end{aligned} \tag{94}$$

and the magnetic field is

$$\begin{aligned}\vec{\boldsymbol{H}}^\epsilon\Big(\frac{\boldsymbol{x}}{\epsilon},z\Big) = \zeta_o^{-1}\int_{|\boldsymbol{\kappa}|<1}\frac{d(k\boldsymbol{\kappa})}{(2\pi)^2}\beta^{-\frac{1}{2}}(\boldsymbol{\kappa})\Big\{&\big[a^\epsilon(\boldsymbol{\kappa},z)\,\vec{\boldsymbol{u}}^\perp(\boldsymbol{\kappa}) - a^{\epsilon,\perp}(\boldsymbol{\kappa},z)\,\vec{\boldsymbol{u}}(\boldsymbol{\kappa})\big]e^{i\frac{k}{\epsilon}\vec{\boldsymbol{\kappa}}\cdot\vec{\boldsymbol{x}}}\\ &+\big[b^\epsilon(\boldsymbol{\kappa},z)\,\vec{\boldsymbol{u}}^\perp(\boldsymbol{\kappa}) + b^{\epsilon,\perp}(\boldsymbol{\kappa},z)\,\vec{\boldsymbol{u}}^-(\boldsymbol{\kappa})\big]e^{i\frac{k}{\epsilon}\vec{\boldsymbol{\kappa}}^-\cdot\vec{\boldsymbol{x}}}\Big\},\end{aligned} \tag{95}$$

for $\vec{\boldsymbol{x}} = (\boldsymbol{x},z)$. Here we used the wave vectors $\vec{\boldsymbol{\kappa}} = \big(\boldsymbol{\kappa},\beta(\boldsymbol{\kappa})\big)$ and $\vec{\boldsymbol{\kappa}}^- = \big(\boldsymbol{\kappa},-\beta(\boldsymbol{\kappa})\big)$ of the forward and backward going waves, and

$$\vec{\boldsymbol{u}}(\boldsymbol{\kappa}) = \left(\beta(\boldsymbol{\kappa})\frac{\boldsymbol{\kappa}}{|\boldsymbol{\kappa}|},-|\boldsymbol{\kappa}|\right),\qquad \vec{\boldsymbol{u}}^-(\boldsymbol{\kappa}) = \left(\beta(\boldsymbol{\kappa})\frac{\boldsymbol{\kappa}}{|\boldsymbol{\kappa}|},|\boldsymbol{\kappa}|\right),\qquad \vec{\boldsymbol{u}}^\perp(\boldsymbol{\kappa}) = \left(\frac{\boldsymbol{\kappa}^\perp}{|\boldsymbol{\kappa}|},0\right).$$

The triplets $\{\vec{\boldsymbol{u}}(\boldsymbol{\kappa}),\vec{\boldsymbol{u}}^\perp(\boldsymbol{\kappa}),\vec{\boldsymbol{\kappa}}\}$ and $\{\vec{\boldsymbol{u}}^-(\boldsymbol{\kappa}),\vec{\boldsymbol{u}}^\perp(\boldsymbol{\kappa}),\vec{\boldsymbol{\kappa}}^-\}$ are orthonormal bases of $\mathbb{R}^3$, when $|\boldsymbol{\kappa}| < 1$. Thus, (94) and (95) are decompositions in transverse waves, which are orthogonal to the direction of propagation along the wave vectors $\vec{\boldsymbol{\kappa}}$ and $\vec{\boldsymbol{\kappa}}^-$, respectively. The amplitudes $a^\epsilon(\boldsymbol{\kappa},z)$ and $b^\epsilon(\boldsymbol{\kappa},z)$ are for the forward and backward transverse magnetic plane waves, and $a^{\epsilon,\perp}(\boldsymbol{\kappa},z)$ and $b^{\epsilon,\perp}(\boldsymbol{\kappa},z)$ are the amplitudes of transverse electric plane waves. Note that the forward going part, written in dimensional units, is the same as in (13) and (14).

5. The Markov limit

Here we describe the $\epsilon \to 0$ limit of the random mode amplitudes satisfying the two-point linear boundary value problem (73) with boundary conditions (67)–(70). We begin in Section 5.1 by writing the solution in terms of propagator matrices. Then we explain in Section 5.2 why we can neglect the backward and evanescent waves. The limit of the forward going wave amplitudes is given in Section 5.3.

5.1. Propagator matrices

The 4×4 propagator matrices $\mathbf{P}^\epsilon(\boldsymbol{\kappa}, z; \boldsymbol{\kappa}_o)$ are solutions of the initial value problem

$$\frac{\partial \mathbf{P}^\epsilon(\boldsymbol{\kappa}, z; \boldsymbol{\kappa}_o)}{\partial z} = \frac{ik\alpha}{2\gamma^2\epsilon^{1/2}} \int_{|\boldsymbol{\kappa}'|<1} \frac{d(k\boldsymbol{\kappa}')}{(2\pi)^2} \widehat{\nu}\left(\frac{k(\boldsymbol{\kappa}-\boldsymbol{\kappa}')}{\gamma}, \gamma\frac{z}{\epsilon}\right) \mathbf{F}\left(\boldsymbol{\kappa}, \boldsymbol{\kappa}', \frac{z}{\epsilon}\right) \mathbf{P}^\epsilon(\boldsymbol{\kappa}', z; \boldsymbol{\kappa}_o)$$
$$+ \frac{ik\alpha^2}{2\gamma^2} \int_{|\boldsymbol{\kappa}'|<1} \frac{d(k\boldsymbol{\kappa}')}{(2\pi)^2} \widehat{\nu^2}\left(\frac{k(\boldsymbol{\kappa}-\boldsymbol{\kappa}')}{\gamma}, \gamma\frac{z}{\epsilon}\right) \mathbf{G}\left(\boldsymbol{\kappa}, \boldsymbol{\kappa}', \frac{z}{\epsilon}\right) \mathbf{P}^\epsilon(\boldsymbol{\kappa}', z; \boldsymbol{\kappa}_o), \tag{96}$$

with initial condition $\mathbf{P}^\epsilon(\boldsymbol{\kappa}, z=0; \boldsymbol{\kappa}_o) = \delta(\boldsymbol{\kappa}-\boldsymbol{\kappa}_o)\mathbf{I}$, where $\mathbf{I}$ is the 4×4 identity matrix. The solution of (73) satisfies

$$\boldsymbol{Y}^\epsilon(\boldsymbol{\kappa}, z) = \int_{|\boldsymbol{\kappa}_o|<1} d\boldsymbol{\kappa}_o\, \mathbf{P}^\epsilon(\boldsymbol{\kappa}, z; \boldsymbol{\kappa}_o) \boldsymbol{Y}^\epsilon(\boldsymbol{\kappa}_o, 0),$$

for any $z \in [0, L]$. In particular, at $z = L$ and using boundary conditions (67)–(70),

$$\begin{pmatrix} a^\epsilon(\boldsymbol{\kappa}, L) \\ a^{\epsilon,\perp}(\boldsymbol{\kappa}, L) \\ 0 \\ 0 \end{pmatrix} = \int_{|\boldsymbol{\kappa}_o|<1} d\boldsymbol{\kappa}_o\, \mathbf{P}^\epsilon(\boldsymbol{\kappa}, L; \boldsymbol{\kappa}_o) \begin{pmatrix} a_o(\boldsymbol{\kappa}_o) \\ a_o^\perp(\boldsymbol{\kappa}_o) \\ b^\epsilon(\boldsymbol{\kappa}_o, 0) \\ b^{\epsilon,\perp}(\boldsymbol{\kappa}_o, 0) \end{pmatrix}. \tag{97}$$

5.2. The forward scattering approximation

The $\epsilon \to 0$ limit $\mathbf{P}$ of $\mathbf{P}^\epsilon$ can be obtained and identified as a Markov process, meaning that it satisfies a system of stochastic differential equations. We refer to [11,12] and Appendix A for details, and state here the result.

In the limit $\epsilon \to 0$, the terms of order one in (96) i.e., those involving the kernel $\mathbf{G}$, become equal to their average with respect to the distribution of ν and to the rapid $O(1/\epsilon)$ phase. We denote the average with respect to this phase by $\langle\cdot\rangle$, and obtain

$$\frac{ik\alpha^2}{2\gamma^2} \int_{|\boldsymbol{\kappa}'|<1} \frac{d(k\boldsymbol{\kappa}')}{(2\pi)^2} \mathbb{E}\left[\widehat{\nu^2}\left(\frac{k(\boldsymbol{\kappa}-\boldsymbol{\kappa}')}{\gamma}, \cdot\right)\right] \left\langle \mathbf{G}(\boldsymbol{\kappa}, \boldsymbol{\kappa}', \cdot)\right\rangle \mathbf{P}(\boldsymbol{\kappa}', z; \boldsymbol{\kappa}_o)$$
$$= \frac{ik\alpha^2}{2} \mathcal{R}(\mathbf{0}) \left\langle \mathbf{G}(\boldsymbol{\kappa}, \boldsymbol{\kappa}, \cdot)\right\rangle \mathbf{P}(\boldsymbol{\kappa}, z; \boldsymbol{\kappa}_o). \tag{98}$$

Due to the large phases of the off-diagonal blocks in $\mathbf{G}$ we have

$$\langle \mathbf{G}(\boldsymbol{\kappa}, \boldsymbol{\kappa}, \cdot)\rangle = \frac{|\boldsymbol{\kappa}|^2}{\beta(\boldsymbol{\kappa})} \begin{pmatrix} -1 & 0 & 0 & 0 \\ 0 & 0 & 0 & 0 \\ 0 & 0 & 1 & 0 \\ 0 & 0 & 0 & 0 \end{pmatrix},$$

a diagonal matrix, so the order one terms in (96) do not introduce any wave coupling.

The order $O(\epsilon^{-1/2})$ part in (96) i.e., involving $\mathbf{F}$, gives diffusive terms. Let us split the propagator matrix into four blocks:

$$\mathbf{P}^\epsilon = \begin{pmatrix} \mathbf{P}^{aa,\epsilon} & \mathbf{P}^{ab,\epsilon} \\ \mathbf{P}^{ba,\epsilon} & \mathbf{P}^{bb,\epsilon} \end{pmatrix}$$

and consider first only the propagating waves. The stochastic differential equations for the limit entries of $\mathbf{P}^{ab,\epsilon}(\boldsymbol{\kappa}, z; \boldsymbol{\kappa}_o)$ and $\mathbf{P}^{ba,\epsilon}(\boldsymbol{\kappa}, z; \boldsymbol{\kappa}_o)$ are coupled to the limit entries of $\mathbf{P}^{aa,\epsilon}(\boldsymbol{\kappa}, z; \boldsymbol{\kappa}_o)$ and $\mathbf{P}^{bb,\epsilon}(\boldsymbol{\kappa}, z; \boldsymbol{\kappa}_o)$ through the coefficients

$$\int_{\mathbb{R}} dr_z\, \widehat{\mathcal{R}}\left(\frac{k(\boldsymbol{\kappa}-\boldsymbol{\kappa}')}{\gamma}, \gamma r_z\right) e^{-ik\left[\beta(\boldsymbol{\kappa})+\beta(\boldsymbol{\kappa}')\right]r_z} = \int_{\mathbb{R}^3} d\vec{\boldsymbol{r}}\, \mathcal{R}(\gamma\vec{\boldsymbol{r}}) e^{-ik\left[(\boldsymbol{\kappa}-\boldsymbol{\kappa}')\cdot\boldsymbol{r}+(\beta(\boldsymbol{\kappa})+\beta(\boldsymbol{\kappa}'))r_z\right]}$$
$$= \frac{1}{\gamma^3} \widetilde{\mathcal{R}}\left(\frac{k(\vec{\boldsymbol{\kappa}}-\vec{\boldsymbol{\kappa}}'^{-})}{\gamma}\right). \tag{99}$$

Here $\widehat{\mathcal{R}}$ is the Fourier transform of $\mathcal{R}$ with respect to the cross-range variable, and $\widetilde{\mathcal{R}}$ is the three-dimensional Fourier transform (8). The sum $\beta(\boldsymbol{\kappa}) + \beta(\boldsymbol{\kappa}')$ in the phase of (99) is because the phase factors in the matrices $\mathbf{F}^{ab}$ and $\mathbf{F}^{ba}$ are $\pm(\beta(\boldsymbol{\kappa}) + \beta(\boldsymbol{\kappa}'))\zeta$. The coupling between the entries of $\mathbf{P}^{aa,\epsilon}(\boldsymbol{\kappa}', z; \boldsymbol{\kappa}_o)$ and between the entries of $\mathbf{P}^{bb,\epsilon}(\boldsymbol{\kappa}', z; \boldsymbol{\kappa}_o)$ is through the coefficients

$$\int_{\mathbb{R}} dr_z\, \widehat{\mathcal{R}}\left(\frac{k(\boldsymbol{\kappa}-\boldsymbol{\kappa}')}{\gamma}, \gamma r_z\right) e^{-ik\left[\beta(\boldsymbol{\kappa})-\beta(\boldsymbol{\kappa}')\right]r_z} = \int_{\mathbb{R}^3} d\vec{\boldsymbol{r}}\, \mathcal{R}(\gamma\vec{\boldsymbol{r}}) e^{-ik\left[(\boldsymbol{\kappa}-\boldsymbol{\kappa}')\cdot\boldsymbol{r}+(\beta(\boldsymbol{\kappa})-\beta(\boldsymbol{\kappa}'))r_z\right]}$$
$$= \frac{1}{\gamma^3} \widetilde{\mathcal{R}}\left(\frac{k(\vec{\boldsymbol{\kappa}}-\vec{\boldsymbol{\kappa}}')}{\gamma}\right), \tag{100}$$

because the phase factors in matrices $\mathbf{F}^{aa}$ and $\mathbf{F}^{bb}$ are $\pm(\beta(\boldsymbol{\kappa}) - \beta(\boldsymbol{\kappa}'))\zeta$.

We conclude that the interaction of the forward and backward going waves depends on the decay of the power spectral density. Recall that the source gives wave amplitudes supported at $|\boldsymbol{\kappa}| \leq \gamma_J/k < 1$ and $\widetilde{\mathfrak{R}}$ is negligible outside the ball with center at $\mathbf{0}$ and radius one in $\mathbb{R}^3$. From (49) and (57) it is possible to choose some $\kappa_M \in (\gamma_J/k, 1)$ such that γ satisfies

$$\frac{2k\beta(\kappa_M)}{\gamma} > 1. \tag{101}$$

Under these circumstances, for all $\boldsymbol{\kappa}'$ satisfying $|\boldsymbol{\kappa}'| < \kappa_M$, the coupling coefficients (99) vanish, because

$$\frac{k|\vec{\boldsymbol{\kappa}} - \vec{\boldsymbol{\kappa}}'^{-}|}{\gamma} = \frac{k}{\gamma}\left[|\boldsymbol{\kappa} - \boldsymbol{\kappa}'|^2 + \left(\beta(\boldsymbol{\kappa}) + \beta(\boldsymbol{\kappa}')\right)^2\right]^{1/2} \geq \frac{k}{\gamma}\left[\beta(\boldsymbol{\kappa}) + \beta(\boldsymbol{\kappa}')\right] \geq \frac{2k\beta(\kappa_M)}{\gamma} > 1.$$

This means that the forward and backward wave amplitudes are asymptotically decoupled as long as the energy of the wave is supported at the transverse wave vectors $\boldsymbol{\kappa}$ satisfying $|\boldsymbol{\kappa}| \leq \kappa_M$.

Nevertheless, the forward going amplitudes are coupled with each other, because

$$\frac{k|\vec{\boldsymbol{\kappa}} - \vec{\boldsymbol{\kappa}}'|}{\gamma} = \frac{k}{\gamma}\left[|\boldsymbol{\kappa} - \boldsymbol{\kappa}'|^2 + \left(\beta(\boldsymbol{\kappa}) - \beta(\boldsymbol{\kappa}')\right)^2\right]^{1/2}$$

is small for at least a subset of transverse wave vectors satisfying $|\boldsymbol{\kappa}|, |\boldsymbol{\kappa}'| \leq \kappa_M$. Due to this coupling there is diffusion of energy from the waves emitted by the source with $|\boldsymbol{\kappa}| < \gamma_J/k$, to waves at larger values of $|\boldsymbol{\kappa}|$, as explained in Section 8. This is why we take $\kappa_M > \gamma_J/k$ in (101). By assuming that $a^\epsilon(\boldsymbol{\kappa}, z)$ and $a^{\epsilon,\perp}(\boldsymbol{\kappa}, z)$ are supported at $|\boldsymbol{\kappa}| \leq \kappa_M$ we essentially restrict z by Z_M, so that the energy does not diffuse to waves with $|\boldsymbol{\kappa}| > \kappa_M$ for $z \leq Z_M$. Physically, it means that the three-dimensional wave vectors $\vec{\boldsymbol{\kappa}}$ of the forward going waves remain within a cone with opening angle smaller than 180°. We will see that the evolution of the $\boldsymbol{\kappa}$-distribution of the wave energy is described by a radiative transfer equation, which means that the wave energy undergoes a random walk (or diffusion). We will also see that the diffusion coefficient is of the order $\gamma\alpha^2$. Thus, the $\boldsymbol{\kappa}$-distribution of the wave energy reaches κ_M after a propagation distance of the order of Z_M such that $\alpha^2\gamma Z_M = \kappa_M^2$. Recalling the scaling (48) of the standard deviation of the fluctuations and (12), we see that it is possible to choose $Z_M = O(1)$ (i.e., similar to $\bar{L}$ in dimensional units).

The evanescent waves can only couple with the propagating waves with wave vectors of magnitude close to 1. Thus, as long as the energy of the wave is supported at wave vectors satisfying $|\boldsymbol{\kappa}| < \kappa_M$, assumption (101) implies that the evanescent waves do not get excited.

The forward scattering approximation amounts to neglecting all the backward and evanescent waves in the system of stochastic differential equations. It is justified in the limit $\epsilon \to 0$ by the decoupling of the waves, the zero initial condition of the evanescent waves, and the zero condition at $z = L$ of the left going wave amplitudes.

5.3. Markov limit of the forward going mode amplitudes

Under the forward scattering approximation, the wave amplitudes $a^\epsilon(\boldsymbol{\kappa}, z)$ and $a^{\epsilon,\perp}(\boldsymbol{\kappa}, z)$ satisfy the initial value problem

$$\begin{aligned}\frac{\partial}{\partial z}\begin{pmatrix} a^\epsilon(\boldsymbol{\kappa}, z) \\ a^{\epsilon,\perp}(\boldsymbol{\kappa}, z)\end{pmatrix} &= \frac{ik\alpha}{2\gamma^2\epsilon^{1/2}}\int_{|\boldsymbol{\kappa}'|<1}\frac{d(k\boldsymbol{\kappa}')}{(2\pi)^2}\widehat{\nu}\left(\frac{k(\boldsymbol{\kappa}-\boldsymbol{\kappa}')}{\gamma}, \gamma\frac{z}{\epsilon}\right)\mathbf{F}^{aa}\left(\boldsymbol{\kappa}, \boldsymbol{\kappa}', \frac{z}{\epsilon}\right)\begin{pmatrix} a^\epsilon(\boldsymbol{\kappa}', z) \\ a^{\epsilon,\perp}(\boldsymbol{\kappa}', z)\end{pmatrix} \\ &\quad + \frac{ik\alpha^2}{2\gamma^2}\int_{|\boldsymbol{\kappa}'|<1}\frac{d(k\boldsymbol{\kappa}')}{(2\pi)^2}\widehat{\nu^2}\left(\frac{k(\boldsymbol{\kappa}-\boldsymbol{\kappa}')}{\gamma}, \gamma\frac{z}{\epsilon}\right)\mathbf{G}^{aa}\left(\boldsymbol{\kappa}, \boldsymbol{\kappa}', \frac{z}{\epsilon}\right)\begin{pmatrix} a^\epsilon(\boldsymbol{\kappa}', z) \\ a^{\epsilon,\perp}(\boldsymbol{\kappa}', z)\end{pmatrix},\end{aligned} \tag{102}$$

for $z > 0$, and the initial condition

$$\begin{pmatrix} a^\epsilon(\boldsymbol{\kappa}, 0) \\ a^{\epsilon,\perp}(\boldsymbol{\kappa}, 0)\end{pmatrix} = \mathcal{A}_o(\boldsymbol{\kappa}), \tag{103}$$

with $\mathcal{A}_o$ defined in (23). These equations conserve energy, as the special structure of the kernels $\mathbf{F}^{aa}$ and $\mathbf{G}^{aa}$ described in Eqs. (76), (84), and (88) implies that for all $\epsilon > 0$, for all $z \geq 0$,

$$\int_{|\boldsymbol{\kappa}|<1}\frac{d(k\boldsymbol{\kappa})}{(2\pi)^2}\left[|a^\epsilon(\boldsymbol{\kappa}, z)|^2 + |a^{\epsilon,\perp}(\boldsymbol{\kappa}, z)|^2\right] = \int_{|\boldsymbol{\kappa}|<1}\frac{d(k\boldsymbol{\kappa})}{(2\pi)^2}\left[|a_o(\boldsymbol{\kappa})|^2 + |a_o^\perp(\boldsymbol{\kappa})|^2\right]. \tag{104}$$

We refer to Appendix A for the details on the Markov limit $\epsilon \to 0$. In particular, we explain there that the process

$$\boldsymbol{X}^\epsilon(z) = \begin{pmatrix} \mathrm{Re}\left(a^\epsilon(\boldsymbol{\kappa}, z)\right) \\ \mathrm{Im}\left(a^\epsilon(\boldsymbol{\kappa}, z)\right) \\ \mathrm{Re}\left(a^{\epsilon,\perp}(\boldsymbol{\kappa}, z)\right) \\ \mathrm{Im}\left(a^{\epsilon,\perp}(\boldsymbol{\kappa}, z)\right)\end{pmatrix}_{\boldsymbol{\kappa}\in\mathcal{O}}, \quad \text{for } \mathcal{O} = \left\{\boldsymbol{\kappa} \in \mathbb{R}^2,\ |\boldsymbol{\kappa}| < 1\right\},$$

converges weakly in $\mathcal{C}([0,L],\mathcal{D}')$ to a Markov process $\boldsymbol{X}(z)$, where $\mathcal{D}'$ is the space of distributions, dual to the space $\mathcal{D}(\mathcal{O},\mathbb{R}^4)$ of infinitely differentiable vector valued functions in $\mathbb{R}^4$, with compact support. The generator of $\boldsymbol{X}(z)$ is given in Appendix A, and we denote henceforth the limit amplitudes by $a(\boldsymbol{\kappa},z)$ and $a^{\perp}(\boldsymbol{\kappa},z)$. Their first and second moments are described in the next two sections and are summarized in Section 2.4.

6. The coherent field

The vector

$$\mathcal{A}(\boldsymbol{\kappa},z)=\begin{pmatrix}\mathbb{E}[a(\boldsymbol{\kappa},z)]\\ \mathbb{E}[a^{\perp}(\boldsymbol{\kappa},z)]\end{pmatrix}=\lim_{\epsilon\to 0}\mathbb{E}\left[\begin{pmatrix}a^{\epsilon}(\boldsymbol{\kappa},z)\\ a^{\epsilon,\perp}(\boldsymbol{\kappa},z)\end{pmatrix}\right], \tag{105}$$

whose components are the expectations of the limit amplitudes of the modes at wave vector $\vec{\boldsymbol{\kappa}}$, satisfies as explained in Appendix A the initial value problem

$$\partial_z\mathcal{A}(\boldsymbol{\kappa},z)=\mathbf{Q}(\boldsymbol{\kappa})\mathcal{A}(\boldsymbol{\kappa},z),\quad z>0, \tag{106}$$

with initial condition $\mathcal{A}(\boldsymbol{\kappa},0)=\mathcal{A}_o(\boldsymbol{\kappa})$, and 2×2 complex matrix $\mathbf{Q}(\boldsymbol{\kappa})$ given by

$$\begin{aligned}\mathbf{Q}(\boldsymbol{\kappa})=&-\frac{k^2\alpha^2}{4\gamma^3}\int_{|\boldsymbol{\kappa}'|<1}\frac{d(k\boldsymbol{\kappa}')}{(2\pi)^2}\boldsymbol{\Gamma}(\boldsymbol{\kappa},\boldsymbol{\kappa}')\boldsymbol{\Gamma}(\boldsymbol{\kappa}',\boldsymbol{\kappa})\int_0^{\infty}d\zeta\,\widehat{\mathcal{R}}\left(\frac{k(\boldsymbol{\kappa}-\boldsymbol{\kappa}')}{\gamma},\zeta\right)e^{-i\frac{k}{\gamma}\left(\beta(\boldsymbol{\kappa})-\beta(\boldsymbol{\kappa}')\right)\zeta}\\ &-\frac{ik\alpha^2}{2}\mathcal{R}(\mathbf{0})\frac{|\boldsymbol{\kappa}|^2}{\beta(\boldsymbol{\kappa})}\begin{pmatrix}1&0\\0&0\end{pmatrix}.\end{aligned} \tag{107}$$

In dimensional units this is the same as (25), with $\boldsymbol{\Gamma}$ given by (26), which equals $\boldsymbol{\Gamma}^{aa}$ defined in (80).

As stated in Section 2.4.1, the real part of $\mathbf{Q}(\boldsymbol{\kappa})$ is a symmetric, negative definite matrix

$$\mathrm{Re}[\mathbf{Q}(\boldsymbol{\kappa})]=-\frac{k^2\alpha^2}{8\gamma^3}\int_{|\boldsymbol{\kappa}'|<1}\frac{d(k\boldsymbol{\kappa}')}{(2\pi)^2}\widetilde{\mathcal{R}}\left(\frac{k(\vec{\boldsymbol{\kappa}}-\vec{\boldsymbol{\kappa}}')}{\gamma}\right)\boldsymbol{\Gamma}(\boldsymbol{\kappa},\boldsymbol{\kappa}')\boldsymbol{\Gamma}(\boldsymbol{\kappa}',\boldsymbol{\kappa}), \tag{108}$$

because $\widetilde{\mathcal{R}}$ is non-negative and $\boldsymbol{\Gamma}(\boldsymbol{\kappa}',\boldsymbol{\kappa})=\boldsymbol{\Gamma}(\boldsymbol{\kappa},\boldsymbol{\kappa}')^T$. It is an effective diffusion term in (106), which removes energy from the mean field and gives it to the incoherent fluctuations. This causes the randomization or loss of coherence of the waves. The imaginary part of $\mathbf{Q}(\boldsymbol{\kappa})$ is the sum of two terms. The first, given by

$$\frac{k^2\alpha^2}{4\gamma^3}\int_{|\boldsymbol{\kappa}'|<1}\frac{d(k\boldsymbol{\kappa}')}{(2\pi)^2}\int_0^{\infty}d\zeta\,\widehat{\mathcal{R}}\left(\frac{k(\boldsymbol{\kappa}-\boldsymbol{\kappa}')}{\gamma},\zeta\right)\sin\left[\frac{k}{\gamma}\big(\beta(\boldsymbol{\kappa})-\beta(\boldsymbol{\kappa}')\big)\zeta\right]\boldsymbol{\Gamma}(\boldsymbol{\kappa},\boldsymbol{\kappa}')\boldsymbol{\Gamma}(\boldsymbol{\kappa}',\boldsymbol{\kappa}),$$

is an effective dispersion term, which does not remove energy from the mean field and ensures causality.[1] The second term in (107) is a homogenization effect due to the $\widehat{\nu^2}$ part in (102). It accounts for the slightly different velocities of the transverse electric and transverse magnetic waves, with discrepancy of the order of $O(\epsilon)$.

7. The transport equation

To describe the transport of energy, we study the z-evolution of the Hermitian positive definite coherence matrix

$$\mathcal{P}(\boldsymbol{\kappa},z)=\lim_{\epsilon\to 0}\mathbb{E}\left[\begin{pmatrix}a^{\epsilon}(\boldsymbol{\kappa},z)\\ a^{\epsilon,\perp}(\boldsymbol{\kappa},z)\end{pmatrix}\begin{pmatrix}a^{\epsilon}(\boldsymbol{\kappa},z)\\ a^{\epsilon,\perp}(\boldsymbol{\kappa},z)\end{pmatrix}^{\dagger}\right]. \tag{109}$$

The diagonal entries of $\mathcal{P}$ are the mode powers. The evolution equation is derived as explained in Appendix A,

$$\begin{aligned}\partial_z\mathcal{P}(\boldsymbol{\kappa},z)=&\,\mathbf{Q}(\boldsymbol{\kappa})\mathcal{P}(\boldsymbol{\kappa},z)+\mathcal{P}(\boldsymbol{\kappa},z)\mathbf{Q}(\boldsymbol{\kappa})^{\dagger}\\ &+\frac{k^2\alpha^2}{4\gamma^3}\int_{|\boldsymbol{\kappa}'|<1}\frac{d(k\boldsymbol{\kappa}')}{(2\pi)^2}\boldsymbol{\Gamma}(\boldsymbol{\kappa},\boldsymbol{\kappa}')\mathcal{P}(\boldsymbol{\kappa}',z)\boldsymbol{\Gamma}(\boldsymbol{\kappa}',\boldsymbol{\kappa})\widetilde{\mathcal{R}}\left(\frac{k(\vec{\boldsymbol{\kappa}}-\vec{\boldsymbol{\kappa}}')}{\gamma}\right),\end{aligned} \tag{110}$$

for $z>0$, with initial condition $\mathcal{P}(\boldsymbol{\kappa},0)=\mathcal{A}_o(\boldsymbol{\kappa})\mathcal{A}_o(\boldsymbol{\kappa})^{\dagger}$. In dimensional units this is the same as (36).

We have from (104) that

$$\int_{|\boldsymbol{\kappa}|<1}\frac{d(k\boldsymbol{\kappa})}{(2\pi)^2}\Big[\mathbb{E}\big[|a^{\epsilon}(\boldsymbol{\kappa},z)|^2\big]+\mathbb{E}\big[|a^{\epsilon,\perp}(\boldsymbol{\kappa},z)|^2\big]\Big]=\int_{|\boldsymbol{\kappa}|<1}\frac{d(k\boldsymbol{\kappa})}{(2\pi)^2}\Big[|a_o(\boldsymbol{\kappa})|^2+|a_o^{\perp}(\boldsymbol{\kappa})|^2\Big],$$

[1] If we write the coherent wave fields in the time domain, using the inverse Fourier transform with respect to the frequency ω, we obtain a causal result.

for all $z > 0$ and $0 < \epsilon \ll 1$, so energy conservation must hold in the limit $\epsilon \to 0$. This is derived from (110) using the commutation properties of the trace, as stated in (37).

By studying the second moments of the wave amplitudes, we can also quantify the decorrelation of the waves due to scattering in the random medium. The calculation of these moments uses the generator in Appendix A and the result is that the wave amplitudes at different transverse wave vectors $\boldsymbol{\kappa} \neq \boldsymbol{\kappa}'$ are decorrelated

$$\lim_{\epsilon\to 0} \mathbb{E}\left[\begin{pmatrix} a^{\epsilon}(\boldsymbol{\kappa}, z) \\ a^{\epsilon,\perp}(\boldsymbol{\kappa}, z)\end{pmatrix}\begin{pmatrix} a^{\epsilon}(\boldsymbol{\kappa}', z) \\ a^{\epsilon,\perp}(\boldsymbol{\kappa}', z)\end{pmatrix}^{\dagger}\right] = \mathcal{A}(\boldsymbol{\kappa}, z)\mathcal{A}(\boldsymbol{\kappa}', z)^{\dagger}.$$

Intuitively, this is because these waves travel in different directions and see a different region of the random medium. It is only when $|\boldsymbol{\kappa} - \boldsymbol{\kappa}'| = O(\epsilon)$ that the waves are correlated, and we can calculate the energy density (Wigner transform)

$$\mathcal{W}(\boldsymbol{\kappa}, \boldsymbol{x}, z) = \lim_{\epsilon\to 0} \int \frac{d(k\boldsymbol{q})}{(2\pi)^2} \exp\Big[ik\boldsymbol{q}\cdot\big(\nabla\beta(\boldsymbol{\kappa})z + \boldsymbol{x}\big)\Big]\mathbb{E}\left[\begin{pmatrix} a^{\epsilon}\big(\boldsymbol{\kappa} + \frac{\epsilon\boldsymbol{q}}{2}, z\big) \\ a^{\epsilon,\perp}\big(\boldsymbol{\kappa} + \frac{\epsilon\boldsymbol{q}}{2}, z\big)\end{pmatrix}\begin{pmatrix} a^{\epsilon}\big(\boldsymbol{\kappa} - \frac{\epsilon\boldsymbol{q}}{2}, z\big) \\ a^{\epsilon,\perp}\big(\boldsymbol{\kappa} - \frac{\epsilon\boldsymbol{q}}{2}, z\big)\end{pmatrix}^{\dagger}\right]. \tag{111}$$

It satisfies the transport equation

$$\begin{aligned}\partial_z \mathcal{W}(\boldsymbol{\kappa}, \boldsymbol{x}, z) - \nabla\beta(\boldsymbol{\kappa})\cdot\nabla_{\boldsymbol{x}}\mathcal{W}(\boldsymbol{\kappa}, \boldsymbol{x}, z) &= \mathbf{Q}(\boldsymbol{\kappa})\mathcal{W}(\boldsymbol{\kappa}, \boldsymbol{x}, z) + \mathcal{W}(\boldsymbol{\kappa}, \boldsymbol{x}, z)\mathbf{Q}(\boldsymbol{\kappa})^{\dagger} \\ &+ \frac{k^2\alpha^2}{4\gamma^3}\int_{|\boldsymbol{\kappa}'|<1} \frac{d(k\boldsymbol{\kappa}')}{(2\pi)^2}\,\mathbf{\Gamma}(\boldsymbol{\kappa}, \boldsymbol{\kappa}')\mathcal{W}(\boldsymbol{\kappa}', \boldsymbol{x}, z)\mathbf{\Gamma}(\boldsymbol{\kappa}', \boldsymbol{\kappa})\widetilde{\mathcal{R}}\left(\frac{k(\vec{\boldsymbol{\kappa}} - \vec{\boldsymbol{\kappa}}')}{\gamma}\right),\end{aligned} \tag{112}$$

for $z > 0$. In dimensional units this is the same as (34). When the initial condition is smooth, we have from (111) that

$$\mathcal{W}(\boldsymbol{\kappa}, \boldsymbol{x}, 0) = \delta(\boldsymbol{x})\mathcal{A}_o(\boldsymbol{\kappa})\mathcal{A}_o(\boldsymbol{\kappa})^{\dagger}, \tag{113}$$

and therefore at $z > 0$

$$\mathcal{W}(\boldsymbol{\kappa}, \boldsymbol{x}, z) = \delta\left(\boldsymbol{x} + \nabla\beta(\boldsymbol{\kappa})z\right)\mathcal{P}(\boldsymbol{\kappa}, z), \tag{114}$$

so energy is transported on the characteristic

$$\boldsymbol{x} = -\nabla\beta(\boldsymbol{\kappa})z = \frac{\boldsymbol{\kappa}}{\beta(\boldsymbol{\kappa})}z.$$

Remark 2. It can also be shown, with an analysis similar to that in Appendix A, that the waves decorrelate over frequency offsets larger than ϵ. Thus, one can study the energy density resolved over both time and space i.e., the space–time Wigner transform. We do not consider this here, as we limit our study to a single frequency.

8. Illustration of the scattering effects in statistically isotropic media

In this section we give numerical illustrations of the net scattering effects in isotropic media. We already stated that in transverse isotropic media, where $\mathcal{R}$ depends only on $|\boldsymbol{x}|$ and z, the matrix $\mathbf{Q}(\boldsymbol{\kappa})$ defined in (107) is diagonal, and depends only on $|\boldsymbol{\kappa}|$. We also defined in (28) the scattering mean free paths $\mathcal{S}(\boldsymbol{\kappa})$ and $\mathcal{S}^{\perp}(\boldsymbol{\kappa})$, which depend only on $|\boldsymbol{\kappa}|$. The illustrations in this section are for statistically isotropic media, where $\mathcal{R}(\vec{\boldsymbol{x}}) = \mathcal{R}_{\text{iso}}(|\vec{\boldsymbol{x}}|)$ and as shown in Appendix B, the real part of matrix $\mathbf{Q}(\boldsymbol{\kappa})$ is a multiple of the identity. Therefore $\mathcal{S}(\boldsymbol{\kappa}) = \mathcal{S}^{\perp}(\boldsymbol{\kappa})$, meaning that both components of the waves lose coherence on the same $|\boldsymbol{\kappa}|$-dependent range scale.

In Fig. 2 we plot the scattering mean free paths for a Gaussian autocorrelation $\mathcal{R}(\vec{\boldsymbol{x}}) = \exp(-|\vec{\boldsymbol{x}}|^2/2)$, and for three different values of $\gamma = \lambda/\ell$ equal to $2\pi/50, 2\pi/17$ and $2\pi/10$. We observe that the scattering mean free paths decrease with γ, meaning that higher frequency waves lose coherence faster. The scattering mean free paths also decrease monotonically with $|\boldsymbol{\kappa}|$. We may understand this intuitively by noting that at a given range z, the length of the path of the waves with transverse vector $|\boldsymbol{\kappa}|$ is $z/\beta(\boldsymbol{\kappa})$. This increases with $|\boldsymbol{\kappa}|$, and the waves lose coherence faster because they travel a longer distance in the random medium. The monotonicity of the scattering mean free paths can also be seen clearly in Section 9.1, where we study the high-frequency limit $\gamma \to 0$.

To illustrate the evolution of the coherence matrix $\mathcal{P}(\boldsymbol{\kappa}, z)$, satisfying the evolution equation (110), we consider first the case of isotropic initial conditions, where $\mathcal{A}_o(\boldsymbol{\kappa})$ depends only on $|\boldsymbol{\kappa}|$, and we excite either the transverse magnetic or electric waves. From (63) we see that this corresponds to a current source with $\widehat{J}_z = 0$ and $\widehat{\boldsymbol{J}}$ along $\boldsymbol{\kappa}$ or $\boldsymbol{\kappa}^{\perp}$. In the spatial coordinates, the latter means that $\boldsymbol{J}$ is the gradient or the perpendicular gradient of a scalar valued function. When the initial conditions are isotropic, the diagonal and off-diagonal terms of the coherence matrix $\mathcal{P}(\boldsymbol{\kappa}, z)$ decouple. Indeed, there is no coupling in the first two terms of Eq. (110), because $\mathbf{Q}(\boldsymbol{\kappa})$ is diagonal. The integral in (110) can be analyzed with a Picard iteration. For each iterate we obtain by explicit calculation, using integration in polar coordinates, that the coupling terms of the kernel

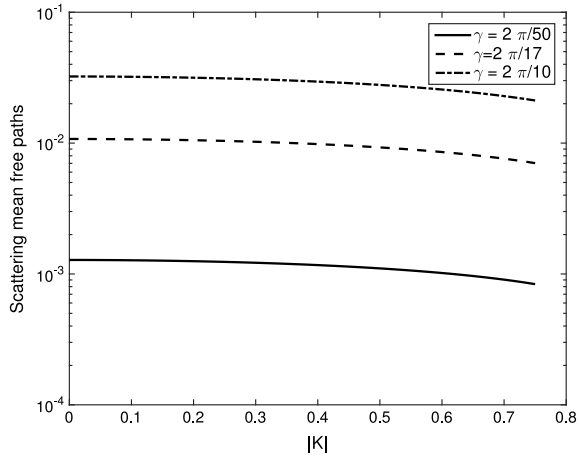

Fig. 2. Illustration of the scattering mean free paths in an isotropic medium with Gaussian autocorrelation, for three different values of $\gamma = \lambda/\ell$, as indicated in the legend. The abscissa is the magnitude $|\boldsymbol{\kappa}|$ of the transverse wave number.

vanish, and that the result preserves the isotropic dependence on $\boldsymbol{\kappa}$. We obtain two autonomous systems of equations for the power vector

$$\begin{pmatrix} \mathcal{P}_{11}(\boldsymbol{\kappa}, z) \\ \mathcal{P}_{22}(\boldsymbol{\kappa}, z) \end{pmatrix} = \lim_{\epsilon \to 0} \begin{pmatrix} \mathbb{E}\left[|a^{\epsilon}(\boldsymbol{\kappa}, z)|^2\right] \\ \mathbb{E}\left[|a^{\epsilon,\perp}(\boldsymbol{\kappa}, z)|^2\right] \end{pmatrix}, \tag{115}$$

and the off-diagonal terms

$$\mathcal{P}_{12}(\boldsymbol{\kappa}, z) = \lim_{\epsilon \to 0} \mathbb{E}\left[a^{\epsilon}(\boldsymbol{\kappa}, z)\overline{a^{\epsilon,\perp}(\boldsymbol{\kappa}, z)}\right]. \tag{116}$$

This means in particular that if the wave is transverse electric or magnetic initially, so that $\mathcal{P}_{12}(\boldsymbol{\kappa}, 0) = 0$, the coherence matrix $\mathcal{P}(\boldsymbol{\kappa}, z)$ remains diagonal for all z.

We illustrate the transfer of power between the modes due to scattering by displaying in Fig. 3 the z-evolution of the power vector (115) for the initial condition

$$\begin{pmatrix} \mathcal{P}_{11}(\boldsymbol{\kappa}, z) \\ \mathcal{P}_{22}(\boldsymbol{\kappa}, z) \end{pmatrix} = \begin{pmatrix} |a_o(\boldsymbol{\kappa})|^2 \\ |a_o^{\perp}(\boldsymbol{\kappa})|^2 \end{pmatrix}, \quad |a_o(\boldsymbol{\kappa})|^2 = \exp\left(-\frac{|\boldsymbol{\kappa}|^2}{2\gamma_J^2}\right), \; a_o^{\perp}(\boldsymbol{\kappa}) = 0.$$

The electromagnetic plane wave at wave vector $\vec{\boldsymbol{\kappa}}$ is transverse magnetic initially and we have in terms of the Stokes vector defined in (18)

$$\mathfrak{S}(\boldsymbol{\kappa}, 0) = \exp\left(-\frac{|\boldsymbol{\kappa}|^2}{2\gamma_J^2}\right)(1, 1, 0, 0)\,.$$

In Fig. 3 we show the results for $\gamma = 2\pi/10$, $\gamma_J = \gamma$ and $\gamma_J = 3.5\gamma$. We plot $\mathcal{P}_{11}$ and $\mathcal{P}_{22}$ as functions of $|\boldsymbol{\kappa}|$, for $z = 0$, $z = 2 \times 10^{-3}$ and $z = 5 \times 10^{-3}$. Note from Fig. 2 that the scattering mean free paths at $\boldsymbol{\kappa} = 0$ are approximately 1.3×10^{-3}. Thus, in the last line of the plots in Fig. 3 the waves have traveled approximately five scattering mean free paths. We observe from the figure that energy from the transverse magnetic waves, which are the only ones excited initially, is transmitted to the transverse electric modes. This energy transfer is faster at smaller $|\boldsymbol{\kappa}|$, so the modes have equal power at five scattering mean free paths in the case $\gamma_J = \gamma$, whereas for $\gamma_J = 3.5\gamma$, the transverse magnetic modes still carry more energy. Recalling the Stokes vector (18), we note that when the transverse electric and magnetic waves have equal power, we have $\mathfrak{S}(\boldsymbol{\kappa}, z) = 2\mathcal{P}_{11}(\boldsymbol{\kappa}, z)\,(1, 0, 0, 0)$ since $\mathcal{P}_{12} = 0$ in the simulation, and the electromagnetic plane wave at wave vector $\vec{\boldsymbol{\kappa}}$ is unpolarized. Aside from the transfer of energy between the transverse electric and magnetic components of the waves, we note in Fig. 3 the diffusion of energy at higher $|\boldsymbol{\kappa}|$. For example, in the case of $\gamma_J = \gamma$, the support of the energy is at $|\boldsymbol{\kappa}| < 0.1$ initially (top left plot) but it extends to $|\boldsymbol{\kappa}| < 0.2$ at five scattering mean free paths (bottom left plot).

Fig. 4 is another illustration of the effect of the initial conditions on the power exchange between the modes. We consider there, in addition to $\gamma_J = \gamma$ and 3.5γ, the case of an even larger γ_J, equal to 7γ. We plot in Fig. 4 the coefficient of power distribution $C_{\mathcal{P}}(z)$, calculated as the difference of the mode powers, normalized by the total power, which is constant in z,

$$C_{\mathcal{P}}(z) = \frac{\int_{|\boldsymbol{\kappa}|<1} d\boldsymbol{\kappa}\left[\mathcal{P}_{11}(\boldsymbol{\kappa}, z) - \mathcal{P}_{22}(\boldsymbol{\kappa}, z)\right]}{\int_{|\boldsymbol{\kappa}|<1} d\boldsymbol{\kappa}\left[\mathcal{P}_{11}(\boldsymbol{\kappa}, z) + \mathcal{P}_{22}(\boldsymbol{\kappa}, z)\right]}. \tag{117}$$

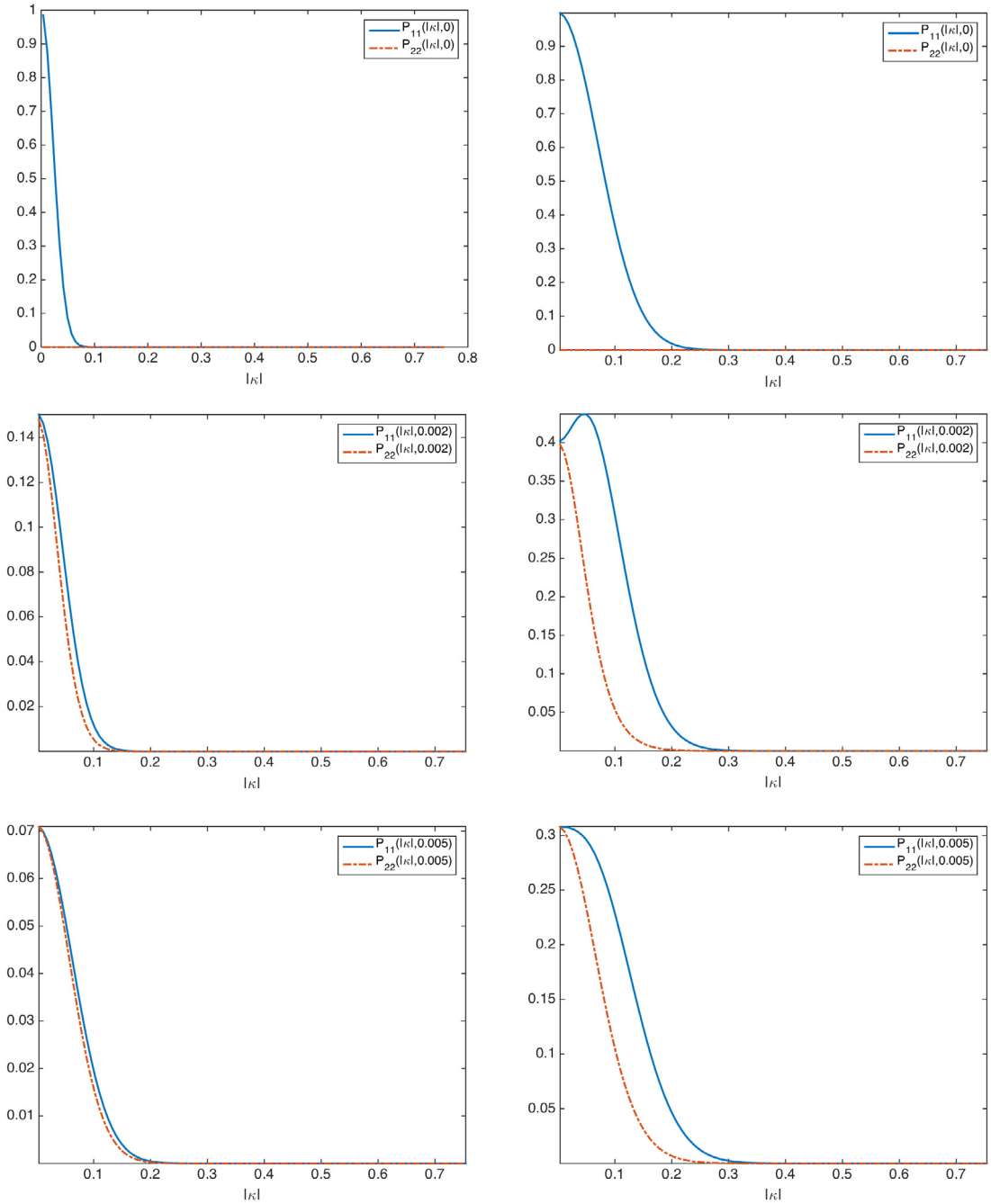

Fig. 3. Display of $\mathcal{P}_{11}(\boldsymbol{\kappa}, z)$ (full blue line) and $\mathcal{P}_{22}(\boldsymbol{\kappa}, z)$ (dashed red line) as a function of $|\boldsymbol{\kappa}|$, for three different values of z: Top line is for $z = 0$, middle line is for $z = 2 \times 10^{-3}$ and the bottom line for $z = 5 \times 10^{-3}$. We take $\gamma = 2\pi/50$, $\gamma_J = \gamma$ in the left column and $\gamma_J = 3.5\gamma$ in the right column. (For interpretation of the references to colour in this figure legend, the reader is referred to the web version of this article.)

Consistent with the left bottom plot in Fig. 3, $C_{\mathcal{P}}$ is almost zero at $z = 5 \times 10^{-3}$ for $\gamma_J = \gamma$. However, when $\gamma_J = 7\gamma$ i.e., when the diameter X of the source is 7 times smaller and the opening angle of the emitted wave cone is 7 times larger, $C_{\mathcal{P}}$ is still large, so the waves still remember the initial excitation. We terminate the plot for $\gamma_J = 7\gamma$ at $z < 0.04$, where the opening angle of the cone comes close to 180° and the evanescent waves start to get excited.

The results in Fig. 5 display the z-evolution of the entries $\mathcal{P}_{jl}(\boldsymbol{\kappa}, z)$ of the coherence matrix, for the anisotropic initial condition

$$|a_o(\boldsymbol{\kappa})|^2 = \exp\left[-\frac{1}{2}\left(\frac{\kappa_1 - \kappa_2}{0.03}\right)^2 - \frac{1}{2}\left(\frac{\kappa_1 + \kappa_2}{0.1}\right)^2\right], \quad a_o^{\perp}(\boldsymbol{\kappa}) = 0.$$

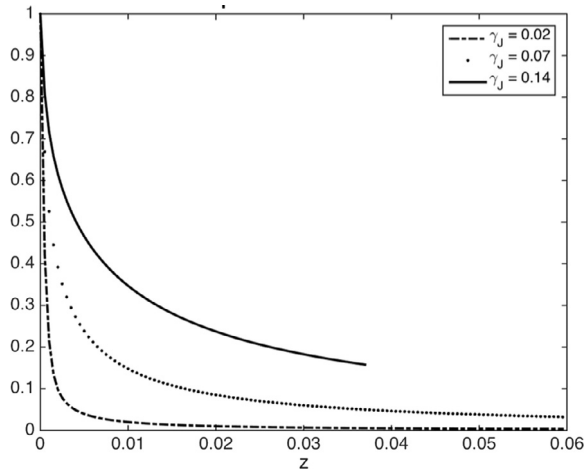

Fig. 4. Plot of the coefficient of power distribution $C_{\mathcal{P}}(z)$. At $z = 0$ there is power only in the transverse magnetic mode. As z grows the other mode gains power, and eventually the energy becomes equally distributed between the modes.

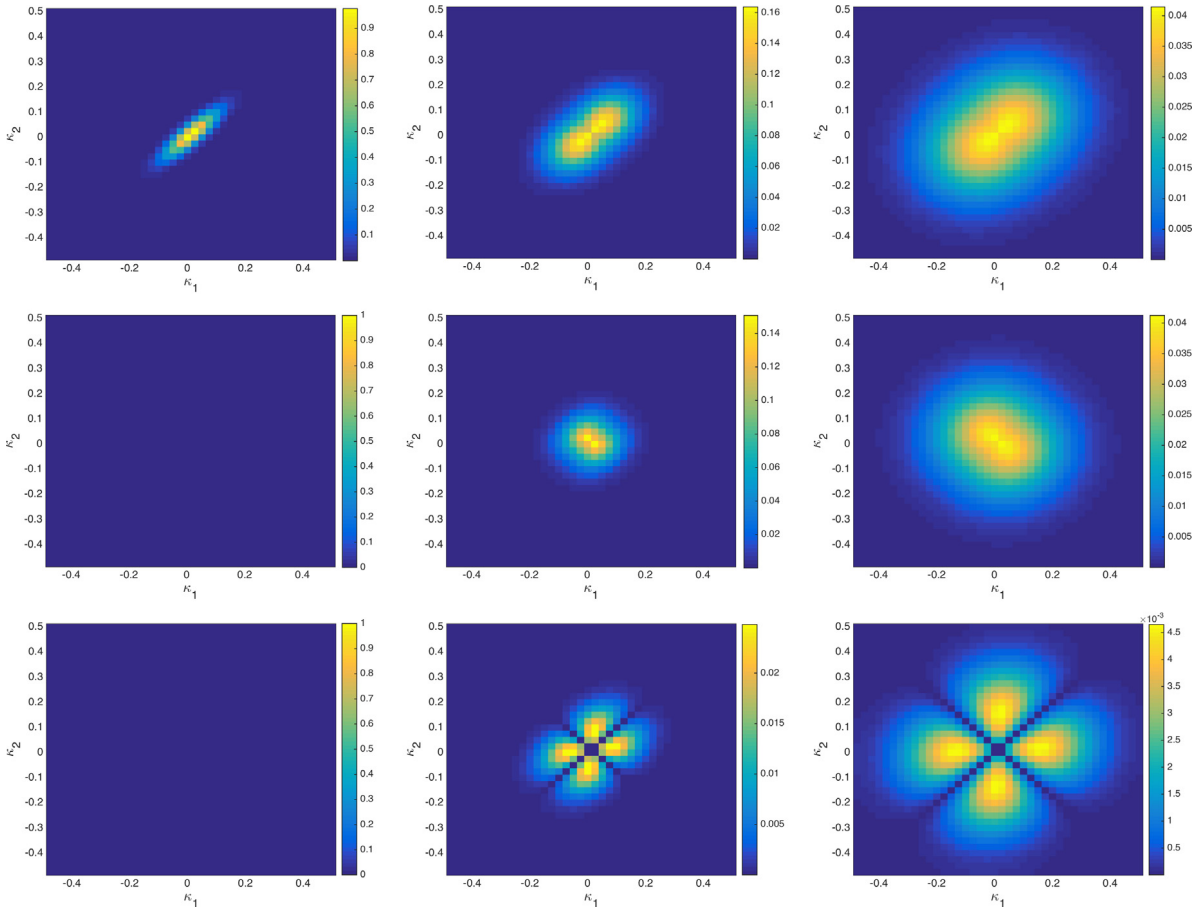

Fig. 5. Display of $\mathcal{P}_{11}(\boldsymbol{\kappa}, z)$ (top line), $\mathcal{P}_{22}(\boldsymbol{\kappa}, z)$ (middle line) and $|\mathcal{P}_{12}(\boldsymbol{\kappa}, z)|$ (bottom line) as a function of $\boldsymbol{\kappa} = (\kappa_1, \kappa_2)$, for $\gamma = 2\pi/50$ and three different values of z: Left column $z = 0$, middle column $z = 5 \times 10^{-3}$ and right column $z = 2.5 \times 10^{-2}$.

Again, we observe the transfer of energy from the transverse magnetic components to the transverse electric ones, which is more efficient at $|\boldsymbol{\kappa}| \approx 0$. We also note the diffusion of energy to waves with larger wave vectors, which means physically that the focused (beam-like) field emitted by the source spreads out as it propagates along z. The off-diagonal components

of the coherence matrix are no longer zero, due to the anisotropic initial condition. However, the solution approaches an isotropic one as z grows, and the off-diagonal components decay.

9. High-frequency analysis

In this section we analyze in detail the net scattering effects of the random medium by considering the high-frequency limit $\gamma \to 0$. We begin with the quantification of the scattering mean free paths and then analyze the coherence matrix.

9.1. Scattering mean free paths

In transverse isotropic random media the matrix $\mathbf{Q}(\boldsymbol{\kappa})$ is diagonal. We are interested in its real part which defines the scattering mean free paths (28). We have

$$\mathrm{Re}\big[\mathrm{Q}_{11}(\boldsymbol{\kappa})\big] = -\frac{k^2\alpha^2}{8\gamma^3}\int_{|\boldsymbol{\kappa}'|<1}\frac{d(k\boldsymbol{\kappa}')}{(2\pi)^2}\widetilde{\mathcal{R}}\left(\frac{k(\vec{\boldsymbol{\kappa}}-\vec{\boldsymbol{\kappa}}')}{\gamma}\right)\Big[\Gamma_{11}^2(\boldsymbol{\kappa}',\boldsymbol{\kappa})+\Gamma_{21}^2(\boldsymbol{\kappa}',\boldsymbol{\kappa})\Big], \tag{118}$$

and

$$\mathrm{Re}\big[\mathrm{Q}_{22}(\boldsymbol{\kappa})\big] = -\frac{k^2\alpha^2}{8\gamma^3}\int_{|\boldsymbol{\kappa}'|<1}\frac{d(k\boldsymbol{\kappa}')}{(2\pi)^2}\widetilde{\mathcal{R}}\left(\frac{k(\vec{\boldsymbol{\kappa}}-\vec{\boldsymbol{\kappa}}')}{\gamma}\right)\Big[\Gamma_{22}^2(\boldsymbol{\kappa}',\boldsymbol{\kappa})+\Gamma_{12}^2(\boldsymbol{\kappa}',\boldsymbol{\kappa})\Big], \tag{119}$$

where we recall that $\vec{\boldsymbol{\kappa}}-\vec{\boldsymbol{\kappa}}' = \big(\boldsymbol{\kappa}-\boldsymbol{\kappa}', \beta(\boldsymbol{\kappa})-\beta(\boldsymbol{\kappa}')\big)$. Let us change variables $\boldsymbol{\kappa}' = \boldsymbol{\kappa}-\gamma\boldsymbol{u}$, and expand in powers of γ

$$\beta(\boldsymbol{\kappa})-\beta(\boldsymbol{\kappa}-\gamma\boldsymbol{u}) = \gamma\boldsymbol{u}\cdot\nabla\beta(\boldsymbol{\kappa})+O(\gamma^2) = -\gamma\frac{\boldsymbol{u}\cdot\boldsymbol{\kappa}}{\beta(\boldsymbol{\kappa})}+O(\gamma^2). \tag{120}$$

For the diagonal entries of $\boldsymbol{\Gamma}$ we have

$$\Gamma_{jj}(\boldsymbol{\kappa}-\gamma\boldsymbol{u},\boldsymbol{\kappa}) = \frac{1}{\beta(\boldsymbol{\kappa})}-\gamma\frac{\boldsymbol{u}\cdot\boldsymbol{\kappa}}{2\beta^3(\boldsymbol{\kappa})}+O(\gamma^2), \quad j=1,2, \tag{121}$$

and for the off-diagonal ones

$$\Gamma_{21}(\boldsymbol{\kappa}-\gamma\boldsymbol{u},\boldsymbol{\kappa}) = \gamma\frac{\boldsymbol{u}\cdot\boldsymbol{\kappa}^{\perp}}{|\boldsymbol{\kappa}||\boldsymbol{\kappa}-\gamma\boldsymbol{u}|}+O(\gamma^2), \tag{122}$$

and similar for Γ_{12}, with a negative sign. Substituting into (118)–(119) and then into the definition (28) of the scattering mean free paths, we obtain using the identity

$$\begin{aligned}\int_{\mathbb{R}^2} d\boldsymbol{u}\,\widetilde{\mathcal{R}}\big(k\boldsymbol{u}, k\boldsymbol{u}\cdot\nabla\beta(\boldsymbol{\kappa})\big) &= \int_{\mathbb{R}^2} d\boldsymbol{u}\int_{\mathbb{R}^2} d\boldsymbol{r}\int_{-\infty}^{\infty} d\zeta\,\mathcal{R}(\boldsymbol{r},\zeta)e^{-ik(\boldsymbol{r},\zeta)\cdot(\boldsymbol{u},\boldsymbol{u}\cdot\nabla\beta(\boldsymbol{\kappa}))}\\ &= \int_{\mathbb{R}^2} d\boldsymbol{r}\int_{-\infty}^{\infty} d\zeta\,\mathcal{R}(\boldsymbol{r},\zeta)(2\pi)^2\delta\big[k\big(\boldsymbol{r}+\zeta\nabla\beta(\boldsymbol{\kappa})\big)\big]\\ &= \frac{(2\pi)^2}{k^2}\int_{-\infty}^{\infty} d\zeta\,\mathcal{R}\left(\frac{\boldsymbol{\kappa}\zeta}{\beta(\boldsymbol{\kappa})},\zeta\right),\end{aligned}$$

that

$$\mathcal{S}(\boldsymbol{\kappa}) = \frac{\gamma}{k^2}\frac{8\beta^2(\boldsymbol{\kappa})}{\alpha^2\int_{-\infty}^{\infty} d\zeta\,\mathcal{R}\left(\frac{\boldsymbol{\kappa}\zeta}{\beta(\boldsymbol{\kappa})},\zeta\right)}+O(\gamma^2), \qquad \mathcal{S}^{\perp}(\boldsymbol{\kappa})-\mathcal{S}(\boldsymbol{\kappa}) = O(\gamma^2). \tag{123}$$

This result shows that when $\gamma \ll 1$, the scattering mean free paths are almost the same. They are proportional to γ and decrease as the negative power of 2 with the frequency i.e., the wave number k. That the waves at higher frequency lose coherence faster, is expected, as observed in Fig. 2.

Remark 3. If $\mathcal{R}(\vec{\boldsymbol{x}})$ depends only on $|\vec{\boldsymbol{x}}|$, i.e. $\mathcal{R}(\vec{\boldsymbol{x}}) = \mathcal{R}_{\mathrm{iso}}(|\vec{\boldsymbol{x}}|)$, then we find from (B.21) in Appendix B that $\mathrm{Re}\big[\mathbf{Q}(\boldsymbol{\kappa})\big]$ is proportional to the 2×2 identity matrix, and

$$\mathcal{S}(\boldsymbol{\kappa}) = \mathcal{S}^{\perp}(\boldsymbol{\kappa}) = \frac{\gamma}{k^2}\frac{4\beta(\boldsymbol{\kappa})}{\alpha^2\int_0^{\infty} d\zeta\,\mathcal{R}_{\mathrm{iso}}(\zeta)}+O(\gamma^2). \tag{124}$$

This is in agreement with (123) because

$$\mathcal{R}\left(\frac{\boldsymbol{\kappa}\zeta}{\beta(\boldsymbol{\kappa})},\zeta\right)=\mathcal{R}_{\rm iso}\left(\sqrt{\frac{|\boldsymbol{\kappa}|^2\zeta^2}{\beta^2(\boldsymbol{\kappa})}+\zeta^2}\right)=\mathcal{R}_{\rm iso}\left(\frac{|\zeta|}{\beta(\boldsymbol{\kappa})}\right).$$

Remark 4. These results hold also when $|\boldsymbol{\kappa}|\lesssim\gamma$, and we have

$$\mathcal{S}(\gamma\boldsymbol{\kappa})=\frac{\gamma}{k^2}\frac{8}{\alpha^2\int_{-\infty}^{\infty}d\zeta\,\mathcal{R}\big(\mathbf{0},\zeta\big)}+O(\gamma^2),\qquad \mathcal{S}^{\perp}(\gamma\boldsymbol{\kappa})-\mathcal{S}(\gamma\boldsymbol{\kappa})=O(\gamma^2). \tag{125}$$

This shows that in the high-frequency regime, in the dimensional variables, the scattering mean free paths for small wave vectors are equal to $8/[\alpha^2k^2\ell\int_{-\infty}^{\infty}\mathcal{R}(\mathbf{0},\zeta)d\zeta]$. These are the scattering mean free paths obtained in the white-noise paraxial regime as described in Appendix C, Eq. (C.6). The agreement is expected because when $\gamma\to 0$ we look at a narrow cone beam propagating through a random medium, as in the paraxial regime.

9.2. Evolution of the coherence matrix

In this section we consider the coherence matrix in the high-frequency regime, denoted by

$$\mathcal{P}_{\rm hf}(\boldsymbol{\kappa},z)=\lim_{\gamma\to 0}\gamma^4\mathcal{P}(\gamma\boldsymbol{\kappa},\gamma z), \tag{126}$$

and compare it to the coherence matrix in the paraxial regime. We rescaled z by γ because we know from (125) that the waves lose coherence over such propagation distances, and we see below that energy exchange between the transverse electric and magnetic modes occurs at the same scale. We also rescaled $\boldsymbol{\kappa}$ by γ because the initial condition generates such wave vectors when γ_J is of the same order as γ, as we assume here. Taking the limit of (110) as $\gamma\to 0$, and using

$$\lim_{\gamma\to 0}\boldsymbol{\Gamma}(\gamma\boldsymbol{\kappa},\gamma\boldsymbol{\kappa}')=\boldsymbol{\Gamma}_{\rm hf}(\boldsymbol{\kappa},\boldsymbol{\kappa}'):=\frac{1}{|\boldsymbol{\kappa}|\,|\boldsymbol{\kappa}'|}\begin{pmatrix}\boldsymbol{\kappa}\cdot\boldsymbol{\kappa}' & -\boldsymbol{\kappa}^{\perp}\cdot\boldsymbol{\kappa}'\\ \boldsymbol{\kappa}^{\perp}\cdot\boldsymbol{\kappa}' & \boldsymbol{\kappa}\cdot\boldsymbol{\kappa}'\end{pmatrix} \tag{127}$$

and

$$\lim_{\gamma\to 0}\gamma\mathbf{Q}(\gamma\boldsymbol{\kappa})=\mathbf{Q}_{\rm hf}(\boldsymbol{\kappa}):=-\left[\frac{k^4\alpha^2}{8}\int_{\mathbb{R}^2}\frac{d\boldsymbol{u}}{(2\pi)^2}\widetilde{\mathcal{R}}(k\boldsymbol{u},0)\right]\mathbf{I}, \tag{128}$$

we find that $\mathcal{P}_{\rm hf}(\boldsymbol{\kappa},z)$ satisfies

$$\partial_z\mathcal{P}_{\rm hf}(\boldsymbol{\kappa},z)=2\mathbf{Q}_{\rm hf}(\boldsymbol{\kappa})\mathcal{P}_{\rm hf}(\boldsymbol{\kappa},z)+\frac{k^2\alpha^2}{4}\int_{\mathbb{R}^2}\frac{d(k\boldsymbol{\kappa}')}{(2\pi)^2}\boldsymbol{\Gamma}_{\rm hf}(\boldsymbol{\kappa},\boldsymbol{\kappa}')\mathcal{P}_{\rm hf}(\boldsymbol{\kappa}',z)\boldsymbol{\Gamma}_{\rm hf}(\boldsymbol{\kappa}',\boldsymbol{\kappa})\widetilde{\mathcal{R}}\big(k(\boldsymbol{\kappa}-\boldsymbol{\kappa}'),0\big), \tag{129}$$

starting from $\mathcal{P}_{\rm hf}(\boldsymbol{\kappa},0)=\mathcal{A}_{{\rm hf},o}(\boldsymbol{\kappa})\mathcal{A}_{{\rm hf},o}(\boldsymbol{\kappa})^{\dagger}$, with

$$\mathcal{A}_{{\rm hf},o}(\boldsymbol{\kappa})=\begin{pmatrix}a_{{\rm hf},o}(\boldsymbol{\kappa})\\ a^{\perp}_{{\rm hf},o}(\boldsymbol{\kappa})\end{pmatrix},\qquad a_{{\rm hf},o}(\boldsymbol{\kappa})=-\frac{\boldsymbol{\kappa}}{2|\boldsymbol{\kappa}|}\cdot\widehat{\boldsymbol{J}}\left(\frac{k\boldsymbol{\kappa}}{\bar{\kappa}_J}\right),\qquad a^{\perp}_{{\rm hf},o}(\boldsymbol{\kappa})=-\frac{\boldsymbol{\kappa}^{\perp}}{2|\boldsymbol{\kappa}|}\cdot\widehat{\boldsymbol{J}}\left(\frac{k\boldsymbol{\kappa}}{\bar{\kappa}_J}\right), \tag{130}$$

and $\bar{\kappa}_J=\lim_{\gamma\to 0}\gamma_J/\gamma=O(1)$. More explicitly, Eq. (129) written componentwise is

$$\begin{aligned}
\partial_z\mathcal{P}_{{\rm hf},11}(\boldsymbol{\kappa},z)&=\frac{k^2\alpha^2}{4}\int_{\mathbb{R}^2}\frac{d(k\boldsymbol{\kappa}')}{(2\pi)^2}\widetilde{\mathcal{R}}\big(k(\boldsymbol{\kappa}-\boldsymbol{\kappa}'),0\big)\Big[-\mathcal{P}_{{\rm hf},11}(\boldsymbol{\kappa},z)\\
&\quad+\frac{(\boldsymbol{\kappa}\cdot\boldsymbol{\kappa}')^2\mathcal{P}_{{\rm hf},11}(\boldsymbol{\kappa}',z)-(\boldsymbol{\kappa}\cdot\boldsymbol{\kappa}')(\boldsymbol{\kappa}^{\perp}\cdot\boldsymbol{\kappa}')(\mathcal{P}_{{\rm hf},12}(\boldsymbol{\kappa}',z)+\mathcal{P}_{{\rm hf},21}(\boldsymbol{\kappa}',z))+(\boldsymbol{\kappa}^{\perp}\cdot\boldsymbol{\kappa}')^2\mathcal{P}_{{\rm hf},22}(\boldsymbol{\kappa}',z)}{|\boldsymbol{\kappa}|^2|\boldsymbol{\kappa}'|^2}\Big],\\
\partial_z\mathcal{P}_{{\rm hf},12}(\boldsymbol{\kappa},z)&=\frac{k^2\alpha^2}{4}\int_{\mathbb{R}^2}\frac{d(k\boldsymbol{\kappa}')}{(2\pi)^2}\widetilde{\mathcal{R}}\big(k(\boldsymbol{\kappa}-\boldsymbol{\kappa}'),0\big)\Big[-\mathcal{P}_{{\rm hf},12}(\boldsymbol{\kappa},z)\\
&\quad+\frac{(\boldsymbol{\kappa}\cdot\boldsymbol{\kappa}')(\boldsymbol{\kappa}^{\perp}\cdot\boldsymbol{\kappa}')(\mathcal{P}_{{\rm hf},11}(\boldsymbol{\kappa}',z)-\mathcal{P}_{{\rm hf},22}(\boldsymbol{\kappa}',z))+(\boldsymbol{\kappa}\cdot\boldsymbol{\kappa}')^2\mathcal{P}_{{\rm hf},12}(\boldsymbol{\kappa}',z)-(\boldsymbol{\kappa}^{\perp}\cdot\boldsymbol{\kappa}')^2\mathcal{P}_{{\rm hf},21}(\boldsymbol{\kappa}',z)}{|\boldsymbol{\kappa}|^2|\boldsymbol{\kappa}'|^2}\Big],\\
\partial_z\mathcal{P}_{{\rm hf},21}(\boldsymbol{\kappa},z)&=\frac{k^2\alpha^2}{4}\int_{\mathbb{R}^2}\frac{d(k\boldsymbol{\kappa}')}{(2\pi)^2}\widetilde{\mathcal{R}}\big(k(\boldsymbol{\kappa}-\boldsymbol{\kappa}'),0\big)\Big[-\mathcal{P}_{{\rm hf},21}(\boldsymbol{\kappa},z)\\
&\quad+\frac{(\boldsymbol{\kappa}\cdot\boldsymbol{\kappa}')(\boldsymbol{\kappa}^{\perp}\cdot\boldsymbol{\kappa}')(\mathcal{P}_{{\rm hf},11}(\boldsymbol{\kappa}',z)-\mathcal{P}_{{\rm hf},22}(\boldsymbol{\kappa}',z))-(\boldsymbol{\kappa}^{\perp}\cdot\boldsymbol{\kappa}')^2\mathcal{P}_{{\rm hf},12}(\boldsymbol{\kappa}',z)+(\boldsymbol{\kappa}\cdot\boldsymbol{\kappa}')^2\mathcal{P}_{{\rm hf},21}(\boldsymbol{\kappa}',z)}{|\boldsymbol{\kappa}|^2|\boldsymbol{\kappa}'|^2}\Big],\\
\partial_z\mathcal{P}_{{\rm hf},22}(\boldsymbol{\kappa},z)&=\frac{k^2\alpha^2}{4}\int_{\mathbb{R}^2}\frac{d(k\boldsymbol{\kappa}')}{(2\pi)^2}\widetilde{\mathcal{R}}\big(k(\boldsymbol{\kappa}-\boldsymbol{\kappa}'),0\big)\Big[-\mathcal{P}_{{\rm hf},22}(\boldsymbol{\kappa},z)\\
&\quad+\frac{(\boldsymbol{\kappa}^{\perp}\cdot\boldsymbol{\kappa}')^2\mathcal{P}_{{\rm hf},11}(\boldsymbol{\kappa}',z)+(\boldsymbol{\kappa}\cdot\boldsymbol{\kappa}')(\boldsymbol{\kappa}^{\perp}\cdot\boldsymbol{\kappa}')(\mathcal{P}_{{\rm hf},12}(\boldsymbol{\kappa}',z)+\mathcal{P}_{{\rm hf},21}(\boldsymbol{\kappa}',z))+(\boldsymbol{\kappa}\cdot\boldsymbol{\kappa}')^2\mathcal{P}_{{\rm hf},22}(\boldsymbol{\kappa}',z)}{|\boldsymbol{\kappa}|^2|\boldsymbol{\kappa}'|^2}\Big].
\end{aligned}$$

This system can be simplified by changing of coordinates, as follows. Let us introduce (for $\boldsymbol{\kappa} = (\kappa_1, \kappa_2)$)

$$a_1^\epsilon(\boldsymbol{\kappa}, z) = \frac{\kappa_1 a^\epsilon(\boldsymbol{\kappa}, z) - \kappa_2 a^{\epsilon,\perp}(\boldsymbol{\kappa}, z)}{|\boldsymbol{\kappa}|}, \qquad a_2^\epsilon(\boldsymbol{\kappa}, z) = \frac{\kappa_2 a^\epsilon(\boldsymbol{\kappa}, z) + \kappa_1 a^{\epsilon,\perp}(\boldsymbol{\kappa}, z)}{|\boldsymbol{\kappa}|}, \tag{131}$$

and note from (94) that they are the Fourier coefficients of the electric field on the x_1 and x_2 axes. Define also the coherence matrix

$$\widetilde{\mathcal{P}}_{\rm hf}(\boldsymbol{\kappa}, z) = \lim_{\gamma\to 0} \gamma^4 \widetilde{\mathcal{P}}(\gamma\boldsymbol{\kappa}, \gamma z), \qquad \widetilde{\mathcal{P}}(\boldsymbol{\kappa}, z) = \lim_{\epsilon\to 0} \mathbb{E}\left[\begin{pmatrix} a_1^\epsilon(\boldsymbol{\kappa}, z) \\ a_2^\epsilon(\boldsymbol{\kappa}, z)\end{pmatrix}\begin{pmatrix} a_1^\epsilon(\boldsymbol{\kappa}, z) \\ a_2^\epsilon(\boldsymbol{\kappa}, z)\end{pmatrix}^\dagger\right], \tag{132}$$

which is related to $\mathcal{P}_{\rm hf}(\boldsymbol{\kappa}, z)$ as

$$\widetilde{\mathcal{P}}_{{\rm hf},11}(\boldsymbol{\kappa}, z) = \frac{\kappa_1^2 \mathcal{P}_{{\rm hf},11}(\boldsymbol{\kappa}, z) + \kappa_2^2 \mathcal{P}_{{\rm hf},22}(\boldsymbol{\kappa}, z) - \kappa_1\kappa_2(\mathcal{P}_{{\rm hf},12}(\boldsymbol{\kappa}, z) + \mathcal{P}_{{\rm hf},21}(\boldsymbol{\kappa}, z))}{|\boldsymbol{\kappa}|^2},$$

$$\widetilde{\mathcal{P}}_{{\rm hf},12}(\boldsymbol{\kappa}, z) = \frac{\kappa_1\kappa_2(\mathcal{P}_{{\rm hf},11}(\boldsymbol{\kappa}, z) - \mathcal{P}_{{\rm hf},22}(\boldsymbol{\kappa}, z)) + \kappa_1^2 \mathcal{P}_{{\rm hf},12}(\boldsymbol{\kappa}, z) - \kappa_2^2 \mathcal{P}_{{\rm hf},21}(\boldsymbol{\kappa}, z)}{|\boldsymbol{\kappa}|^2},$$

$$\widetilde{\mathcal{P}}_{{\rm hf},21}(\boldsymbol{\kappa}, z) = \frac{\kappa_1\kappa_2(\mathcal{P}_{{\rm hf},11}(\boldsymbol{\kappa}, z) - \mathcal{P}_{{\rm hf},22}(\boldsymbol{\kappa}, z)) - \kappa_2^2 \mathcal{P}_{{\rm hf},12}(\boldsymbol{\kappa}, z) + \kappa_1^2 \mathcal{P}_{{\rm hf},21}(\boldsymbol{\kappa}, z)}{|\boldsymbol{\kappa}|^2},$$

$$\widetilde{\mathcal{P}}_{{\rm hf},22}(\boldsymbol{\kappa}, z) = \frac{\kappa_2^2 \mathcal{P}_{{\rm hf},11}(\boldsymbol{\kappa}, z) + \kappa_1^2 \mathcal{P}_{{\rm hf},22}(\boldsymbol{\kappa}, z) + \kappa_1\kappa_2(\mathcal{P}_{{\rm hf},12}(\boldsymbol{\kappa}, z) + \mathcal{P}_{{\rm hf},21}(\boldsymbol{\kappa}, z))}{|\boldsymbol{\kappa}|^2}.$$

Elementary calculations then show that $\widetilde{\mathcal{P}}_{\rm hf}(\boldsymbol{\kappa}, z)$ satisfies

$$\partial_z \widetilde{\mathcal{P}}_{\rm hf}(\boldsymbol{\kappa}, z) = \frac{k^2\alpha^2}{4} \int_{\mathbb{R}^2} \frac{d(k\boldsymbol{\kappa}')}{(2\pi)^2} \widetilde{\mathcal{R}}\big(k(\boldsymbol{\kappa} - \boldsymbol{\kappa}'), 0\big)\Big[-\widetilde{\mathcal{P}}_{\rm hf}(\boldsymbol{\kappa}, z) + \widetilde{\mathcal{P}}_{\rm hf}(\boldsymbol{\kappa}', z)\Big], \tag{133}$$

starting from $\widetilde{\mathcal{P}}_{\rm hf}(\boldsymbol{\kappa}, 0) = \widetilde{\mathcal{A}}_{{\rm hf},o}(\boldsymbol{\kappa})\widetilde{\mathcal{A}}_{{\rm hf},o}(\boldsymbol{\kappa})^\dagger$, with

$$\widetilde{\mathcal{A}}_{{\rm hf},o}(\boldsymbol{\kappa}) = -\frac{1}{2}\begin{pmatrix} \widehat{J}_1\Big(\dfrac{k\boldsymbol{\kappa}}{\bar{\kappa}_J}\Big) \\ \widehat{J}_2\Big(\dfrac{k\boldsymbol{\kappa}}{\bar{\kappa}_J}\Big)\end{pmatrix}. \tag{134}$$

This equation agrees to the one found in the white noise paraxial regime, as described in Appendix C, Eq. (C.7). It says that in this high frequency scaling there is no polarization exchange. If the electric field is along the x_1 axis initially, it remains along the x_1 axis for distances that are comparable to the scattering mean free path.

Remark 5. The polarization conservation described here happens only in the high-frequency regime, where the transport equation reduces to (133). It does not hold in general, and Eq. (110) exhibits polarization exchange.

10. Summary

We presented a detailed analysis of cumulative scattering effects on electromagnetic waves that propagate long distances in random media with small fluctuations of the wave speed. The results are derived from first principles, by studying Maxwell's equations with random electric permittivity, in a regime of separation of scales modeled by two parameters. The first is ϵ, the ratio of the wavelength and the distance of propagation, and the second is γ, the ratio of the wavelength and correlation length of the random fluctuations, which is similar to the spatial support of the source. By controlling γ, we ensure that the source emits a cone wave beam which propagates along a preferred direction, called range. Depending on γ, the opening angle of the cone may be much larger than in paraxial regimes. However, the angle is smaller than 180°, so that evanescent and backscattered waves can be neglected.

The analysis of the solution of Maxwell's equation is in the long range limit $\epsilon \to 0$. It involves the decomposition of the waves in transverse electric and magnetic plane wave components, whose amplitudes are random fields. They satisfy a stochastic system of differential equations driven by the random fluctuations of the electric permittivity. These equations model the evolution in range of the random amplitudes, starting from the initial values determined by the source of excitation. The $\epsilon \to 0$ limit of the solution of the system of stochastic differential equations is obtained with the Markov limit theorem.

We study in detail the first two statistical moments of the limit amplitudes. Their expectation decays exponentially with range, on length scales called scattering mean free paths. This is the manifestation of the randomization of the waves, due to scattering in the random medium. The second moments of the amplitudes describe the decorrelation of the waves over directions, and the transport of energy. Of particular interest is the energy density (mean Wigner transform), which

characterizes the state of polarization of the waves and the diffusion of energy over directions. The transport equations with polarization satisfied by the energy density are derived with the Markov limit theorem, and the result is related to the radiative transport theory. In the high frequency limit $\gamma \to 0$ the equations simplify, and are related to those satisfied by the Wigner transform of the solution of the paraxial wave equation in random media. We quantify the transfer of energy between the components of the wave field, and illustrate the results with numerical simulations.

Acknowledgments

Liliana Borcea's work was partially supported by grant #339153 from the Simons Foundation and by AFOSR Grant FA9550-15-1-0118.

Appendix A. The Markov limit

Let $\mathcal{O}$ be an open set in $\mathbb{R}^d$ and $\mathcal{D}(\mathcal{O}, \mathbb{R}^p)$ the space of infinitely differentiable functions with compact support. We consider the process $\boldsymbol{X}^\epsilon$ in $\mathcal{C}([0, L], \mathcal{D}')$, the solution of

$$\frac{d\boldsymbol{X}^\epsilon}{dz} = \frac{1}{\sqrt{\epsilon}}\mathcal{F}\left(\frac{z}{\epsilon}, \frac{z}{\epsilon}\right)\boldsymbol{X}^\epsilon + \mathcal{G}\left(\frac{z}{\epsilon}, \frac{z}{\epsilon}\right)\boldsymbol{X}^\epsilon, \tag{A.1}$$

where $\mathcal{F}(\zeta, \zeta')$ and $\mathcal{G}(\zeta, \zeta')$ are random linear operators from $\mathcal{D}'$ to $\mathcal{D}'$. We assume that the mappings $\zeta \to \mathcal{F}(\zeta, \zeta')$ and $\zeta \to \mathcal{G}(\zeta, \zeta')$ are stationary and possess strong ergodic properties, and that $\mathcal{F}(\zeta, \zeta')$ has mean zero. Moreover, the mappings $\zeta' \to \mathcal{F}(\zeta, \zeta')$ and $\zeta' \to \mathcal{G}(\zeta, \zeta')$ are periodic.

We are interested in particular in Eq. (102), where the process $\boldsymbol{X}^\epsilon$ is in $\mathcal{D}'(\mathcal{O}, \mathbb{R}^4)$, defined by

$$\boldsymbol{X}^\epsilon(z) = \begin{pmatrix} \mathrm{Re}\big(a^\epsilon(\boldsymbol{\kappa}, z)\big) \\ \mathrm{Im}\big(a^\epsilon(\boldsymbol{\kappa}, z)\big) \\ \mathrm{Re}\big(a^{\epsilon,\perp}(\boldsymbol{\kappa}, z)\big) \\ \mathrm{Im}\big(a^{\epsilon,\perp}(\boldsymbol{\kappa}, z)\big) \end{pmatrix}, \quad \text{for } \boldsymbol{\kappa} \in \mathcal{O} = \{\boldsymbol{\kappa} \in \mathbb{R}^2,\ |\boldsymbol{\kappa}| < 1\}. \tag{A.2}$$

The operator $\mathcal{F}(\zeta, \zeta')$ is

$$\big\langle \mathcal{F}(\zeta, \zeta')\boldsymbol{X}, \boldsymbol{\phi}\big\rangle = \sum_{j=1}^{4} \int_{\mathcal{O}} d\boldsymbol{\kappa}\, [\mathcal{F}(\zeta, \zeta')\boldsymbol{X}]_j(\boldsymbol{\kappa})\phi_j(\boldsymbol{\kappa}) = \int_{\mathcal{O}} d\boldsymbol{\kappa}\, \boldsymbol{\phi}(\boldsymbol{\kappa}) \cdot \int_{\mathcal{O}} d\boldsymbol{\kappa}'\, \mathbb{F}(\boldsymbol{\kappa}, \boldsymbol{\kappa}', \zeta, \zeta')\boldsymbol{X}(\boldsymbol{\kappa}'), \tag{A.3}$$

for $\boldsymbol{\phi} \in \mathcal{D}(\mathcal{O}, \mathbb{R}^4)$ with components ϕ_j, and $\boldsymbol{X} \in \mathcal{D}'(\mathcal{O}, \mathbb{R}^4)$ with components X_j. The kernel matrix $\mathbb{F}(\boldsymbol{\kappa}, \boldsymbol{\kappa}', \zeta, \zeta')$ in (A.3) is given by

$$\mathbb{F} = \begin{pmatrix} \mathcal{F}^{\mathrm{r}}_{11} & -\mathcal{F}^{\mathrm{i}}_{11} & \mathcal{F}^{\mathrm{r}}_{12} & -\mathcal{F}^{\mathrm{i}}_{12} \\ \mathcal{F}^{\mathrm{i}}_{11} & \mathcal{F}^{\mathrm{r}}_{11} & \mathcal{F}^{\mathrm{i}}_{12} & \mathcal{F}^{\mathrm{r}}_{12} \\ \mathcal{F}^{\mathrm{r}}_{21} & -\mathcal{F}^{\mathrm{i}}_{21} & \mathcal{F}^{\mathrm{r}}_{22} & -\mathcal{F}^{\mathrm{i}}_{22} \\ \mathcal{F}^{\mathrm{i}}_{21} & \mathcal{F}^{\mathrm{r}}_{21} & \mathcal{F}^{\mathrm{i}}_{22} & \mathcal{F}^{\mathrm{r}}_{22} \end{pmatrix}, \tag{A.4}$$

in terms of

$$\mathcal{F}^{\mathrm{r}}_{jl}(\boldsymbol{\kappa}, \boldsymbol{\kappa}', \zeta, \zeta') = \mathrm{Re}\Big[\frac{ik^3\alpha}{2(2\pi)^2\gamma^2}\widehat{\nu}\left(\frac{k(\boldsymbol{\kappa} - \boldsymbol{\kappa}')}{\gamma}, \gamma\zeta\right) F^{aa}_{jl}\big(\boldsymbol{\kappa}, \boldsymbol{\kappa}', \zeta'\big)\Big], \tag{A.5}$$

$$\mathcal{F}^{\mathrm{i}}_{jl}(\boldsymbol{\kappa}, \boldsymbol{\kappa}', \zeta, \zeta') = \mathrm{Im}\Big[\frac{ik^3\alpha}{2(2\pi)^2\gamma^2}\widehat{\nu}\left(\frac{k(\boldsymbol{\kappa} - \boldsymbol{\kappa}')}{\gamma}, \gamma\zeta\right) F^{aa}_{jl}\big(\boldsymbol{\kappa}, \boldsymbol{\kappa}', \zeta'\big)\Big], \tag{A.6}$$

where we recall from (76) to (80) the expression of $F^{aa}_{jl}(\boldsymbol{\kappa}, \boldsymbol{\kappa}', \zeta')$. The adjoint operator $\mathcal{F}^*(\zeta, \zeta')$ is defined by

$$\big\langle \mathcal{F}(\zeta, \zeta')\boldsymbol{X}, \boldsymbol{\phi}\big\rangle = \big\langle \boldsymbol{X}, \mathcal{F}^*(\zeta, \zeta')\boldsymbol{\phi}\big\rangle$$

for $\boldsymbol{\phi} \in \mathcal{D}(\mathcal{O}, \mathbb{R}^4)$ and $\boldsymbol{X} \in \mathcal{D}'(\mathcal{O}, \mathbb{R}^4)$, and has kernel $\mathbb{F}^*(\boldsymbol{\kappa}, \boldsymbol{\kappa}', \zeta, \zeta') = \mathbb{F}^T(\boldsymbol{\kappa}', \boldsymbol{\kappa}, \zeta, \zeta')$. Similar expressions hold for $\mathcal{G}$.

To obtain the Markov limit we use the results in [12]. The interested reader can find a self-contained introduction to such limit theorems in [20, Chapter 6] or in [21, Appendix A]. We get that $\boldsymbol{X}^\epsilon(z)$ converges weakly in $\mathcal{C}([0, L], \mathcal{D}')$ to $\boldsymbol{X}(z)$, which is the solution of a martingale problem with generator $\mathcal{L}$ defined by:

$$\begin{aligned} \mathcal{L}f\left(\langle \boldsymbol{X}, \boldsymbol{\phi}\rangle\right) = &\int_0^\infty d\zeta \lim_{Z\to\infty} \frac{1}{Z}\int_0^Z dh\, \mathbb{E}\Big[\big\langle \boldsymbol{X}, \mathcal{F}^*(0, h)\boldsymbol{\phi}\big\rangle \big\langle \boldsymbol{X}, \mathcal{F}^*(\zeta, \zeta + h)\boldsymbol{\phi}\big\rangle\Big] f''\left(\langle \boldsymbol{X}, \boldsymbol{\phi}\rangle\right) \\ &+ \int_0^\infty d\zeta \lim_{Z\to\infty} \frac{1}{Z}\int_0^Z dh\, \mathbb{E}\Big[\big\langle \boldsymbol{X}, \mathcal{F}^*(0, h)\mathcal{F}^*(\zeta, \zeta + h)\boldsymbol{\phi}\big\rangle\Big] f'\left(\langle \boldsymbol{X}, \boldsymbol{\phi}\rangle\right) \\ &+ \lim_{Z\to\infty} \frac{1}{Z}\int_0^Z dh\, \mathbb{E}\Big[\big\langle \boldsymbol{X}, \mathcal{G}^*(0, h)\boldsymbol{\phi}\big\rangle\Big] f'\left(\langle \boldsymbol{X}, \boldsymbol{\phi}\rangle\right), \end{aligned} \tag{A.7}$$

for any $\boldsymbol{X} \in \mathcal{D}'(\mathcal{O}, \mathbb{R}^4)$, $\boldsymbol{\phi} \in \mathcal{D}(\mathcal{O}, \mathbb{R}^4)$, and smooth $f : \mathbb{R} \to \mathbb{R}$. This means that, for any $\boldsymbol{\phi} \in \mathcal{D}(\mathcal{O}, \mathbb{R}^4)$ and smooth function $f : \mathbb{R} \to \mathbb{R}$, the real-valued process

$$f\left(\langle \boldsymbol{X}(z), \boldsymbol{\phi}\rangle\right) - \int_0^z dz'\, \mathcal{L}f\left(\langle \boldsymbol{X}(z'), \boldsymbol{\phi}\rangle\right)$$

is a martingale. More generally, if $n \in \mathbb{N}$, $\boldsymbol{\phi}_1, \ldots, \boldsymbol{\phi}_n \in \mathcal{D}(\mathcal{O}, \mathbb{R}^4)$, and $f : \mathbb{R}^n \to \mathbb{R}$ is a smooth function, then

$$f\left(\langle \boldsymbol{X}(z), \boldsymbol{\phi}_1\rangle, \ldots, \langle \boldsymbol{X}(z), \boldsymbol{\phi}_n\rangle\right) - \int_0^z dz'\, \mathcal{L}^n f\left(\langle \boldsymbol{X}(z'), \boldsymbol{\phi}_1\rangle, \ldots, \langle \boldsymbol{X}(z'), \boldsymbol{\phi}_n\rangle\right)$$

is a martingale, where

$$\begin{aligned}\mathcal{L}^n f\left(\langle \boldsymbol{X}, \boldsymbol{\phi}_1\rangle, \ldots, \langle \boldsymbol{X}, \boldsymbol{\phi}_n\rangle\right) = \Bigg\{ &\sum_{j,l=1}^n \int_0^\infty d\zeta \lim_{Z\to\infty} \frac{1}{Z}\int_0^Z dh\, \mathbb{E}\Big[\langle \boldsymbol{X}, \mathcal{F}^*(0,h)\boldsymbol{\phi}_j\rangle \langle \boldsymbol{X}, \mathcal{F}^*(\zeta, \zeta+h)\boldsymbol{\phi}_l\rangle\Big]\, \partial^2_{jl} \\ &+ \sum_{j=1}^n \int_0^\infty d\zeta \lim_{Z\to\infty} \frac{1}{Z}\int_0^Z dh\, \mathbb{E}\Big[\langle \boldsymbol{X}, \mathcal{F}^*(0,h)\mathcal{F}^*(\zeta, \zeta+h)\boldsymbol{\phi}_j\rangle\Big]\, \partial_j \\ &+ \sum_{j=1}^n \lim_{Z\to\infty} \frac{1}{Z}\int_0^Z dh\, \mathbb{E}\Big[\langle X, \mathcal{G}^*(0,h)\phi_j\rangle\Big]\partial_j \Bigg\} f\Big(\langle \boldsymbol{X}, \boldsymbol{\phi}_1\rangle, \ldots, \langle \boldsymbol{X}, \boldsymbol{\phi}_n\rangle\Big). \end{aligned} \tag{A.8}$$

To calculate the first moment of the limit process $\boldsymbol{X}(z)$, let $n = 1$ and $f(y) = y$ in (A.8). We find that

$$\frac{d\,\mathbb{E}\Big[\langle \boldsymbol{X}(z), \boldsymbol{\phi}\rangle\Big]}{dz} = \mathbb{E}\Big[\langle \boldsymbol{X}(z), \overline{\mathcal{F}}^*\boldsymbol{\phi}\rangle\Big] + \mathbb{E}\Big[\langle \boldsymbol{X}(z), \overline{\mathcal{G}}^*\boldsymbol{\phi}\rangle\Big],$$

where

$$\overline{\mathcal{F}}^* = \int_0^\infty d\zeta \lim_{Z\to\infty} \frac{1}{Z}\int_0^Z dh\, \mathbb{E}\big[\mathcal{F}^*(0,h)\mathcal{F}^*(\zeta, \zeta+h)\big],$$

$$\overline{\mathcal{G}}^* = \lim_{Z\to\infty} \frac{1}{Z}\int_0^Z dh\, \mathbb{E}\big[\mathcal{G}^*(0,h)\big].$$

This shows that

$$\overline{\boldsymbol{X}}(z) = \mathbb{E}\big[\boldsymbol{X}(z)\big],$$

satisfies a closed system of ordinary differential equations

$$\frac{d\,\langle \overline{\boldsymbol{X}}(z), \boldsymbol{\phi}\rangle}{dz} = \langle \overline{\boldsymbol{X}}(z), \overline{\mathcal{F}}^*\boldsymbol{\phi}\rangle + \langle \overline{\boldsymbol{X}}(z), \overline{\mathcal{G}}^*\boldsymbol{\phi}\rangle,$$

or, equivalently in $\mathcal{D}'$,

$$\frac{d\overline{\boldsymbol{X}}(z)}{dz} = \overline{\mathcal{F}}\,\overline{\boldsymbol{X}}(z) + \overline{\mathcal{G}}\,\overline{\boldsymbol{X}}(z), \tag{A.9}$$

where $\overline{\mathcal{F}}$, resp. $\overline{\mathcal{G}}$, is the adjoint of $\overline{\mathcal{F}}^*$, resp. $\overline{\mathcal{G}}^*$.

Recalling from (A.3) to (A.6) the expression of the kernel $\mathbb{F}^T(\kappa', \boldsymbol{\kappa}, \zeta, \zeta')$ of $\mathcal{F}^*(\zeta, \zeta')$, we obtain

$$\overline{\mathcal{F}}^*_{jl}(\boldsymbol{\kappa}, \boldsymbol{\kappa}') = \sum_{q=1}^4 \int_{\mathcal{O}} d\boldsymbol{\kappa}'' \int_0^\infty d\zeta \lim_{Z\to\infty} \frac{1}{Z}\int_0^Z dh\, \mathbb{E}\big[\mathbb{F}_{lq}(\boldsymbol{\kappa}', \boldsymbol{\kappa}'', \zeta, \zeta+h)\mathbb{F}_{qj}(\boldsymbol{\kappa}'', \boldsymbol{\kappa}, 0, h)\big],$$

for $j, l = 1, \ldots, 4$. For instance,

$$\begin{aligned}\overline{\mathcal{F}}^*_{11}(\boldsymbol{\kappa}, \boldsymbol{\kappa}') = &\int_{\mathcal{O}} d\boldsymbol{\kappa}'' \int_0^\infty d\zeta \lim_{Z\to\infty} \frac{1}{Z}\int_0^Z dh\, \mathbb{E}\big[\mathcal{F}^{\mathrm{r}}_{11}(\boldsymbol{\kappa}', \boldsymbol{\kappa}'', \zeta, \zeta+h)\mathcal{F}^{\mathrm{r}}_{11}(\boldsymbol{\kappa}'', \boldsymbol{\kappa}, 0, h)\big] \\ &- \int_{\mathcal{O}} d\boldsymbol{\kappa}'' \int_0^\infty d\zeta \lim_{Z\to\infty} \frac{1}{Z}\int_0^Z dh\, \mathbb{E}\big[\mathcal{F}^{\mathrm{i}}_{11}(\boldsymbol{\kappa}', \boldsymbol{\kappa}'', \zeta, \zeta+h)\mathcal{F}^{\mathrm{i}}_{11}(\boldsymbol{\kappa}'', \boldsymbol{\kappa}, 0, h)\big] \\ &+ \int_{\mathcal{O}} d\boldsymbol{\kappa}'' \int_0^\infty d\zeta \lim_{Z\to\infty} \frac{1}{Z}\int_0^Z dh\, \mathbb{E}\big[\mathcal{F}^{\mathrm{r}}_{12}(\boldsymbol{\kappa}', \boldsymbol{\kappa}'', \zeta, \zeta+h)\mathcal{F}^{\mathrm{r}}_{21}(\boldsymbol{\kappa}'', \boldsymbol{\kappa}, 0, h)\big] \\ &- \int_{\mathcal{O}} d\boldsymbol{\kappa}'' \int_0^\infty d\zeta \lim_{Z\to\infty} \frac{1}{Z}\int_0^Z dh\, \mathbb{E}\big[\mathcal{F}^{\mathrm{i}}_{12}(\boldsymbol{\kappa}', \boldsymbol{\kappa}'', \zeta, \zeta+h)\mathcal{F}^{\mathrm{i}}_{21}(\boldsymbol{\kappa}'', \boldsymbol{\kappa}, 0, h)\big],\end{aligned}$$

and using (A.5)–(A.6), we get

$$\overline{\mathcal{F}}^*_{11}(\boldsymbol{\kappa},\boldsymbol{\kappa}') = \mathrm{Re}\Bigg\{\left(\frac{ik^3\alpha}{2(2\pi)^2\gamma^2}\right)^2 \int_{\mho} d\boldsymbol{\kappa}'' \int_0^\infty d\zeta \lim_{Z\to\infty}\frac{1}{Z}\int_0^Z dh \\ \times \mathbb{E}\left[\widehat{\nu}\left(\frac{k(\boldsymbol{\kappa}'-\boldsymbol{\kappa}'')}{\gamma},\gamma\zeta\right)\widehat{\nu}\left(\frac{k(\boldsymbol{\kappa}''-\boldsymbol{\kappa})}{\gamma},0\right)\right] \\ \times \left[\mathbf{F}^{aa}(\boldsymbol{\kappa}',\boldsymbol{\kappa}'',\zeta+h)\mathbf{F}^{aa}(\boldsymbol{\kappa}'',\boldsymbol{\kappa},h)\right]_{11}\Bigg\}.$$

Moreover, using the identity

$$\mathbb{E}\left[\widehat{\nu}\left(\frac{k(\boldsymbol{\kappa}'-\boldsymbol{\kappa}'')}{\gamma},\gamma\zeta\right)\widehat{\nu}\left(\frac{k(\boldsymbol{\kappa}''-\boldsymbol{\kappa})}{\gamma},0\right)\right] = \left(\frac{2\pi\gamma}{k}\right)^2\delta(\boldsymbol{\kappa}-\boldsymbol{\kappa}')\widehat{\mathcal{R}}\left(\frac{k(\boldsymbol{\kappa}-\boldsymbol{\kappa}'')}{\gamma},\gamma\zeta\right),$$

derived from the definition of the autocorrelation with straightforward algebraic manipulations, and obtaining from (76) that

$$\mathbf{F}^{aa}(\boldsymbol{\kappa},\boldsymbol{\kappa}'',\zeta+h)\mathbf{F}^{aa}(\boldsymbol{\kappa}'',\boldsymbol{\kappa},h) = \boldsymbol{\Gamma}^{aa}(\boldsymbol{\kappa},\boldsymbol{\kappa}'')\boldsymbol{\Gamma}^{aa}(\boldsymbol{\kappa}'',\boldsymbol{\kappa})e^{ik(\beta(\boldsymbol{\kappa}'')-\beta(\boldsymbol{\kappa}))\zeta},$$

we get

$$\overline{\mathcal{F}}^*_{11}(\boldsymbol{\kappa},\boldsymbol{\kappa}') = -\frac{k^4\alpha^2}{16\pi^2\gamma^2}\mathrm{Re}\Bigg\{\int_{\mho} d\boldsymbol{\kappa}''\int_0^\infty d\zeta\,\widehat{\mathcal{R}}\left(\frac{k(\boldsymbol{\kappa}-\boldsymbol{\kappa}'')}{\gamma},\gamma\zeta\right)e^{ik(\beta(\boldsymbol{\kappa}'')-\beta(\boldsymbol{\kappa}))\zeta} \\ \times\left[\boldsymbol{\Gamma}^{aa}(\boldsymbol{\kappa},\boldsymbol{\kappa}'')\boldsymbol{\Gamma}^{aa}(\boldsymbol{\kappa}'',\boldsymbol{\kappa})\right]_{11}\delta(\boldsymbol{\kappa}-\boldsymbol{\kappa}')\Bigg\}.$$

The expressions of the other components of $\overline{\mathcal{F}}^*_{jl}(\boldsymbol{\kappa},\boldsymbol{\kappa}')$ are of the same type. Similarly, we calculate $\overline{\mathcal{G}}^\star$, and substituting into (A.9) we obtain the explicit expression of the differential equations satisfied by the mean wave amplitudes. This is Eq. (106), written in complex form.

The calculation of the second moments is similar, by letting $n = 1$ and $f(y) = y^2$ in (A.8), and carrying the lengthy calculations.

Appendix B. Connection to the radiative transport theory

To connect our transport equation (112) (see also (110)) to the radiative transport theory in [13,9,10], we adhere to the notation in [9]. First note that in [9] the random medium is assumed to be statistically isotropic, i.e. $\mathcal{R}(\vec{\boldsymbol{x}})$ depends only on $|\vec{\boldsymbol{x}}|$.

For any $\vec{\mathcal{K}} \in \mathbb{R}^3$, consider the orthonormal basis $\{\vec{\boldsymbol{z}}^{(0)}(\vec{\mathcal{K}}), \vec{\boldsymbol{z}}^{(1)}(\vec{\mathcal{K}}), \vec{\boldsymbol{z}}^{(2)}(\vec{\mathcal{K}})\}$ of $\mathbb{R}^3$, defined by

$$\vec{\boldsymbol{z}}^{(0)}(\vec{\mathcal{K}}) = \frac{\vec{\mathcal{K}}}{|\vec{\mathcal{K}}|} = \frac{1}{|\vec{\mathcal{K}}|}(\mathcal{K},\mathcal{K}_z), \qquad \vec{\boldsymbol{z}}^{(1)}(\vec{\mathcal{K}}) = \frac{1}{|\vec{\mathcal{K}}|}\left(\mathcal{K}_z\frac{\mathcal{K}}{|\mathcal{K}|},-|\mathcal{K}|\right), \qquad \vec{\boldsymbol{z}}^{(2)}(\vec{\mathcal{K}}) = \left(\frac{\mathcal{K}^\perp}{|\mathcal{K}|},0\right), \tag{B.1}$$

and satisfying

$$\vec{\boldsymbol{z}}^{(0)}\times\vec{\boldsymbol{z}}^{(1)} = \vec{\boldsymbol{z}}^{(2)}, \qquad \vec{\boldsymbol{z}}^{(0)}\times\vec{\boldsymbol{z}}^{(2)} = -\vec{\boldsymbol{z}}^{(1)}. \tag{B.2}$$

In [9] the vector $\vec{\boldsymbol{z}}^{(0)}$ is denoted by $\widehat{\boldsymbol{k}}$. We call it $\vec{\boldsymbol{z}}^{(0)}$ to avoid confusion with the wavenumber k. Note that when $\vec{\mathcal{K}} = k\vec{\boldsymbol{\kappa}}$, with $|\vec{\boldsymbol{\kappa}}| = 1$, then $\vec{\boldsymbol{z}}^{(0)} = \vec{\boldsymbol{\kappa}}$, and the vectors $\vec{\boldsymbol{z}}^{(1)}$ and $\vec{\boldsymbol{z}}^{(2)}$ are the same as $\vec{\boldsymbol{u}}$ and $\vec{\boldsymbol{u}}^\perp$ defined in (17).

Following the notation in [9], we define

$$f_j(\vec{\mathcal{K}},\vec{\boldsymbol{x}}) = \frac{2\pi}{\sqrt{2}\epsilon}\left[\vec{\boldsymbol{E}}^\epsilon(\vec{\boldsymbol{x}})\cdot\vec{\boldsymbol{z}}^{(j)}(\vec{\mathcal{K}}) + \zeta_o\vec{\boldsymbol{H}}^\epsilon(\vec{\boldsymbol{x}})\cdot\left(\vec{\boldsymbol{z}}^{(0)}(\vec{\mathcal{K}})\times\vec{\boldsymbol{z}}^{(j)}(\vec{\mathcal{K}})\right)\right], \quad j = 1,2, \tag{B.3}$$

where we use a different constant of proportionality than in [9], to simplify the relation (B.5). The Wigner transform $\mathbf{W}(\vec{\mathcal{K}},\vec{\boldsymbol{x}})$ is the 2×2 matrix with components

$$W_{lq}(\vec{\mathcal{K}},\vec{\boldsymbol{x}}) = \int\frac{d\vec{\boldsymbol{y}}}{(2\pi)^3}f_l\left(\vec{\boldsymbol{x}}-\frac{\epsilon\vec{\boldsymbol{y}}}{2},\vec{\mathcal{K}}\right)\overline{f_q\left(\vec{\boldsymbol{x}}+\frac{\epsilon\vec{\boldsymbol{y}}}{2},\vec{\mathcal{K}}\right)}e^{i\vec{\mathcal{K}}\cdot\vec{\boldsymbol{y}}}, \quad l,q = 1,2, \tag{B.4}$$

where the bar denotes complex conjugate. Substituting the wave decompositions (94)–(95) into (B.3), and keeping only the forward propagating modes, we obtain after some algebraic manipulations that

$$\mathbf{W}(\vec{\mathcal{K}},\vec{\boldsymbol{x}}) = \frac{\delta\left[\mathcal{K}_z - k\beta(\mathcal{K}/k)\right]}{\beta(\mathcal{K}/k)}\mathcal{W}(\mathcal{K}/k,\boldsymbol{x},z), \tag{B.5}$$

with $\mathcal{W}$ the Wigner transform in (111), satisfying (112).

The transport equation in [9] is

$$\vec{\nabla}\omega(\vec{\mathcal{K}})\cdot\vec{\nabla}_{\vec{\boldsymbol{x}}}\mathbf{W}(\vec{\mathcal{K}},\vec{\boldsymbol{x}}) = \int d\vec{\mathcal{K}}'\sigma(\vec{\mathcal{K}},\vec{\mathcal{K}}')[\mathbf{W}(\vec{\mathcal{K}}',\vec{\boldsymbol{x}})] - \Sigma(\vec{\mathcal{K}})\mathbf{W}(\vec{\mathcal{K}},\vec{\boldsymbol{x}}), \tag{B.6}$$

for the dispersion relation

$$\omega(\vec{\mathcal{K}}) = c_o|\vec{\mathcal{K}}|.$$

The integral kernel in the right hand side of (B.6) is the differential scattering cross section, defined by [9]

$$\begin{aligned}\sigma(\vec{\mathcal{K}},\vec{\mathcal{K}}')[\mathbf{W}(\vec{\mathcal{K}}',\vec{\boldsymbol{x}})] = {} & \frac{\pi c_o^2 k^2\alpha^2}{2(2\pi)^3\gamma^3}\widetilde{\mathcal{R}}\left(\frac{\vec{\mathcal{K}}-\vec{\mathcal{K}}'}{\gamma}\right)\\ & \times\delta[\omega(\vec{\mathcal{K}})-\omega(\vec{\mathcal{K}}')]\mathbf{T}(\vec{\mathcal{K}},\vec{\mathcal{K}}')\mathbf{W}(\vec{\mathcal{K}}',\vec{\boldsymbol{x}})\mathbf{T}(\vec{\mathcal{K}}',\vec{\mathcal{K}}),\end{aligned} \tag{B.7}$$

with the 2×2 matrix

$$\mathbf{T}(\vec{\mathcal{K}},\vec{\mathcal{K}}') = \left(\vec{\boldsymbol{z}}^{(l)}(\vec{\mathcal{K}})\cdot\vec{\boldsymbol{z}}^{(q)}(\vec{\mathcal{K}}')\right)_{l,q=1,2}.$$

The scalar $\Sigma(\vec{\mathcal{K}})$ is the total scattering cross section, which is shown in [9] to satisfy

$$\Sigma(\vec{\mathcal{K}})\mathbf{I} = \int d\vec{\mathcal{K}}'\sigma(\vec{\mathcal{K}},\vec{\mathcal{K}}')[\mathbf{I}]. \tag{B.8}$$

Since (B.5) gives that $\mathbf{W}(\vec{\mathcal{K}},\vec{\boldsymbol{x}})$ is supported at vectors $\vec{\mathcal{K}}$ of the form $\vec{\mathcal{K}} = k\vec{\boldsymbol{\kappa}}$, with $\vec{\boldsymbol{\kappa}} = (\boldsymbol{\kappa},\beta(\boldsymbol{\kappa}))$, we see that the operator on the left hand side of (B.6) is given by

$$\vec{\nabla}\omega(\vec{\mathcal{K}})\cdot\vec{\nabla}_{\vec{\boldsymbol{x}}} = c_o\frac{\vec{\mathcal{K}}}{|\vec{\mathcal{K}}|}\cdot\vec{\nabla}_{\vec{\boldsymbol{x}}} = c_o\Big[\boldsymbol{\kappa}\cdot\nabla_{\boldsymbol{x}}+\beta(\boldsymbol{\kappa})\partial_z\Big] = c_o\beta(\boldsymbol{\kappa})\Big[\partial_z-\nabla\beta(\boldsymbol{\kappa})\cdot\nabla_{\boldsymbol{x}}\Big]. \tag{B.9}$$

Again, using (B.5), we see that the integral kernel in the right hand side of (B.6) is supported at vectors $\vec{\mathcal{K}}' = k\vec{\boldsymbol{\kappa}}'$, with $\vec{\boldsymbol{\kappa}}' = (\boldsymbol{\kappa}',\beta(\boldsymbol{\kappa}'))$, so the Dirac distribution in (B.7) is

$$\delta\Big[\omega(\vec{\mathcal{K}})-\omega(k\vec{\boldsymbol{\kappa}}')\Big] = \delta\Big[c_o\sqrt{|\mathcal{K}|^2+|\mathcal{K}_z|^2}-c_o k\Big] = \frac{\delta\big[\mathcal{K}_z-k\beta(\mathcal{K}/k)\big]}{c_o\beta(\mathcal{K}/k)}. \tag{B.10}$$

Thus, the integral in (B.6) is supported at $\vec{\mathcal{K}} = k\vec{\boldsymbol{\kappa}}$, with $\vec{\boldsymbol{\kappa}} = (\boldsymbol{\kappa},\beta(\boldsymbol{\kappa}))$. For such vectors, the matrix $\mathbf{T}$ equals

$$\mathbf{T}(k\vec{\boldsymbol{\kappa}},k\vec{\boldsymbol{\kappa}}') = \sqrt{\beta(\boldsymbol{\kappa})\beta(\boldsymbol{\kappa}')}\boldsymbol{\Gamma}(\boldsymbol{\kappa},\boldsymbol{\kappa}'). \tag{B.11}$$

From (B.5) and (B.9), we obtain that

$$\vec{\nabla}\omega(\vec{\mathcal{K}})\cdot\vec{\nabla}_{\vec{\boldsymbol{x}}}\mathbf{W}(\vec{\mathcal{K}},\vec{\boldsymbol{x}}) = c_o\delta\big[\mathcal{K}_z-k\beta(\mathcal{K}/k)\big]\big[\partial_z-\nabla\beta(\mathcal{K}/k)\cdot\nabla_{\boldsymbol{x}}\big]\mathcal{W}(\mathcal{K}/k,\boldsymbol{x},z), \tag{B.12}$$

from (B.5), (B.7), and (B.10)–(B.11), we obtain that

$$\begin{aligned}\int d\vec{\mathcal{K}}'\sigma(\vec{\mathcal{K}},\vec{\mathcal{K}}')[\mathbf{W}(\vec{\mathcal{K}}',\vec{\boldsymbol{x}})] = {} & \frac{c_o k^2\alpha^2}{4\gamma^3}\delta\big[\mathcal{K}_z-k\beta(\mathcal{K}/k)\big]\\ & \times\int_{|\boldsymbol{\kappa}'|\le 1}\frac{d(k\boldsymbol{\kappa}')}{(2\pi)^2}\widetilde{\mathcal{R}}\left(\frac{\mathcal{K}-k\boldsymbol{\kappa}'}{\gamma},\frac{k(\beta(\mathcal{K}/k)-\beta(\boldsymbol{\kappa}'))}{\gamma}\right)\\ & \times\boldsymbol{\Gamma}(\mathcal{K}/k,\boldsymbol{\kappa}')\mathcal{W}(\boldsymbol{\kappa}',\boldsymbol{x},z)\boldsymbol{\Gamma}(\boldsymbol{\kappa}',\mathcal{K}/k).\end{aligned} \tag{B.13}$$

We also find from (B.8) that

$$\Sigma(\vec{\mathcal{K}})\mathbf{I} = \frac{c_o^2k^2\alpha^2}{4(2\pi)^2\gamma^3}\int d\vec{\mathcal{K}}'\delta\big[\omega(\vec{\mathcal{K}}')-\omega(\vec{\mathcal{K}})\big]\widetilde{\mathcal{R}}\left(\frac{\vec{\mathcal{K}}-\vec{\mathcal{K}}'}{\gamma}\right)\mathbf{T}(\vec{\mathcal{K}},\vec{\mathcal{K}}')\mathbf{T}(\vec{\mathcal{K}}',\vec{\mathcal{K}}), \tag{B.14}$$

or equivalently, for $\vec{\mathcal{K}} = k(\boldsymbol{\kappa},\beta(\boldsymbol{\kappa}))$,

$$\Sigma(\vec{\mathcal{K}})\mathbf{I} = \frac{c_o k^2\beta(\boldsymbol{\kappa})\alpha^2}{4\gamma^3}\int_{|\boldsymbol{\kappa}'|<1}\frac{d(k\boldsymbol{\kappa}')}{(2\pi)^2}\widetilde{\mathcal{R}}\left(\frac{k(\boldsymbol{\kappa}-\boldsymbol{\kappa}')}{\gamma},\frac{k(\beta(\boldsymbol{\kappa})-\beta(\boldsymbol{\kappa}'))}{\gamma}\right)\boldsymbol{\Gamma}(\boldsymbol{\kappa},\boldsymbol{\kappa}')\boldsymbol{\Gamma}(\boldsymbol{\kappa}',\boldsymbol{\kappa}), \tag{B.15}$$

so that

$$\begin{aligned}\Sigma(\vec{\mathcal{K}})\mathbf{W}(\vec{\mathcal{K}},\vec{\boldsymbol{x}}) = {} & \frac{c_o k^2\alpha^2}{4\gamma^3}\delta\big[\mathcal{K}_z-k\beta(\mathcal{K}/k)\big]\\ & \times\int_{|\boldsymbol{\kappa}'|<1}\frac{d(k\boldsymbol{\kappa}')}{(2\pi)^2}\widetilde{\mathcal{R}}\left(\frac{\mathcal{K}-k\boldsymbol{\kappa}'}{\gamma},\frac{k\big(\beta(\mathcal{K}/k)-\beta(\boldsymbol{\kappa}')\big)}{\gamma}\right)\\ & \times\boldsymbol{\Gamma}(\mathcal{K}/k,\boldsymbol{\kappa}')\boldsymbol{\Gamma}(\boldsymbol{\kappa}',\mathcal{K}/k)\mathcal{W}(\mathcal{K}/k,\boldsymbol{x},z).\end{aligned} \tag{B.16}$$

Finally, using the transport equation (112) satisfied by $\mathcal{W}(\boldsymbol{\kappa}, \boldsymbol{x}, z)$, and the relation (B.5), we obtain that

$$\vec{\nabla}\omega(\vec{\mathcal{K}}) \cdot \vec{\nabla}_{\vec{\boldsymbol{x}}}\mathbf{W}(\vec{\mathcal{K}}, \vec{\boldsymbol{x}}) = \int d\vec{\mathcal{K}}'\, \sigma(\vec{\mathcal{K}}, \vec{\mathcal{K}}')\mathbf{W}(\vec{\mathcal{K}}', \vec{\boldsymbol{x}}) + c_o\beta(\mathcal{K}/k)\Big[\mathbf{Q}(\mathcal{K}/k)\mathbf{W}(\vec{\mathcal{K}}, \vec{\boldsymbol{x}}) + \mathbf{W}(\vec{\mathcal{K}}, \vec{\boldsymbol{x}})\mathbf{Q}(\mathcal{K}/k)^{\dagger}\Big]. \tag{B.17}$$

This is similar to the transport equation (B.6), except that we do not have the scalar valued total scattering cross section $\Sigma(\vec{\mathcal{K}})$ multiplying $\mathbf{W}(\vec{\mathcal{K}}, \vec{\boldsymbol{x}})$, but a linear operator $-c_o\beta(\mathcal{K}/k)\Big[\mathbf{Q}(\mathcal{K}/k)\mathbf{W}(\vec{\mathcal{K}}, \vec{\boldsymbol{x}}) + \mathbf{W}(\vec{\mathcal{K}}, \vec{\boldsymbol{x}})\mathbf{Q}(\mathcal{K}/k)^{\dagger}\Big]$ acting on $\mathbf{W}(\vec{\mathcal{K}}, \vec{\boldsymbol{x}})$. The results would be exactly the same if $\mathbf{Q}(\boldsymbol{\kappa})$ were a multiple of the identity of the form

$$-2c_o\beta(\boldsymbol{\kappa})\mathbf{Q}(\boldsymbol{\kappa}) = \Sigma(\vec{\mathcal{K}})\mathbf{I}$$

for $\vec{\mathcal{K}} = k(\boldsymbol{\kappa}, \beta(\boldsymbol{\kappa}))$. This turns out to be the case in the high-frequency limit $\gamma \to 0$, as explained in Section 8. It is also the case for the real part of $\mathbf{Q}(\boldsymbol{\kappa})$ in general (provided that $\mathcal{R}$ is isotropic, as assumed throughout this appendix), as we now show.

For $\boldsymbol{\kappa} \in \mathbb{R}^2$ such that $|\boldsymbol{\kappa}| < 1$, we have by (108)

$$\mathrm{Re}\big(\mathbf{Q}(\boldsymbol{\kappa})\big) = -\frac{k^2\alpha^2}{8\gamma^3}\int_{|\boldsymbol{\kappa}'|<1}\frac{d(k\boldsymbol{\kappa}')}{(2\pi)^2}\widetilde{\mathcal{R}}\left(\frac{k(\boldsymbol{\kappa}-\boldsymbol{\kappa}')}{\gamma}, \frac{k\big(\beta(\boldsymbol{\kappa})-\beta(\boldsymbol{\kappa}')\big)}{\gamma}\right)\boldsymbol{\Gamma}(\boldsymbol{\kappa}, \boldsymbol{\kappa}')\boldsymbol{\Gamma}(\boldsymbol{\kappa}', \boldsymbol{\kappa}). \tag{B.18}$$

By comparing with (B.15) and denoting $\vec{\mathcal{K}} = k(\boldsymbol{\kappa}, \beta(\boldsymbol{\kappa}))$, this shows that

$$-2c_o\beta(\boldsymbol{\kappa})\mathrm{Re}\big(\mathbf{Q}(\boldsymbol{\kappa})\big) = \Sigma(\vec{\mathcal{K}})\mathbf{I}, \tag{B.19}$$

which is a multiple of the identity matrix. This also follows by inspection from (B.18), rewritten as

$$\mathrm{Re}\big(\mathbf{Q}(\boldsymbol{\kappa})\big) = -\frac{k^2\alpha^2}{8(2\pi)^2\gamma^3\beta(\boldsymbol{\kappa})}\int_{|\vec{\mathcal{K}}'|=k} dS(\vec{\mathcal{K}}')\widetilde{\mathcal{R}}\left(\frac{\vec{\mathcal{K}}-\vec{\mathcal{K}}'}{\gamma}\right)\mathbf{T}(\vec{\mathcal{K}}, \vec{\mathcal{K}}')\mathbf{T}(\vec{\mathcal{K}}', \vec{\mathcal{K}}). \tag{B.20}$$

Indeed, if we parameterize

$$\boldsymbol{\kappa} = \begin{pmatrix}\sin\theta\cos\phi\\ \sin\theta\sin\phi\end{pmatrix}, \qquad \vec{\mathcal{K}} = k\begin{pmatrix}\sin\theta\cos\phi\\ \sin\theta\sin\phi\\ \cos\theta\end{pmatrix}, \qquad \vec{\mathcal{K}}' = k\begin{pmatrix}\sin\theta'\cos\phi'\\ \sin\theta'\sin\phi'\\ \cos\theta'\end{pmatrix},$$

then we have

$$\mathbf{T}(\vec{\mathcal{K}}, \vec{\mathcal{K}}')\mathbf{T}(\vec{\mathcal{K}}', \vec{\mathcal{K}}) = \begin{pmatrix}1-\kappa_2''^2 & -\kappa_1''\kappa_2''\\ -\kappa_1''\kappa_2'' & 1-\kappa_1''^2\end{pmatrix}, \qquad |\vec{\mathcal{K}}-\vec{\mathcal{K}}'|^2 = 2k^2(1-\kappa_3''),$$

where

$$\vec{\boldsymbol{\kappa}}'' = \begin{pmatrix}\kappa_1''\\ \kappa_2''\\ \kappa_3''\end{pmatrix} = \begin{pmatrix}\sin\theta'\sin(\phi'-\phi)\\ \cos\theta\sin\theta'\cos(\phi'-\phi)+\sin\theta\cos\theta'\\ \sin\theta\sin\theta'\cos(\phi'-\phi)+\cos\theta\cos\theta'\end{pmatrix}.$$

If we introduce the rotation matrix

$$\mathbf{U}_{\boldsymbol{\kappa}} = \begin{pmatrix}-\sin\phi & \cos\phi & 0\\ \cos\theta\cos\phi & \cos\theta\sin\phi & -\sin\theta\\ \sin\theta\cos\phi & \sin\theta\sin\phi & \cos\theta\end{pmatrix},$$

then

$$\mathbf{U}_{\boldsymbol{\kappa}}\vec{\mathcal{K}}' = k\vec{\boldsymbol{\kappa}}''.$$

By carrying out the change of variable $\vec{\boldsymbol{\kappa}}'' = \mathbf{U}_{\boldsymbol{\kappa}}\vec{\mathcal{K}}'/k$ in (B.20), we find that since $\widetilde{\mathcal{R}}(\vec{\boldsymbol{\kappa}}) = \check{\mathcal{R}}_{\mathrm{iso}}(|\vec{\boldsymbol{\kappa}}|)$,

$$\mathrm{Re}\big(\mathbf{Q}(\boldsymbol{\kappa})\big) = -\frac{k^4\alpha^2}{8(2\pi)^2\gamma^3\beta(\boldsymbol{\kappa})}\int_{|\vec{\boldsymbol{\kappa}}''|=1} dS(\vec{\boldsymbol{\kappa}}'')\check{\mathcal{R}}_{\mathrm{iso}}\left(\frac{\sqrt{2(1-\kappa_3'')}}{\gamma}\right)\begin{pmatrix}1-\kappa_2''^2 & -\kappa_1''\kappa_2''\\ -\kappa_1''\kappa_2'' & 1-\kappa_1''^2\end{pmatrix}. \tag{B.21}$$

By changing (κ_1'', κ_2'') into $(-\kappa_2'', \kappa_1'')$ and carrying the integration over the unit sphere, we obtain that $\mathrm{Re}\big(\mathbf{Q}(\boldsymbol{\kappa})\big)$ is proportional to the identity matrix.

Appendix C. Connection to the white-noise paraxial theory

The white-noise paraxial theory is valid when the four length scales satisfy

$$\lambda \ll \ell \sim X \ll \bar{L}, \tag{C.1}$$

with $\lambda\bar{L} \sim X^2$, which corresponds to a Fresnel number of order one. The separation of scales can then be characterized by a unique dimensionless parameter $\epsilon \ll 1$ such that

$$\epsilon = \frac{\lambda}{\bar{L}}, \qquad \frac{\lambda}{\ell} \sim \frac{\lambda}{X} \sim \epsilon^{\frac{1}{2}}. \tag{C.2}$$

We again let $\bar{L}$ be the reference length scale and introduce the scaled length variables

$$\boldsymbol{x}' = \boldsymbol{x}/(\epsilon^{\frac{1}{2}}\bar{L}), \qquad z' = z/\bar{L}, \qquad L' = L/\bar{L}, \qquad \ell' = \ell/(\epsilon^{\frac{1}{2}}\bar{L}), \qquad X' = X/(\epsilon^{\frac{1}{2}}\bar{L}). \tag{C.3}$$

The scaled wavenumber is $k' = k\bar{L}\epsilon = 2\pi$. We finally assume that the standard deviation α of the fluctuations of the random medium in (5) is small, of order $\epsilon^{3/2}$, and we let $\alpha' = \alpha/\epsilon^{3/2}$ be the normalized standard deviation of the fluctuations. If we drop the primes and consider the asymptotic regime $\epsilon \to 0$, then the electric field $\vec{\boldsymbol{E}}^{\epsilon}$ has the form [8]

$$\vec{\boldsymbol{E}}^{\epsilon}(\vec{\boldsymbol{x}}) \approx \begin{pmatrix} \boldsymbol{E}_{\rm par}(\boldsymbol{x}, z) \\ 0 \end{pmatrix} e^{ik\frac{z}{\epsilon}}, \qquad \boldsymbol{E}_{\rm par}(\boldsymbol{x}, z) = \int_{\mathbb{R}^2} T_{\rm par}(\boldsymbol{x}, \boldsymbol{x}', z)\boldsymbol{E}_o(\boldsymbol{x}')d\boldsymbol{x}', \tag{C.4}$$

where the scalar transmission kernel satisfies the Itô-Schrödinger equation

$$dT_{\rm par}(\boldsymbol{x}, \boldsymbol{x}', z) = \frac{i}{2k}\Delta_{\boldsymbol{x}'}T_{\rm par}(\boldsymbol{x}, \boldsymbol{x}', z)dz + \frac{ik}{2}T_{\rm par}(\boldsymbol{x}, \boldsymbol{x}', z) \circ dB(\boldsymbol{x}', z), \tag{C.5}$$

starting from $T_{\rm par}(\boldsymbol{x}, \boldsymbol{x}', z = 0) = \delta(\boldsymbol{x} - \boldsymbol{x}')$. Here $B(\boldsymbol{x}, z)$ is a Brownian field with mean zero and covariance function

$$\mathbb{E}\big[B(\boldsymbol{x}, z)B(\boldsymbol{x}', z')\big] = \min(z, z')\,\alpha^2\ell \int_{-\infty}^{\infty} \Re\left(\frac{\boldsymbol{x} - \boldsymbol{x}'}{\ell}, \zeta\right) d\zeta,$$

and $\circ$ stands for the Stratonovich integral. Using Itô's formula, the coherent field $\boldsymbol{A}_{\rm par}(\boldsymbol{x}, z) = \mathbb{E}[\boldsymbol{E}_{\rm par}(\boldsymbol{x}, z)]$ satisfies [8]

$$\partial_z \boldsymbol{A}_{\rm par}(\boldsymbol{x}, z) = \frac{i}{2k}\Delta_{\boldsymbol{x}}\boldsymbol{A}_{\rm par}(\boldsymbol{x}, z) - \frac{1}{\mathcal{S}_{\rm par}}\boldsymbol{A}_{\rm par}(\boldsymbol{x}, z),$$

which shows that it decays exponentially with z on the scale

$$\mathcal{S}_{\rm par} = \frac{8}{k^2\ell\alpha^2 \int_{-\infty}^{\infty} \Re(\boldsymbol{0}, \zeta)d\zeta}. \tag{C.6}$$

The decay length $\mathcal{S}_{\rm par}$ corresponds to the scattering mean free path $\mathcal{S}(\boldsymbol{\kappa})$ defined by (123) in the high-frequency regime $\gamma \to 0$ with $|\boldsymbol{\kappa}| = O(\gamma)$.

The Wigner transform is

$$\begin{aligned} \mathbf{W}_{\rm par}(\boldsymbol{\kappa}, \boldsymbol{x}, z) &= \int_{\mathbb{R}^2} d\boldsymbol{y}\, e^{ik\boldsymbol{\kappa}\cdot\boldsymbol{y}}\mathbb{E}\Big[\boldsymbol{E}_{\rm par}\Big(\boldsymbol{x} - \frac{\boldsymbol{y}}{2}, z\Big)\boldsymbol{E}_{\rm par}\Big(\boldsymbol{x} + \frac{\boldsymbol{y}}{2}, z\Big)^{\dagger}\Big] \\ &= \int_{\mathbb{R}^2} \frac{d(k\boldsymbol{q})}{(2\pi)^2}\, e^{ik\boldsymbol{q}\cdot\boldsymbol{x}}\mathbb{E}\Big[\widehat{\boldsymbol{E}}_{\rm par}\Big(k\Big(\boldsymbol{\kappa} + \frac{\boldsymbol{q}}{2}\Big), z\Big)\widehat{\boldsymbol{E}}_{\rm par}\Big(k\Big(\boldsymbol{\kappa} - \frac{\boldsymbol{q}}{2}\Big), z\Big)^{\dagger}\Big]. \end{aligned}$$

Using Itô's formula it is shown in [8] to satisfy the transport equation

$$\partial_z \mathbf{W}_{\rm par} + \boldsymbol{\kappa}\cdot\nabla_{\boldsymbol{x}}\mathbf{W}_{\rm par} = \frac{k^2\ell^3\alpha^2}{4}\int_{\mathbb{R}^2} \frac{\mathrm{d}(k\boldsymbol{\kappa}')}{(2\pi)^2}\,\widetilde{\Re}\big(k\ell(\boldsymbol{\kappa} - \boldsymbol{\kappa}'), 0\big)\big[\mathbf{W}_{\rm par}(\boldsymbol{\kappa}') - \mathbf{W}_{\rm par}(\boldsymbol{\kappa})\big], \tag{C.7}$$

which corresponds to (133) in the high-frequency regime $\gamma \to 0$.

References

[1] M.I. Skolnik, Radar Handbook, third ed., McGraw-Hill, New York, 2008.
[2] C. Elachi, Y. Kuga, K. McDonald, K. Sarabandi, F. Ulaby, M. Whitt, H. Zebker, J. van Zyl, Radar Polarimetry for Geoscience Applications, Artech House Inc., Norwood, MA, 1990.
[3] M. Moscoso, Polarization-based optical imaging, in: Inverse Problems and Imaging, in: Lecture Notes in Mathematics, vol. 1943, Springer, 2008, pp. 67–83.
[4] L.C. Andrews, R.L. Phillips, Laser Beam Propagation Through Random Media, Vol. 1, SPIE Press, Bellingham, WA, 2005.
[5] A. Goldsmith, Wireless Communications, Cambridge University Press, Cambridge, 2005.

[6] W. Kohler, G. Papanicolaou, B. White, M. Postel, Reflection of pulsed electromagnetic waves from a randomly stratified half-space, J. Opt. Soc. Am. A 8 (7) (1991) 1109–1125.
[7] R. Alonso, L. Borcea, Electromagnetic wave propagation in random waveguides, SIAM Multiscale Model. Simul. 13 (3) (2015) 847–889.
[8] J. Garnier, K. Sølna, Paraxial coupling of electromagnetic waves in random media, SIAM Multiscale Model. Simul. 7 (4) (2009) 1928–1955.
[9] L. Ryzhik, G. Papanicolaou, J.B. Keller, Transport equations for elastic and other waves in random media, Wave Motion 24 (4) (1996) 327–370.
[10] G. Papanicolaou, G. Bal, L. Ryzhik, Probabilistic theory of transport processes with polarization, SIAM J. Appl. Math. 60 (5) (2000) 1639–1666.
[11] G. Papanicolaou, W. Kohler, Asymptotic theory of mixing stochastic ordinary differential equations, Comm. Pure Appl. Math. 27 (5) (1974) 641–668.
[12] G. Papanicolaou, S. Weinryb, A functional limit theorem for waves reflected by a random medium, Appl. Math. Optim. 30 (3) (1994) 307–334.
[13] S. Chandrasekhar, Radiative Transfer, Dover, New York, 1960.
[14] L. Tsang, J.A. Kong, Scattering of Electromagnetic Waves, John Wiley & Sons, Inc., New York, 2001.
[15] A.C. Fannjiang, Self-averaging radiative transfer for parabolic waves, C. R. Math. 342 (2) (2006) 109–114.
[16] G. Papanicolaou, L. Ryzhik, K. Sølna, Self-averaging from lateral diversity in the ito-schroedinger equation, SIAM Multiscale Model. Simul. (2007) 468–492.
[17] J. Garnier, K. Sølna, Coupled paraxial wave equations in random media in the white-noise regime, Ann. Appl. Probab. 19 (1) (2009) 318–346.
[18] M.C.W. van Rossum, T.M. Nieuwenhuizen, Multiple scattering of classical waves: microscopy, mesoscopy, and diffusion, Biomed. Opt. Express 71 (1999) 313–371.
[19] J.D. Jackson, Classical Electrodynamics, third ed., John Wiley & Sons, Inc., New York, 1999.
[20] J.-P. Fouque, J. Garnier, G. Papanicolaou, K. Sølna, Wave Propagation and Time Reversal in Randomly Layered Media, Springer, New York, 2007.
[21] G. Bal, Waves in Random Media, in: Lecture Notes, Columbia University, 2006.